

# YAP and TAZ have Functionally Redundant Roles in Uveal Melanoma

by

Swanny A. Lamboy Rodríguez  
B.S. Microbiology  
University of Puerto Rico – Humacao, 2018

Submitted to Department of Biology in partial fulfillment of the requirements for the degree of  
Doctor of Philosophy in Biology  
At the  
Massachusetts Institute of Technology  
June 2024

© 2024 Swanny Lamboy Rodríguez. All rights reserved.

The author hereby grants to MIT a nonexclusive, worldwide, irrevocable, royalty-free license to exercise any and all rights under copyright, including to reproduce, preserve, distribute and publicly display copies of the thesis, or release the thesis under an open-access license."

Signature of the Author: \_\_\_\_\_

Department of Biology

Certified by: \_\_\_\_\_

Jacqueline A. Lees  
Virginia and D.K. Ludwig Professor for Cancer Research  
Associate Dean, School of Science  
Associate Director, Koch Institute  
Biology Thesis Supervisor

Accepted by: \_\_\_\_\_

Mary Gehring  
Professor of Biology  
Member, Whitehead Institute  
Director, Biology Graduate Committee

# Acknowledgments

I have found this section to be difficult to write. It feels like an immensely impossible task to find the right words to properly express just how grateful I am for all the support I have received during this journey. Here's to trying.

Firstly, I want to express my deepest gratitude to my thesis supervisor, Dr. Jacqueline Lees. Your never-ending support, counseling, and active listening have made it possible for this project (and me) to reach the finish line. I also want to thank Dr. Matthew Vander Heiden and Dr. Eliezer Calo, my thesis committee, for all your guidance these last few years.

Second, I want to thank team Uveal Melanoma, without you, this project would not have been what it is today. I want to thank Kevin, Griffin, Adam, and Grace for your guidance, mentorship, and overall contributions to this work. I especially want to thank Adam for all of your help these years, particularly in these last few months. I also want to thank Grace for having been such a great peer mentor and even better friend. You were there to guide and teach me when I knew nothing. I learned a lot from you.

I want to thank the Lees lab members, current and past, for having been so welcoming to me when I joined, and for always being such a great group of people to work with. I want to thank Colin for being the best bay-mate ever and a great friend. Thank you for helping me with experiments, thinking about science, and all the coffee breaks. I also want to thank Renin for always keeping an eye out for me, bringing me snacks, helping me learn about the drug assays, always being willing to chat, and your friendship.

To my friends, thank you for making this journey easier to bear. If it wasn't for my little *familia Boricua en la diáspora*, I would not have been able to stand these Cambridge/Boston winters. Thank you for making home not feel so far away and always bringing the warmth with you. Especially, Gaby, Yami, Luis, Javier, Normaris, Zuly, and Leeza. I also want to thank Glorimar & Paola Cristina for being only a video call away all these years, your support, for more than a decade, has never faltered.

I want to thank my family, *los Lamboy y Rodríguez Pérez*, for your love and support. I want to thank my second family, *los Núñez*, for opening your arms and home to me from the first day we met. Especially, I want to thank my in-laws, Maribel & Rolando, as well as Betty, Ricardo, Marie, Jose, Ian, Gabriel, and Marina.

To my parents, Magaly & Axel, I would not be the person I am today if it wasn't for you. *Ustedes son mi inspiración más grande en la vida, los amo una eternidad*. To my sister, Alisha, I miss you every day, I am so incredibly proud of you, you have made me the happiest oldest sister ever, thank you for your support and spending this past holiday with us.

*A mi vida*, Rolando Jaime, thank you for believing in me, even when I didn't. Thank you for inspiring me every day since the moment we met. You held me up when I couldn't stand and cheered me on every step of the way.

Lastly, I want to thank my precious little furbaby, Haru, for being the best cat ever. Having you in our lives these last years has brightened all my days.

# YAP and TAZ have Functionally Redundant Roles in Uveal Melanoma

by

Swanny A. Lamboy Rodríguez

Submitted to the Department of Biology on May 17<sup>th</sup>, 2024, in Partial Fulfillment of the Requirements for the Degree of Doctor of Philosophy in Biology

## Abstract

Uveal Melanoma (UM) is the primary ocular malignancy in adults. The primary tumor is treatable but 50% of patients develop fatal metastases. Most UM are driven by activating mutations in the heterotrimeric G protein alpha subunits paralogs, *GNAQ* or *GNA11*, whose main downstream effectors are MAPK signaling and the transcriptional activator YAP. Recent zebrafish work established the importance of YAP and de-emphasized the role of MAPK in UM. Here we show that deletion of *yap* has no significant effect on the incidence, or kinetics, of *GNAQ*<sup>Q209L</sup>-driven zebrafish UM. Additional experiments revealed the presence of nuclear Taz in the *yap* null tumors. Our data suggest that this reflects functional redundancy between *yap* and its paralog, *taz*, either of which can efficiently drive UM. Furthermore, we show that the tumorigenic effects of YAP and TAZ are TEAD-dependent. To determine the human relevance, multiple YAP or TAZ-deficient clones were generated for two human UM cell lines, Mel202 and MP41. Deletion of either protein had no consistent deleterious effects on cell survival or proliferation, across the two cell lines *in vitro*. Moreover, deletion of YAP or TAZ did not prevent tumor formation in mice after intracardiac injection, and the clones show high liver tropism, modeling human UM metastases. The liver tumors displayed nuclear YAP and/or TAZ, as appropriate for their genotype, and only low-level, heterogenous staining for phospho-ERK. We conclude that the YAP/TAZ signaling plays the dominant role in both zebrafish and human UM, but most tumors can survive without YAP or TAZ due to the functional redundancy of these two proteins.

Thesis Supervisor: Jacqueline Lees

Title: Virginia and D.K. Ludwig Professor for Cancer Research, Associate Dean, School of Science, Associate Director, Koch Institute

# Table of Contents

<b>TITLE PAGE</b>	<b>1</b>
<b>ACKNOWLEDGEMENTS</b>	<b>2</b>
<b>ABSTRACT</b>	<b>3</b>
<b>TABLE OF CONTENTS</b>	<b>4</b>
<b>ABBREVIATIONS</b>	<b>5</b>
<b>CHAPTER I: INTRODUCTION</b>	<b>6</b>
MELANOCYTES AND MELANOMA	7
CUTANEOUS MELANOMA	9
THE MAPK PATHWAY	10
TARGETED THERAPIES AGAINST THE MAPK PATHWAY	13
RESISTANCE TO MAPK INHIBITORS	14
UVEAL MELANOMA	15
THE MAPK PATHWAY IN UM	19
THE YAP/TAZ PATHWAY IN UM	21
DRUG STRATEGIES IN UM	23
UM CELL LINES	25
ANIMAL MODELS IN UM	29
QUESTIONS ADDRESSED IN THIS THESIS	32
REFERENCES	34
<b>CHAPTER II: EITHER YAP OR TAZ IS DISPENSABLE FOR UVEAL MELANOMA, REFLECTING PATHWAY PLASTICITY</b>	<b>55</b>
ABSTRACT	56
INTRODUCTION	56
RESULTS	60
DISCUSSION	75
MATERIALS & METHODS	78
ACKNOWLEDGEMENTS	83
SUPPLEMENTARY MATERIALS/FIGURES	84
REFERENCES	104
<b>CHAPTER III: DISCUSSION AND CONCLUSIONS</b>	<b>111</b>
REFERENCES	119

# Abbreviations

Uveal Melanoma as **UM**

Cutaneous Melanoma as **CM**

Mitogen-Activated Protein Kinase as **MAPK**

GNAQ or GNA11 as **GαQ/11**

phosphatidylinositol 4,5 biphosphate as **PIP2**

diacylglycerol as **DAG**

inositol 1,4,5-triphosphate as **PIP3**

Trio Guanine Nucleotide Exchange Factor as **TRIO**

Focal adenosine kinase as **FAK**

FAK inhibitor as **FAKi**

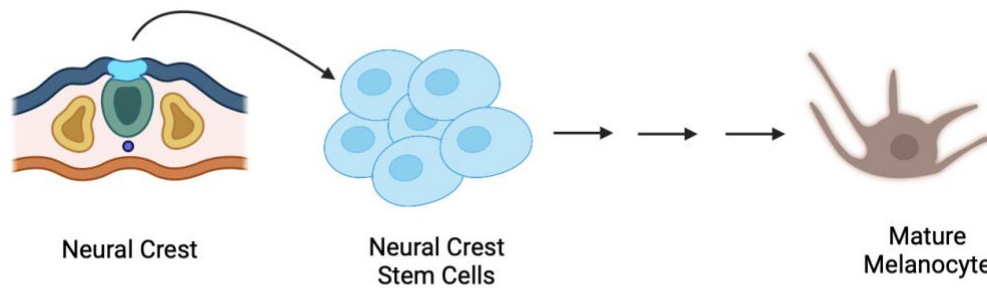
# **Chapter I. Introduction**

The work presented in this thesis was built upon many years of work by previous members of the lab, as well as the broader research community. My work is focused on understanding molecular drivers and contributors to Uveal Melanoma (UM), a subtype of melanoma. In this Chapter, I will begin by discussing general melanocyte biology, and the development, progression, genetics, and treatment approaches of Cutaneous Melanoma (CM), as these have had an overarching influence on the study of UM. I will then describe the biology of, and existing treatments, for UM.

## **I. Melanocytes and Melanoma**

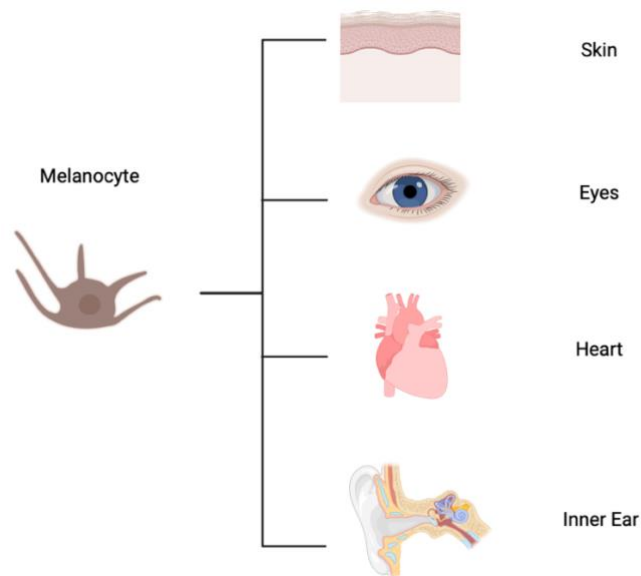
Melanoma is a cancer that arises from transformed melanocytic cells. Melanocytes are a type of cell whose main function is to produce melanin. There are two types of melanin in mammals, eumelanin and pheomelanin. Eumelanin produces dark pigments like brown and black, while pheomelanin contains red-orange pigment (Nasti et al., 2015). These pigments give color to our skin, iris, and hair.

Melanocytes are derived from neural crest stem cells. These cells arise in the neural crest early in embryonic development and migrate throughout the body to distinct sites where they give rise to different cell types, including melanocytes (Fig. 1). Melanocytes are found predominantly in the epidermis, but also exist in the eyes, the heart, inner ear, meninges, bones, and mucosal epithelium (Fig. 2). During neural crest cell migration, melanocyte precursor cells relocate to the future sites of these organs and eventually differentiate into mature melanocytes (Thomas et al., 2008).



**Figure 1. From Neural Crest to Melanocyte** Generalized overview of the developmental trajectory of neural crest cells to melanocytes (adapted from Thomas et al 2008). Created with BioRender.com

The main role of melanocyte cells is to produce pigment to protect the body from UV damage. This explains why most melanocytes are found in the epidermis, the only external organ in the body. The presence of melanocytes at other sites that are not affected by UV rays suggests that melanocytes might have alternate or additional roles. Accordingly, melanocytes in the inner ear have been shown to be important at preventing hearing loss (Price & Fisher 2001), while melanocytes in the eye regulate photo-oxidative stress (Istrate et al., 2020).



**Figure 2. Melanocyte cells localize to many sites in the body** Melanocytes are found in multiple sites throughout the human body, including the skin, eyes, heart, and inner ear. Created with BioRender.com



Cancers are typically categorized based on the cell or tissue type from which they arise. When a melanocyte becomes malignant, the cancer is called a melanoma. Given that melanocytes exist at many locations, they can result in different categories of melanoma. The most common type of melanoma is CM, initiating from transformed skin melanocytes. It is followed by melanomas of the eye, arising from transformed melanocytes in the uvea and conjunctiva of the eye, and then mucosal melanoma, derived from transformed melanocytes that line the mucous membrane. This introduction focuses on the two most prevalent melanoma types, CM and UM. We will dive deeper into the similarities and differences between the two, and how this has shaped the research approach the field has taken to UM.

## **II. Cutaneous Melanoma**

CM is the 5<sup>th</sup> most common cancer in the US (“Melanoma of the Skin” - Cancer Stat Facts, n.d.). The global incidence of CM is about 15-25 cases per 100,000 individuals and the median age at diagnosis is 57 years (Schadendorf et al., 2015). It is most common in fair skin individuals and is mainly caused by mutations associated with UV damage. UV damage causes a mutational signal with base changes of C to T or G to T. As a consequence of UV damage, CM has the highest mutational burden of all cancer types.

Melanoma is generally diagnosed by routine check-ups with a dermatologist. In other instances, patients themselves identify an odd-looking mole that prompts a visit to the doctor. Routine check-ups for melanoma are not an established medical standard, even though they have a slightly higher correlation with better patient outcome than cases where the patient raised concerns with their doctors (Schadendorf et al., 2015). This is likely because trained physicians identify the malignancy at earlier stages, when removal of the cancer is still a relatively curative method of treatment, with less likelihood of metastasis. Only about 10-15% of patients who are diagnosed early and have the primary tumor excised will develop metastasis (Schadendorf et al., 2015).

Other factors that contribute to the aggressiveness of CM are the nature of the acquired mutations within the tumor. As mentioned above, UV rays are the primary causative agent of CM (Schadendorf et al., 2018). CM's commonly associated mutations include *BRAF*, *NRAS*, or *NFI* (Schadendorf et al., 2018). The most prevalent mutation in CM, observed in approximately 50% of patients, is an activating mutation in the serine/threonine kinase *BRAF* (Davies et al., 2002). *BRAF* mutations in CM have an inverse correlation to sun exposure (Bauer et al., 2011; Maldonado et al., 2003; Curtin et al., 2005). *BRAF* is normally regulated by an upstream GTPase, *RAS*, which phosphorylates *BRAF*, allowing it to dimerize and now activate its main downstream target, another kinase known as *MEK* (Goldsmith & Dhanasekaran 2007; Kiuru & Busam et al., 2017). *MEK*, in turn, activates the transcription factor *ERK* by phosphorylation, to form phospho-*ERK* (Goldsmith & Dhanasekaran 2007; Kiuru & Busam et al., 2017). This signaling cascade is termed the MAPK kinase pathway.

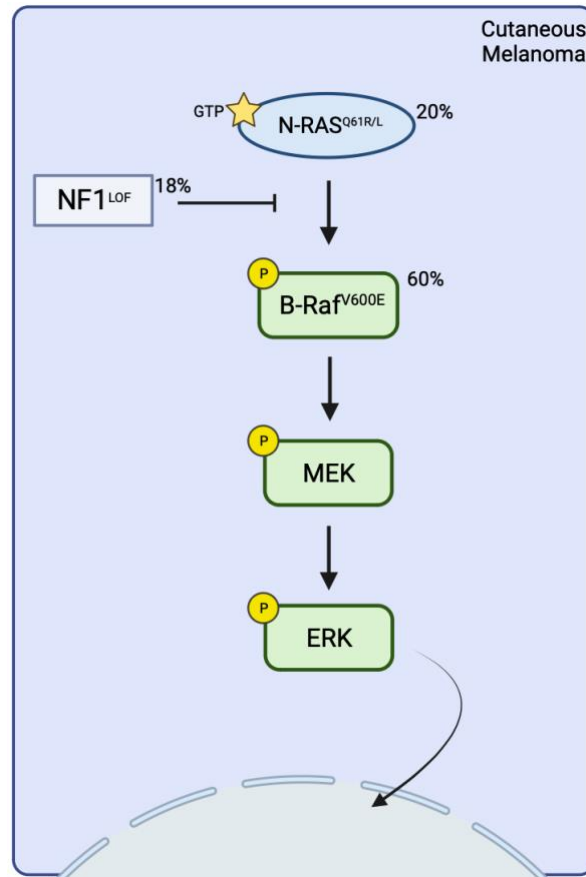
#### **i. The MAPK Kinase Pathway**

The MAPK kinase pathway is frequently mutated in CM. The second and third most prevalent mutations in CM patients, *NRAS* and *NFI*, are also components of this pathway. *NRAS* is mutated in 20% of melanoma cases (Schadendorf et al., 2018). As mentioned previously, *NRAS* is the small GTPase upstream of *BRAF*. *NFI*, a GTPase that downregulates *NRAS* activity, is mutated in 15-18% of cases (Akbani et al., 2015; Trinh et al., 2022). It is a classic tumor suppressor, and the CM mutations delete or inactivate the *NFI* gene or disrupt its ability to inhibit *NRAS*, causing increased or deregulated MAPK pathway activity (Andersen et al., 1993; Nissan et al., 2014; Kiuru & Busam et al 2017). The existence of multiple mutations altering the same pathway highlights its importance in CM.

The MAPK pathway normally regulates cell growth, proliferation, differentiation, and apoptosis (Morrison 2012; Ottaviano et al., 2021). It becomes active when a membrane receptor protein, such as *KIT* or *EGFR*, bind to their ligands and then stimulate the downstream GTPase,

RAS. In mammalian cells, three RAS proteins are expressed, HRAS, NRAS and KRAS (Prior et al., 2012). All three are proto-oncogenes and are commonly mutated in a variety of cancer types including pancreatic cancer, colon cancer, lung cancer, thyroid cancer, myeloid cancer, and skin cancer (Bos J.L. 1990). RAS proteins become active when bound to GTP in their GDP/GTP binding pocket. *RAS* mutations localize predominantly to this binding pocket, eliminating the GTPase function, thus locking RAS in the GTP bound active form (Prior et al., 2012). *N-RAS* mutations in CM typically occur at the codon 61, which also affect its GDP/GTP pocket and lead to constitute activation (Akbari et al., 2015).

After RAS becomes activated, it phosphorylates RAF and activates its kinase function. There are three RAF proteins in mammalian cells: CRAF, BRAF, and ARAF, and all are mutated to a certain extent in cancers. RAF proteins have three distinct domains, CR1, CR2, and CR3. CR1 has a RAS binding domain (RBD), CR2 contains a 14-3-3 binding domain and a serine/threonine rich domain, and CR3 has the catalytic serine/threonine kinase domain (Ottaviano et al., 2021). The most common mutation of *BRAF* is substitution of V600 for acid residues, followed by mutations in codons L597, K601, G469, which all result in constitutive activity (Ottaviano et al., 2021). Once active, RAF dimerizes with itself and then phosphorylates the kinase MEK to activate it (Morrison & Davis 2003).



**Figure 3. MAPK Pathway Mutations in CM** The most common mutations in CM that alter the MAPK pathway. BRAF mutations account for 60% of the mutations that alter the MAPK pathway, followed by NRAS with 20%, and NF1 with 18%. Created with BioRender.com

MEK phosphorylates members of the Mitogen-Activated Protein Kinase (MAPK) family, otherwise known as the ERK1 and ERK2 proteins. These are the last effectors of the MAPK pathway. Once activated, ERKs dimerize and translocate to the nucleus to regulate transcription factors that will further activate the cell proliferation, differentiation, or growth pathways (Fig. 3) (Khokhlatchev et al., 1998; Chang & Karin 2001; Guo et al., 2019). The precise effect depends on the transcription factors that get activated, but common ERK targets include c-FOS, c-MYC, ATF2, as well as others (Guo et al., 2019). ERKs are not commonly mutated in cancers, but increased levels of activity have been demonstrated to be present in, and established as an important driver of, many cancer types.

In CM, *BRAF* mutations are present in approximately 50% of melanomas, with the vast majority affecting the V600 codon (Akbari et al., 2015). This activating mutation promotes tumor progression and invasion via multiple mechanisms. One mechanism is through the increased level of signaling to promote cell proliferation and growth. Another is to promote a more de-differentiated state by modulating the protein levels of differentiation factors, especially MITF, the master melanocyte transcription factor (Wellbrock et al., 2008). Finally, *BRAF* V600 mutations also promote immune evasion by secretion of immunosuppressive cytokines (Mandala et al., 2017), mediation of MHC I (Bradley et al., 2015), and downregulation of the tumor promoting cytokine gene *CCL2* (Mandala et al., 2017). *BRAF* mutant patients also have a more aggressive form of the disease with higher trends of brain and liver metastasis (Adler et al., 2017). Many targeted therapies have been implemented towards the betterment of melanoma patients.

## **ii. Targeted therapies against the MAPK pathway**

DNA sequencing has made it possible to identify the mutations present within a patient's cancer. This advancement allowed for the development of targeted therapies, geared towards disrupting the driving pathways of cancer. Given the high incidence of *BRAF* mutations in melanoma, specific BRAF inhibitors were developed and subsequently approved for treatment. Before targeted therapy, the standard of care for cutaneous melanoma was surgical removal of the primary tumor, followed by chemotherapy ("Melanoma Treatment", NCI). Dacarbazine is a chemotherapeutic agent approved by the FDA to treat metastatic melanoma (Ascierto et al., 2012). Median survival for melanoma patients with dacarbazine was 5 to 7.8 months, with a response rate of 7 to 12% (Ascierto et al., 2012). With the introduction of BRAF inhibitors, median overall survival improved to 13.6 months (Chapman et al., 2017).

The first BRAF inhibitor to be approved by the FDA was vemurafenib on August 17<sup>th</sup>, 2011(Ascierto et al., 2012). It works by inhibiting the kinase function of BRAF, thus suppressing the MAPK signaling cascade. Other approved BRAF inhibitors include dabrafenib and

encorafenib (FDA orange book: approved drugs). However, despite the significant improvement in overall survival of patients conferred by these monotherapies, resistance and reemergence eventually occurs. To combat resistance, combination/dual therapies were tested and approved.

### **iii. Resistance to MAPK inhibitors**

Resistance to BRAF inhibitors in melanoma has been shown to occur in multiple ways. A common mechanism of resistance is reactivation of the MAPK signaling cascade (Long et al., 2014). While generally, mutations in MAPK are mutually exclusive, tumors that carry BRAF mutations and acquire resistance to BRAF inhibitors have been found to harbor activating mutations in N-RAS or MEK (Long et al., 2014; Kaplan et al., 2011). To address this, inhibitors against MEK were tested for their efficacy in treating BRAF inhibitor resistant tumors. This strategy showed an initial response but eventually the tumors resurged (Caunt et al., 2015). Another approved strategy has been the combination of BRAF and MEK inhibitor treatment from the onset of therapy administration. Many such drug combinations are now approved by the FDA including: dabrafenib plus trametinib, vemurafenib plus cobimetinib, and encorafenib plus binimetinib (Ottaviano et al., 2021; FDA).

Besides acquiring resistance to BRAF inhibitors through reactivation of the MAPK pathway, these tumors activate other pathways to promote tumorigenesis, regardless of BRAF inhibition. Some common pathways that lead to resistance include the activation of the PI3K/AKT/mTOR pathway and the hippo effector YAP/TAZ-TEAD pathway. Loss of *PTEN*, a negative regulator of PI3K, is present in 30% of melanomas (Scatena et al., 2021). *PTEN* loss of function mutations have been shown to prevent tumor apoptosis in the presence of a BRAF inhibitor and thus give the cells a survival advantage (Paraiso et al., 2011). Furthermore, a study of a small cohort of patient tumor samples comparing the mutational landscape of treatment-naïve versus regressed tumors found newly acquired mutations in PI3K pathway genes only in the regressed tumors (Van Allen et al., 2014). However, it is unknown how important these mutations

were for the acquired resistance to the BRAF inhibitor. In a screen conducted to identify potential mediators of resistance to BRAF and MEK inhibitors, *YAPI* was the highest scoring gene (Li et al., 2015). Additionally, when comparing YAP in patients' tumors before and after treatment, there was a clear increase in the levels of nuclear YAP, which constitutes the active form of this protein, in the post-treatment samples (Li et al., 2015). Notably, UM typically shows poor response in the clinic to MAPK inhibitors. As I will discuss in detail below, these tumors are characterized by high levels of nuclear YAP, offering a potential reason as to why these treatments are unsuccessful for UM.

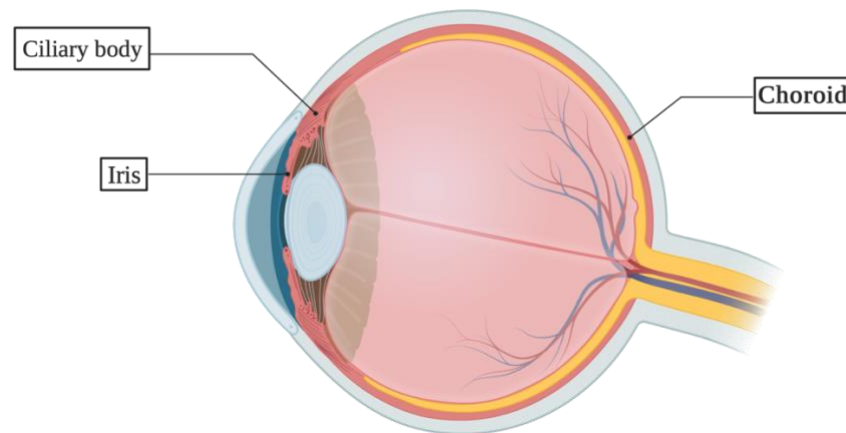
### **III. Uveal Melanoma**

UM accounts for 90% of melanomas of the eye and represents 5% of all melanoma diagnoses (Branisteanu et al., 2021). UM is the most common adult cancer of the eye, with a yearly prevalence of 1-9 per 1,000,000 individuals (Jager et al., 2020). UM arises from the transformation of melanocytes found in the uvea of the eye, which is composed of the choroid, the iris, and the ciliary body (Fig. 4). 90% of UM arise in the choroid, ~6% in the ciliary body, followed by ~4% in the iris (Jager et al., 2020). They are also sometimes categorized as anterior (iris and ciliary body) versus posterior (choroid) melanomas. Posterior UMs, along with the size of the primary tumor, correlate with a worse prognosis (Jager et al., 2020). The primary tumor is highly treatable, mainly by localized radiotherapy, but unfortunately 50% of patients develop metastases. Of these, up to 80-90% develop liver metastasis (Kaliki & Shields 2017). After metastasis diagnosis, the median survival decreases to about 4-15 months (Kaliki & Shields 2017).

Clinical outcomes for patients with UM have not progressed since 1973 (Aronow et al., 2018), contrary to CM patients who have increased survival thanks to new successful therapies (Kahlon et al., 2022). The differences in response to therapies CM versus UM, has puzzled clinicians and researchers; because both melanomas share key oncogenic signalling pathways (as I describe below) there was some expectation that CM treatments would also work in UM.

However, the two have distinct features, besides the location of origin, which very likely explain their differential responses.

#### UVEA OF THE EYE



**Figure 4. Anatomy of the Uvea** The Uvea of the eye is made up of the iris, the choroid, and the ciliary body. Created with BioRender.com

The main difference between CM and UM, besides location, is the oncogenic drivers. While the oncogenes that promote CM are commonly activated *BRAF* or *NRAS*, the main initiating oncogene in UM is an activating mutation in the small alpha subunit of the GTPase *GNAQ*, or its paralogue *GNA11* (Van Raamsdonk et al., 2009; Van Raamsdonk et al., 2010). I will use  $G\alpha Q/11$  as the nomenclature when referring to these proteins, as they are interchangeable drivers of UM. There are no known *BRAF* mutations in UM patients (Rimoldi et al., 2003), but a small percentage (~2%) of CM cases do carry a *G $\alpha$ Q/11* mutation (Larribère & Utikal, 2020).

Another oncogene found in UM patients is an activating mutation in the G-protein coupled receptor (GPCR) upstream of  $G\alpha Q/11$ , *CYSLTR2*. The mutation affects codon 129, substituting a leucine for glutamine, and causing *CYSLTR2* to constitutively activate  $G\alpha Q/11$



(Moore et al., 2016). *CYSLTR2*<sup>L129Q</sup> is mutually exclusive with the *GαQ/11*<sup>Q209</sup>. These two mutations affect genetic components of the same pathway, cementing the conclusion that the GαQ/11 pathway is the main driver of UM tumorigenesis.

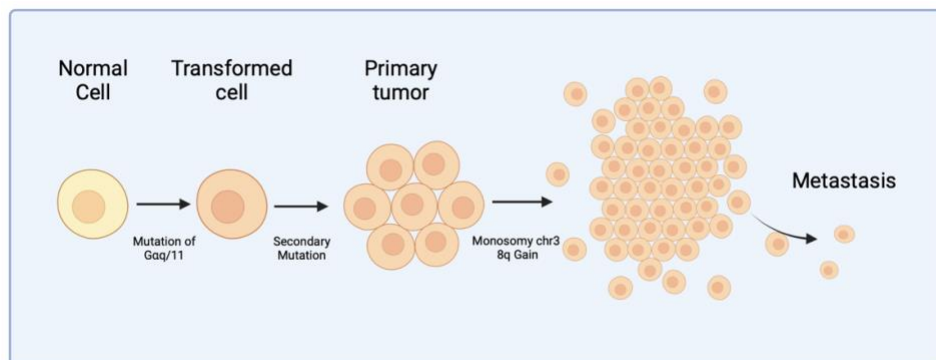
Secondary mutations in UM are found in the BRCA1-associated protein-1, *BAP1*, a known tumor suppressor gene whose role is to remove ubiquitin marks (Ventii et al., 2008). *BAP1* is mutated in ~47% to 50% of patients and this is associated with worse prognosis and metastasis (Harbour et al., 2010). *BAP1* is located on chromosome 3p21.1, and it is the only gene found to have a mutation on this chromosome (Harbour et al., 2010). *BAP1* is inactivated when this mutation is combined with monosomy of chromosome 3, a common hallmark of metastatic UM (Harbour et al., 2010; Robertson et al., 2017). Interestingly, there is considerable debate as to which event occurs first, as some studies report that *BAP1* mutations can occur prior to monosomy 3 (Harbour et al., 2010; Shain et al., 2019), while others propose that monosomy occurs before *BAP1* mutation (Robertson et al., 2017).

Two alternate secondary mutations, *SF3B1* and *EIF1AX*, are found in 24 % and 15% of UM patients respectively (Jager et al., 2020). *SF3B1* encodes a core protein component of the spliceosome, and *EIF1AX* has an important role in translation initiation. Mutations in *EIF1AX* are associated with favorable prognosis and less likely to develop metastasis, while *SF3B1* mutations are associated with late-onset metastasis development (Yavuzytoglu et al., 2016). These secondary mutations are acquired later during UM tumor evolution and exert their effect in the presence of a remaining wildtype allele.

Chromosomal alterations are tightly linked to cancer (Gordon et al., 2012). Before the identification of the gene mutations driving UM, the karyotype of UM patient samples was examined and monosomy of chromosome 3 and trisomy of chromosome 8q were found in most cases (Horsman & White 1993). These two chromosomal changes are associated with poorer prognosis for patient survival and increased metastatic risk; both monosomy 3 and 8q gain independently increase the risk of metastasis by 37% and 48%, respectively, after 7 years (Shields

et al., 2017). Monosomy 3 is an early event in the evolutionary trajectory of UM tumors (Robertson et al., 2017). On the other hand, 8q gain occurs after monosomy 3, and the number of 8q increases throughout the trajectory from primary tumor to metastasis (Shain et al., 2019). As mentioned above, it was subsequently discovered that *BAP1* is associated with monosomy 3 (Harbour et al., 2010). Other chromosomal alterations found in UM include loss of 1p, 6q, 8p and 9p, along with 1q and 6p gain (Harbour 2012). 6p gain in UM appears to correlate with a better prognosis (White et al., 1998; Robertson et al., 2017). *MYC*, a prominent proto-oncogene, is in chromosome 8q24 and 8q gains in UM are highly correlated with an increased activity of *MYC* (Parella et al., 2001; Schaub et al., 2018). Loss of 1p is found only in UM metastases, meaning it is a late occurrence in tumor evolution and presumably provides some benefit to metastatic outgrowth (Aalto et al., 2001).

Tumor evolution studies have shown that acquiring these mutational events happens in a stepwise manner, with *GαQ/11* mutations being the first event, followed by secondary mutations, such as *BAP1* mutation and monosomy of chromosome 3, and then 8q gain and 1q gain happening at the latest stages (Fig. 5) (Shain et al., 2019).



**Figure 5. Mutation evolution during UM progression** The first mutational event in UM is the occurrence of the *GαQ/11* mutation, followed by a secondary mutation, and later on, chromosomal aberrations prior and during metastasis. Created with BioRender.com

Monosomy 3 and 8q gain largely contributed to characterizing UM tumors. Specifically, UM was divided into Class I or Class II, where Class I is associated with decreased risk of

metastasis, and chromosomal changes, while Class II is associated with a higher risk of metastasis and includes tumors with monosomy 3 and 8q gain (Onken et al., 2004; Barbagallo et al., 2023). These classes can be further divided into subclasses based on more recent molecular profiling (Robertson et al., 2017).

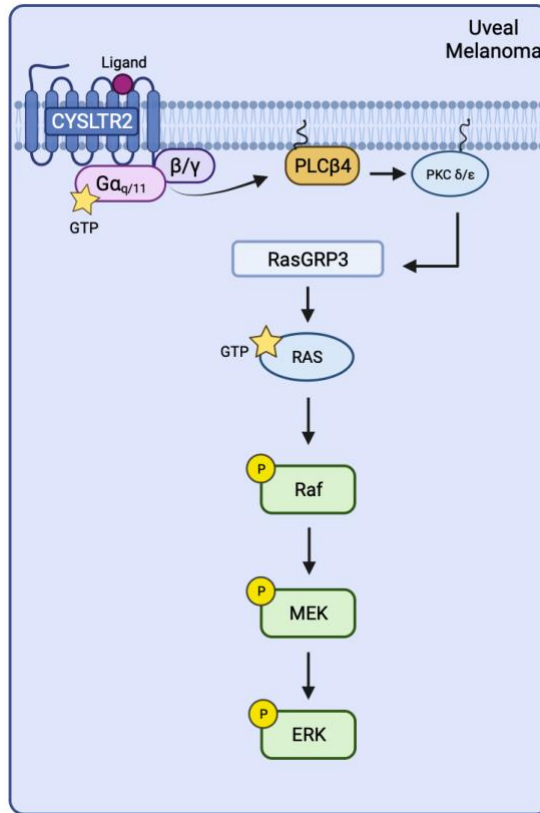
### **i. The MAPK Pathway in UM**

As introduced above, about 80 to 90% of UM carry mutations in either *GNAQ* or *GNA11* (Silva-Rodriguez et al., 2022). These mutations cluster to the GTP binding pocket, affecting its GTPase activity, similarly to the mutation of codon 61 of *N-RAS* in CM (Van Raamsdonk et al., 2009; Burd et al., 2014). *GαQ/11* mutations were identified in UM patients through sequencing of patient samples and transformation of melanocyte cells with oncogenic versions of *GNAQ* or *GNA11* (Van Raamsdonk et al., 2009; Van Raamsdonk et al., 2010). The most affected codon is Q209, where the amino acid, glutamine, is substituted by a leucine. This change prevents  $G\alpha Q/11^{Q209L}$  from hydrolyzing GTP, maintaining  $G\alpha Q/11$  in its active conformation. When active,  $G\alpha Q/11$  signals to downstream effectors that lead to activation of both the MAPK and YAP/TAZ pathways.

$G\alpha Q/11$  promotes MAPK activity through its interaction with the phospholipase c, PLC $\beta$ 4 (Lee et al 1994). PLC $\beta$ 4 converts phosphatidylinositol 4,5 biphosphate (PIP2) into diacylglycerol (DAG) and inositol 1,4,5-triphosphate (PIP3) (Kadamur et al., 2012). PIP3 activates calcium signaling, while DAG interacts with PKC isoforms, PKC $\delta/\epsilon$ , to activate RASGRP3 (Chen et al 2017; Moore et al 2018). RASGRP3 then activates the MAPK signaling cascade (Fig 6). The commonality of this MAPK signaling pathway between UM and CM, and its well documented importance in CM, was a major factor in thinking that treating UM patients with MAPK inhibitors would provide a similar level of success as seen in CM patients. Furthermore, another initiating mutation identified in UM patients is D630Y in *PLC $\beta$ 4* (Johansson et al., 2015). *PLC $\beta$ 4<sup>D630Y</sup>* is a relatively uncommon mutation, present in less than 3% of UM cases (Robertson et al., 2017;

TCGA). However, it is mutually exclusive with mutations in *GαQ/11* and has been shown to be both constitutively active and able to promote tumorigenesis *in vivo* (Phan et al., 2021). These findings reinforced the notion that activation of MAPK signaling, through constitutive activation of either GNAQ/11 or PLCβ4, was a key driver for UM.

The presence of overactive MAPK signalling in many UM cell lines (Zuidevaart et al., 2005), along with the discovery of the PLCβ4 mutation, drove the field to test the dependency of UM on this pathway. Thus began the use of MAPK inhibitors in UM cell lines to test its effect on cell viability and tumor potential. Multiple studies have shown a decrease in viability of UM cells when treated with inhibitors that target some element of the MAPK pathway (Ambrosini et al., 2012; Amirouchene-Angelozzi et al., 2014; Sugase et al., 2020). Soon after, clinical trials began to test the efficacy of MAPK inhibitors in patients with metastatic UM (mUM). Although MAPK inhibition showed initial promise in a phase II clinical trial, with better patient outcomes when compared to chemotherapy (Carvajal et al., 2014), the phase III failed to show improvement in progression free survival when compared to chemotherapy alone (Carvajal et al., 2018). In a similar manner, in Moore et al., (2018) showed that when UM tumors *in vivo* are treated with a MEK inhibitor, UM tumors are not responsive to treatment. These unexpected results propelled the field to identify other drivers and druggable targets in UM.



**Figure 6. MAPK Pathway activity in UM** Signaling from Gαq/11 towards MAPK pathway activation through its interaction with PLCβ4. Created with BioRender.com

## ii. The YAP/TAZ Pathway in UM

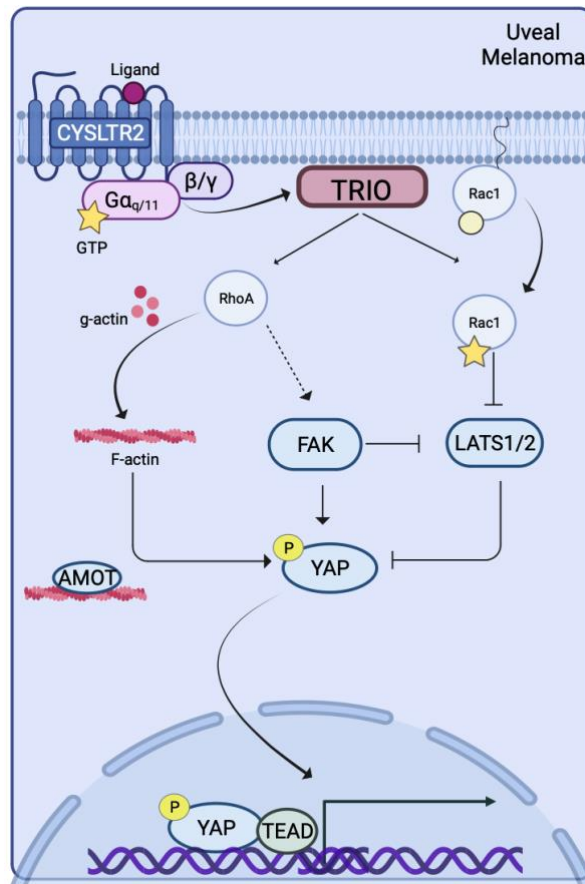
The second identified pathway in UM is the YAP pathway. YAP is an effector of the Hippo Pathway. It was first identified in drosophila as *Yorkie*, where its constitutive activation via loss of function mutations in its upstream negative regulator, lead to increased/uncontrolled organ size (Huang et al., 2005). The Hippo pathway is a negative regulator of YAP activity; when the Hippo pathway is on, YAP is off. The pathway contains multiple upstream kinases, including LATS1/2, which deposits negative phosphorylation marks unto serine residues of YAP, such as serine 127 (S127). This phosphorylation causes the cytoplasmic sequestration of YAP by 14-3-3 proteins and AMOT (Zhao et al., 2007; Freeman & Morrison, 2011; Jang et al., 2018). When the Hippo pathway is off, the S127 phosphorylation is removed, and a new phosphorylation is added at tyrosine 357

(Y357), a positive regulatory site, allowing YAP translocation to the nucleus (Smoot et al., 2017). Here, YAP functions as a transcriptional co-activator. It does not contain a DNA binding domain itself and thus requires interactions with transcription factors. YAP has been shown to interact with p73 (Strano et al., 2001), Runx2 (Vassilev et al., 2001), ErbB4 (Komuro et al., 2003), and TEAD (Yagi et al., 1999). However, the main factors, and certainly the ones through which YAP exerts its Hippo pathway effector role, is the TEAD family (Reggiani et al., 2021).

YAP's role in UM was found when searching for non-canonical pathways downstream of *GαQ/11*. As a result of the lack of efficacy of MAPK inhibitors in UM patients, researchers went looking for alternative pathways that may be activated by *GαQ/11*<sup>Q209L</sup>. In two studies published in 2014, oncogenic *GαQ/11* was demonstrated to lead to YAP nuclear localization, while wild-type *GαQ/11* cells lacked nuclear YAP (Feng et al., 2014 and Yu et al., 2014). The ability of oncogenic *GαQ/11* to increase YAP activity was found to occur independent of Hippo signalling, and it has propelled the field into studying the contributions of this pathway, versus the PLCβ4-MAPK pathway, in UM.

Understanding how *GαQ/11* promotes YAP activity has also been key in identifying other potential drug targets in UM. For *GαQ/11* to promote YAP nuclear localization, it first interacts with the Trio Guanine Nucleotide Exchange Factor (TRIO) (Feng et al., 2014). TRIO mediates this event through members of the Rho-family of small GTPases, RHOA and RAC1. RHOA and RAC1 have both been linked to regulation of actomyosin contractility and cell motility (Nguyen et al., 2018). Moreover, this pathway has been implicated in regulating tumor plasticity and increasing metastatic potential of CM (Sanz-Moreno et al., 2008; Sanz-Moreno & Marshall, 2009). The role of RHOA and RAC1 in UM is to promote YAP activity. RAC1 negatively regulates LATS1/2, while RHOA activates its downstream effector ROCK, a Rho-associated kinase, to promote g-actin polymerization to f-actin (Feng et al., 2014). AMOT, which sequesters YAP in the cytoplasm, is activated by LATS1/2 phosphorylation (Dai et al., 2013). AMOT is inhibited through f-actin binding, thus when ROCK promotes f-actin polymerization, YAP is free to localize

to the nucleus (Mana-Capelli et al., 2014). Therefore, RHOA and RAC1 function to promote YAP activity through inhibition of AMOT and preventing LATS1/2 activation. With the use of a bioinformatics pipeline, analysis of TCGA data identified *PTK2*, the gene encoding for focal adhesion tyrosine kinase (FAK), as being amplified in 18% of UM cases (Feng et al., 2019). Additional studies confirmed that FAK was downstream of RHOA-ROCK and able to promote YAP activity by two mechanisms: promoting positive phosphorylation marks on YAP and inhibiting the activity of LATS1/2 (Fig. 7) (Feng et al., 2019).



**Figure 7.  $G\alpha q/11$  -YAP pathway in UM** “Alternate” pathway of  $G\alpha q/11$  signaling, where  $G\alpha q/11$  leads to the activation of YAP, independently from the Hippo pathway, via TRIO. Created with BioRender.com

### iii. Drug strategies in UM

Understanding the interplay and contributions of oncogene activated pathways has been the focus of the UM field for the last decade. Many papers have shown the effectiveness of

inhibitors against one of the two major “arms” downstream of GαQ11, referring to the MAPK pathway and the YAP pathway, in cell line models and *in vivo* mouse models. Here I’ll discuss what was known at the beginning of my thesis work.

Targeting the main oncogenic driver is a common therapeutic approach to treat cancer, including treating CM with inhibitors that specifically target B-RAF. There are two inhibitors, YM-254890 and FR900359, that have been shown to selectively inhibit GαQ/11 (Lapadula & Benovic, 2021). YM-254890 acts by binding to the hydrophobic pocket of GαQ/11 and inhibiting the GDP for GTP exchange, locking GαQ/11 in its GDP bound, inactive state (Lapadula & Benovic, 2021). FR900359 functions in a similar manner but has higher binding affinity and potency than YM-254890 (Schrage et al., 2015; Lapadula & Benovic, 2021). This mechanism of action, maintaining the GDP bound state of GαQ/11, lead to the fear that these inhibitors would not effectively inhibit mutated versions of GαQ/11, given that GαqQ11<sup>Q209</sup> is constitutively bound to GTP. However, multiple studies have shown that treatment of UM cell lines with YM-254890 or FR900359 can affect their cell proliferation, cell cycle phasing, YAP nuclear localization, and MAPK signaling (Onken et al., 2018; Lapadula et al., 2019, Annala et al., 2019). Treatment with FR900359 in an *in vivo* subcutaneous transplant mouse experiment showed significant tumor regression, but once treatment was stopped, the tumors regrew (Onken et al., 2021). This suggests that other strategies are still needed to achieve better and/or more sustainable results.

As previously mentioned, monotherapies that have been proposed for UM patients have mainly focused on MAPK inhibitors. This is due to the findings that oncogenic mutations in GαQ/11, CYSLTR2, and PLCβ4 all contribute to MAPK activity, as well as the effectiveness of these drugs in CM. However, this didn’t translate to effective responses when studied in clinical trials (Carvajal et al., 2018).

After identifying FAK as a critical factor in promoting YAP activity in UM, FAK inhibitors were tested to determine the effects it had on UM cell lines. Either of two FAK inhibitors (FAKi), VS4718 and PF5622771, at the highest dose tested (10μM), decreased the viability of UM cells to



20% and decreased YAP activity (Feng et al., 2019). A follow up study showed that treating flank engrafted UM tumors with FAKi slowed tumor progression but didn't yield complete tumor regression (Paradis et al., 2021). This raised the possibility of the tumor developing resistance mechanisms to FAK inhibition. To get ahead of this possibility, studies have identified other targets that would work synergistically combination with FAKi to improve positive outcomes (Arang et al., 2022).

#### **iv. UM cell lines**

Most of the discoveries and breakthroughs associated with the UM literature has been made using a relatively limited number of human UM cell lines or animal models. While many of the main oncogenes were identified through patient sample sequencing, they were accompanied by the confirmation of the presence of these mutations in available UM cell lines, or by engineering cell line models that expressed the relevant oncogenes. The majority of UM cell lines currently used in the field arose from patient samples, but there is a variation in mutations, derivation, and more.

The first successfully growth of UM cells in culture was in 1929 but these cells only survived for 10 days (Kirby 1929). The first permanently established UM cell lines were derived in 1984 from donated enucleated eyes. The resulting six cell lines are OM421, OM431, OM439, OM443, OM449, and HL165 (Albert et al., 1984). In 1931, Callender, categorized UM cells into 6 morphological groups: spindle A, spindle B, fascicular, mixed, epithelioid, and necrotic (Iwamoto et al., 1972). This classification was used to both confirm and characterized the derived cell lines. As the subcategories of spindle cells (A and B) varying only by size of their nucleoli (Iwamoto et al., 1972), for simplicity, I will classify cells in two broad categories, spindle or epithelioid. Spindle cells are elongated, while epithelioid cells are round or polygonal. Cell lines OM443, OM439 and OM449 were spindle cells, while OM431 was epithelioid, and both OM421

and HL165 had a combination of spindle and epithelioid cells. Unfortunately, none of these six cell lines grow out beyond 100 passages, and thus are no longer available for study.

In 1989, a second group managed to successfully establish 2 UM cell lines from xenografted tumors into the anterior chamber of rabbit eyes (Kan-Mitchel et al., 1989). These two cell lines, OCM1 and OCM2, were from primary choroidal melanomas that were spindle or mixed (spindle and epithelioid) morphologies. However, despite their claim that these are UM cell lines, subsequent genetic analyses showed that neither harbored a *GNAQ* or *GNA11* mutation but instead both had *B-RAF* mutation (Griewanak et al., 2012). This makes it more likely that these were derived from either conjunctival melanoma, which do carry *BRAF* mutations, or CM. The cell lines IPC 211, IPC 227E, IPC 227F, IPC281, were established by Aubert et al 1993 and maintained in culture for multiple years. IPC 211, IPC 227F were spindle morphology, IPC 227E was epithelioid and IPC 281 was mixed morphology. The best known and most frequently used UM cell line, 92.1, was established in 1995 from a primary UM tumor, and it shows a dendritic morphology, which are elongated with multiple outward extending protrusions (De Waard-Siebinga et al., 1995). This cell line is still used today in UM research.

The first metastatic UM cell lines were established in 1996, along with 2 more primary UM cell lines. The primary cells are EOM-3 and EOM-29, and they have epithelioid and spindle morphologies respectively (Luyten et al., 1996). The metastasis derived cell lines OMM1, OMM2 and OMM3 were obtained from three different patients. OMM1, was a subcutaneous metastatic lesion from a UM patient that was confirmed to have originated from the primary UM tumor (Luyten et al., 1996). OMM2 and OMM3 were derived from subcutaneous metastatic lesions, but less is known about the patients (Luyten et al., 1996). Other UM cell lines generated include a panel of cell lines, made from UM tumor donations to the Bascom Palmer Eye Institute, called Mel202, Mel203, Mel270, Mel285, and Mel290 (Ksander et al., 1991; Chen et al., 1997; Jager et al., 2016) Additionally, metastasis-derived UM cell lines OMM1.3 and OMM 1.5 were generated from a liver metastasis of the same patient from which the Mel270 cell lines was generated, and

subsequently their names were changed to OMM2.3 and OMM2.5 (Griewank et al., 2012; Jager et al., 2016). Cell lines TJU-UM001, TJU-UM003, and TJU-UM004 were established by the lab of Takami Sato, from liver metastasis, retroperitoneal metastasis, and orbital metastasis respectively (Yoshida et al., 2013; Cheng et al., 2015).

Notably, none of the established cell lines described above carried the full complement of chromosomal abnormalities characteristic of aggressive UM; in particular, they all lacked chromosome 3 monosomy, even though several of these lines had been generated from metastatic lesions. The established cell lines UPMM1 and UPMM2, both derived from primary UM, were the first cell lines to be confirmed to have monosomy of chromosome 3 (Nareyeck et al., 2006). Later, the cell lines UPMM3, UPMM4 and UPMD1 were established by the same group, with only 2 out of the four having monosomy 3 (Nareyeck et al., 2009). More recently, a panel of UM cell lines were successfully established by transplanting patient-derived UM tumor cells directly into the kidney capsules of mice, serially passaging them in mice, and subsequently generating 2D cultured cell lines (Nemati et al., 2010; Amirouchene-Angelozzi et al., 2014). These cell lines include MP38, MP41, MP46, MP65, MM28, MM33 and MM66, which display varying morphologies. Other studies have moved towards using primary cell lines from UM patient samples (Aughton et al., 2020).

Out of all these cell lines, the most frequently used for published UM studies are: 92.1, Mel202, Mel270, Mel290, Mel285, OMM1, OMM2.3, OMM2.5, UPMM1, UPMM2, UPMM3, UPMM4, UPDM1, and the MP and MM series of cell lines. Sequencing of these cell lines has been conducted to determine the mutational status of UM relevant genes (Griewank et al., 2012; Jager et al 2016; Amirouchene-Angelozzi et al., 2014; Yoshida et al., 2013; Cheng et al., 2015), showing that most carried mutations in either *GNAQ* or *GNAI1*, as expected (see Table 1). Mel290 and Mel285 lacked mutations for either of these genes, or for *B-RAF*, and unfortunately no sequencing was done to identify *PLC $\beta$ 4* or *CYSLTR2* mutations (Griewank et al., 2012;

Amirouchene-Angelozzi et al., 2014). For the work presented in this thesis, we will use two of these established UM cell lines, MP41<sup>GNA11-Q209</sup> and Mel202<sup>GNAQ-Q209</sup>.

Table 1. Status of driver oncogene, Chromosome 3/BAP1 and morphology of key UM cell lines.

<b>CELL LINE</b>	<b>ONCOGENES</b>	<b>CHROMOSOME 3/BAP1</b>	<b>MORPHOLOGY</b>
92.1	<i>GNAQ</i> <sup>Q209L</sup> ; <i>EIF1AX</i> <sup>G6D</sup>	BAP1 protein expressed	Mixed (Epithelial and spindle)
EOM-3	ND	Disomy	Epithelial
EOM-29	ND	Disomy	Spindle
OMM1	<i>GNA11</i> <sup>Q209L</sup>	Partial loss of 3q BAP1 protein expressed	Mixed
OMM2	ND	Disomy	Spindle
OMM3	ND	Disomy	Spindle
OMM2.3	<i>GNAQ</i> <sup>Q209P</sup>	ND	ND
OMM2.5	<i>GNAQ</i> <sup>Q209L</sup>	BAP1 Protein	Mixed
Mel202	<i>GNAQ</i> <sup>Q209L</sup> ; <i>SF3B1</i> <sup>R625G</sup>	BAP1 Protein Expressed	Epithelial
Mel270	<i>GNAQ</i> <sup>Q209P</sup>	BAP1 Protein Expressed Loss of 3q21.2-3q24	Mixed
Mel285	WT( <i>GNAQ</i> , <i>GNA11</i> )	BAP1 Protein Expressed Loss of 3p26-pter	Mixed
Mel290	WT ( <i>GNAQ</i> , <i>GNA11</i> )	BAP1 Protein Expressed Loss of 3p26-pter	Epithelial
TJU-UM001	<i>GNAQ</i> <sup>Q209P</sup>	BAP1 WT	ND
TJU-UM003	<i>GNAQ</i> <sup>Q209L</sup>	BAP1 WT	ND
TJU-UM004	<i>GNAQ</i> <sup>Q209P</sup>	ND	ND
UPMM1	<i>GNAQ</i> <sup>R183Q</sup>	Monosomy 3	ND
UPMM2	<i>GNAQ</i> <sup>Q209L</sup>	Disomy	ND
UPMM3	<i>GNAQ</i> <sup>Q209P</sup>	Monosomy 3	ND
UPMM4	WT( <i>GNAQ</i> , <i>GNA11</i> )	ND	ND
UPMD1	<i>GNA11</i> <sup>Q209L</sup>	ND	ND
MP38	<i>GNAQ</i> <sup>Q209L</sup>	BAP1 deletion; loss of 3q	spindle
MP41	<i>GNA11</i> <sup>Q209L</sup>	Monosomy chromosome 3; BAP1 protein expressed	mixed
MP46	<i>GNAQ</i> <sup>Q209L</sup>	No BAP1 protein expressed	mixed
MP65	<i>GNA11</i> <sup>Q209L</sup>	BAP1 deletion	spindle
MM28	<i>GNA11</i> <sup>Q209L</sup>	BAP1 point mutation; loss of 3q	mixed
MM33	<i>GNAQ</i> <sup>Q209L</sup>	Disomy; BAP1 protein expressed	Spindle
MM66	<i>GNA11</i> <sup>Q209L</sup>	Disomy; BAP1 protein expressed	Mixed

## v. Animal models of UM

Equally important in the field have been the use of animal models to better understand the molecular contributors, drug response, and pathology of UM. These consist of transgenic models harboring the oncogenes found in UM and transplant models, mostly in the context of mouse, zebrafish, or chicken. Rabbits have also been used specifically to grow-out patient-derived UM xenografts, but since I have not been able to find studies that use them for modeling UM progression or pathogenesis, I will not include them in this summary.

Murine mouse models have been used extensively in the field. Genetically engineered mouse models have been developed to express oncogenic *GαQ/11*. Tyr-CreER; *Gnaq*<sup>Q209L</sup> mice were generated, but these didn't develop tumors (Huang et al., 2015; Moore et al., 2018). Interestingly, alongside their analyses of Tyr-CreER; *Gnaq*<sup>Q209L</sup> mice, Moore et al. tested Tyr-CreER; *Gna11*<sup>Q209L</sup> animals and found that this gene developed tumor lesions within 4 weeks at multiple sites across the body (Moore et al., 2018). When the Tyr-CreER; *GNA11*<sup>Q209L</sup> was crossed with a *Bap1*<sup>Lox/Lox</sup> mouse, to generate *Gna11*<sup>Q209L</sup> *Bap1*<sup>KO</sup> mice, these rapidly developed tumors, including in the eye, however, they also developed very aggressive skin melanomas to which they succumbed (Moore et al., 2018). Another group generated a *Gnaq*<sup>Q209L</sup> conditional mouse model, expressing Cre under the control of the master melanocyte transcription factor, *Mitf* (Huang et al., 2015). These mice developed tumors without requiring an added cooperating mutation (Huang et al., 2015). However, the construction of this model results in a significant reduction in the expression level of the endogenous *Mitf* gene (Huang et al., 2015), and work from our lab shows that the absence of *mitf* can cooperate with *GNAQ*<sup>Q209L</sup> to drive UM in zebrafish (Phelps, Hagen et al., 2022). In the mouse models, the UM tumors bear the core hallmarks of human UM, including high levels of nuclear YAP. However, these tumors develop in many sites of the body, beyond the eye, making it hard to distinguish between distant primary tumors or metastasis. To get around this caveat, one group took advantage of the adeno-associated virus delivery system to

deliver Cre into the eye of mice carrying conditional *Lats1<sup>fl/fl</sup>*; *Lats2<sup>fl/fl</sup>* alleles (Li et al., 2019). The presence of Cre inactivates these Hippo pathway regulators, resulting in increased YAP and TAZ activity, which was sufficient to drive tumors in the eye (Li et al., 2019).

Mice are also commonly used for tumor or cell line transplantation, allowing for local delivery at orthotopic sites or additional sites to model progression and/or metastasis. Transplant models of UM cells into different organs, such as the liver, spleen, kidney, have been described previously by various groups (Kageyama et al., 2017, Sugase et al., 2020, Terai et al., 2021,). In this work, we will take advantage of this mouse transplantation to assess tumorigenicity the tumorigenicity of genetically modified human UM cell lines.

Another model used in UM has been chick embryos for transplantation. Human UM cells have been injected into the chorioallantoic membrane or the optic cup (Uner et al., 2022). These cells eventually grow out and form tumors. However, only about half of the injected cohort will develop tumors, so there is a lower success rate for tumor outgrowth compared to mouse transplantation models.

Zebrafish have also served as models of UM. Human UM cell lines have been transplanted into zebrafish to study tumor dissemination and drug response (Van der Ent et al., 2014). The Lees lab has used zebrafish to model and extensively study UM. We developed a transgenic zebrafish model that was conceptually based upon the previously developed zebrafish model of CM, which expresses human *B-RAF<sup>V600E</sup>* under the promoter of the zebrafish *mitf* paralog, *mitfa*. We first expressed human *GNAQ<sup>Q209L</sup>* under the *mitfa* promoter and found that this altered melanocyte biology early in development, increasing the number of melanocytes, but rarely resulted in tumors (Perez et al., 2018). Thus, we crossed the *Tg(mitfa:GNAQ<sup>Q209L</sup>)* transgenic strain with a *tp53* mutant fish and these fish developed tumors with complete penetrance (Perez et al., 2018). We validated that the tumors recapitulated UM biology by dissecting the tumors and performing IHC for YAP and pERK and found expression of both present in tumor (Perez et al., 2018; Phelps, Hagen et al 2022). Zebrafish have also been used to efficiently assess genes of interest for tumor-

forming potential by injecting them into fish embryos using transposon vectors that allow integration into the genome in a mosaic manner without establishing germ-line transgenics (Ceol et al., 2011). We modified this system and used it to evaluate the contributions to UM tumorigenesis of *CYSLTR2<sup>L129Q</sup>*, *PLC $\beta$ <sup>D630Y</sup>*, and an activated form of *YAPI*, *YAP<sup>AA</sup>*, alongside *GNAQ<sup>Q209L</sup>* as a positive control for this vector system (Phelps, Hagen et al., 2022). *GNAQ<sup>Q209L</sup>*, *CYSLTR2<sup>L129Q</sup>* and *YAP<sup>AA</sup>* all drove tumors when injected into *tp53* mutant embryos, with *YAP<sup>AA</sup>* being particularly effective (Phelps, Hagen et al., 2022). In contrast, *PLC $\beta$ <sup>D630Y</sup>* barely yielded any tumors, and these arose with very long latency suggesting that they might be dependent on additional, sporadic events. These findings strongly suggested that YAP signaling, rather than the MAPK pathway, might be the most important pathway downstream of *GNAQ<sup>Q209L</sup>* in driving UM.

The Lees lab also showed that the master melanocyte transcription factor, *MITF*, can function as a tumor suppressor in the context of the *Tg(mitfa:GNAQ<sup>Q209L</sup>)* zebrafish model, and that losing expression of *mitfa* is sufficient to serve as a second hit (instead of *tp53* mutation) and promote tumorigenesis (Phelps, Hagen et al., 2022). *Tg(mitfa:GNAQ<sup>Q209L</sup>); mitfa<sup>-/-</sup>* fish tumors developed more rapidly than *Tg(mitfa:GNAQ<sup>Q209L</sup>); mitfa<sup>wt</sup>*. Seeing that *mitfa* loss led to rapid tumorigenesis, we assessed the oncogenicity of other UM driving oncogenes, *CYSLTR2<sup>L129Q</sup>*, *PLC $\beta$ <sup>D630Y</sup>*, and *YAP<sup>AA</sup>* in a *mitfa<sup>-/-</sup>* background. We found that all these oncogenes drove tumors in a *tp53<sup>-/-</sup>; mitfa<sup>-/-</sup>* background, and the kinetics of tumor development was typically more rapid than in the *tp53<sup>-/-</sup>; mitfa<sup>+/+</sup>* context. Still, *YAP<sup>AA</sup>* was the most potent driver of all. Further, in the context of *mitfa* loss, now *PLC $\beta$ <sup>D630Y</sup>* drove tumors with reasonable frequency. However, when we performed IHC on these *PLC $\beta$ <sup>D630Y</sup>*-driven tumors we saw a lack of pERK signal, and instead detected YAP nuclear localization (Phelps, Hagen et al., 2022). These results further de-emphasized the role of pERK, and highlighted the importance of YAP, in zebrafish UM tumors.

Moreover, taking advantage of the observed embryonic melanocyte phenotype of *GNAQ<sup>Q209L</sup>* fish, the Lees lab also developed an assay to measure drug response. In this assay, we add drug into the water containing either *Tg(mitfa:GNAQ<sup>Q209L</sup>)* or non-transgenic embryos for

several days and then use flow cytometry to quantify the melanocyte population representation (Phelps, Amsterdam et al., 2022). The zebrafish we used for this assay have been crossed with *Tg(mitfa:eGFP)* zebrafish, and thus allows for the use of GFP+ cells in the population to function as a proxy for melanocyte cells. Drugs that affect important contributors to GNAQ driven biology will have a greater effect on the GFP+ population. As previously mentioned, *GNAQ<sup>Q209L</sup>* increases the number of melanocyte cells present in the population (Perez et al., 2018), thus, the *Tg(mitfa:GNAQ<sup>Q209L</sup>)* cohort will have a higher percent of GFP+ cells in the population. To this end, we tested numerous drugs that targeted either the MAPK or YAP pathway and determined which had a greater effect on GNAQ biology. Treatment with the MAPK inhibitor trametinib did not reduce the GFP+ cell population (Phelps, Amsterdam et al., 2022). Similarly, treatment of *Tg(mitfa:GNAQ<sup>Q209L</sup>)* embryos with a PI3K inhibitor, Ly294002, didn't reduce the GFP+ cell population compared to DMSO (Phelps, Amsterdam et al., 2022). On the other hand, treatment with either a YAP inhibitor, verteporfin, or with a FAK inhibitor, PND-1186, significantly reduced the GFP+ cell population in the *Tg(mitfa:GNAQ<sup>Q209L</sup>)* embryos more than *Tg(mitfa:GNAQ<sup>Q209L</sup>)* embryos treated with DMSO, this decrease was not observed in non-transgenic embryos treated with either drug (Phelps, Amsterdam et al., 2022). These results, taken together with the results from the *mitfa<sup>-/-</sup>* fish and the oncogene contributions to tumorigenesis, strongly suggest YAP as a strong proponent of *GNAQ<sup>Q209L</sup>* tumorigenesis.

#### **IV. Questions addressed in this thesis**

Observations from us, and others, have raised several key questions, which I address in this thesis. First, is YAP necessary for UM development in zebrafish? If not, which additional factors or pathways might contribute? Second, to what degree are our observations in fish relevant to human UM? To address whether YAP is necessary for UM tumorigenesis, we generated a *Tg(mitfa:GNAQ<sup>Q209L</sup>);yap<sup>-/-</sup>* zebrafish model and tracked survival and tumorigenesis overtime. In contrast to what we hypothesized, *yap* loss didn't affect *Tg(mitfa:GNAQ<sup>Q209L</sup>)*-driven



tumorigenesis, with both cohorts exhibiting similar kinetics of tumor burden. Notably, there is a paralog of *yap* named *taz* (officially named *wltr1*). TAZ was shown to interact with TEF-1 family members (now called the TEAD family) (Mahoney et al., 2005). Using the rationale that YAP and TAZ are paralogs, they showed that TAZ could interact with TEAD both in vitro and in vivo (Mahoney et al., 2005). Like YAP, TAZ has also been shown to be negatively regulated by sequestration through 14-3-3 protein interaction (Kanai et al., 2000), contains a PDZ domain (Kanai et al., 2000), and is negatively regulated by LATS1/2 phosphorylation (Lei et al., 2008). Additionally, it has been shown that YAP and TAZ regulate many of the same targets mediated by their TEAD interaction (Piccolo et al., 2014). Given these observations, we asked whether there could be compensation from TAZ in the *yap*<sup>-/-</sup> fish tumors. We were able to find nuclear Taz signal in the *yap*<sup>-/-</sup> tumors, suggesting that Taz could be compensating for Yap as the effector of *GNAQ*. Further, we tested if TAZ could drive tumor formation in a similar manner as YAP. After adding an activated form of TAZ, TAZ<sup>AA</sup>, to fish embryos, we saw that TAZ was sufficient to drive rapid tumorigenesis and was even more aggressive than YAP. To further explore the roles of *YAP* and *TAZ* in UM, we knocked-out expression of either paralog in the context of both zebrafish UM tumors, as well as human UM cell lines. We saw little hinderance to viability or cell proliferation *in vitro* as a consequence of *YAP* or *TAZ* deletion. Additionally, we observed formation of tumors *in vivo* from both *YAP* or *TAZ* knockouts, with variable MAPK pathway expression and no upregulation of this pathway, suggesting that MAPK is likely not a main driver of tumorigenesis *in vivo*. These data all point to a high level of adaptability or plasticity of UM both in vitro and in vivo to maintain tumor potential and highlight the difficulty of targeting this tumor effectively in the clinic.

## References

- Aalto, Y., Eriksson, L., Seregard, S., Larsson, O., & Knuutila, S. (2001). Concomitant loss of chromosome 3 and whole arm losses and gains of chromosome 1, 6, or 8 in metastasizing primary uveal melanoma. *PubMed*, *42*(2), 313–317. <https://pubmed.ncbi.nlm.nih.gov/11157859>
- Adler, N. R., Wolfe, R., Kelly, J. W., Haydon, A., McArthur, G. A., McLean, C., & Mar, V. (2017). Tumour mutation status and sites of metastasis in patients with cutaneous melanoma. *British Journal of Cancer*, *117*(7), 1026–1035. <https://doi.org/10.1038/bjc.2017.254>
- Akbani, R., Akdemir, K. C., Aksoy, B. A., Albert, M., Ally, A., Amin, S. B., Arachchi, H., Arora, A., Auman, J. T., Ayala, B., Baboud, J., Balasundaram, M., Balu, S., Barnabas, N., Bartlett, J. M., Bartlett, P., Bastian, B. C., Baylin, S. B., Behera, M., . . . Zou, L. (2015). Genomic classification of cutaneous melanoma. *Cell*, *161*(7), 1681–1696. <https://doi.org/10.1016/j.cell.2015.05.044>
- Ambrosini, G., Pratilas, C.A., Qin, L.X., Tadi, M., Surriga, O., Carvajal, R.D., & Schwartz, G.K. (2012). Identification of unique MEK-dependent genes in GNAQ mutant uveal melanoma involved in cell growth, tumor cell invasion, and MEK resistance. *Clinical Cancer Research*, *18*(13), 3552-3561. <https://doi.org/10.1158/1078-0432.CCR-11-3086>
- Andersen, L. B., Fountain, J. W., Gutmann, D. H., Tarlé, S. A., Glover, T. W., Dracopoli, N. C., Housman, D. E., & Collins, F. S. (1993). Mutations in the neurofibromatosis 1 gene in sporadic malignant melanoma cell lines. *Nature Genetics*, *3*(2), 118–121. <https://doi.org/10.1038/ng0293-118>
- Annala, S., Feng, X., Shridhar, N., Eryilmaz, F., Patt, J., Yang, J. H., Pfeil, E. M., Cervantes-Villagrana, R. D., Inoue, A., Häberlein, F., Slodczyk, T., Reher, R., Kehraus, S., Monteleone, S., Schrage, R., Heycke, N., Rick, U., Engel, S., Pfeifer, A., . . . Kostenis, E.

- (2019). Direct targeting of Gα q and Gα 11 oncoproteins in cancer cells. *Science Signaling*, 12(573). <https://doi.org/10.1126/scisignal.aau5948>
- Arang, N., Lubrano, S., Rigiracciolo, D. C., Nachmanson, D., Lippman, S. M., Mali, P., Harismendy, O., & Gutkind, J. S. (2023). Whole-genome CRISPR screening identifies PI3K/AKT as a downstream component of the oncogenic GNAQ–focal adhesion kinase signaling circuitry. *Journal of Biological Chemistry*, 299(2), 102866. <https://doi.org/10.1016/j.jbc.2022.102866>
- Aronow, M. E., Topham, A., & Singh, A. D. (2017). Uveal Melanoma: 5-Year Update on Incidence, Treatment, and Survival (SEER 1973-2013). *Ocular Oncology and Pathology*, 4(3), 145–151. <https://doi.org/10.1159/000480640>
- Ascierto, P. A., Kirkwood, J. M., Grob, J., Simeone, E., Grimaldi, A., Maio, M., Palmieri, G., Testori, A., Marincola, F. M., & Mozzillo, N. (2012). The role of BRAF V600 mutation in melanoma. *Journal of Translational Medicine*, 10(1). <https://doi.org/10.1186/1479-5876-10-85>
- Aubert, C., Rougé, F., Reillaudou, M., & Metge, P. (1993). Establishment and characterization of human ocular melanoma cell lines. *International Journal of Cancer*, 54(5), 784–792. <https://doi.org/10.1002/ijc.2910540513>
- Aughton, K., Shahidipour, H., Djirackor, L., Coupland, S. E., & Kalirai, H. (2020). Characterization of Uveal melanoma cell lines and primary tumor samples in 3D culture. *Translational Vision Science & Technology*, 9(7), 39. <https://doi.org/10.1167/tvst.9.7.39>
- Barbagallo, C., Stella, M., Broggi, G., Russo, A., Caltabiano, R., & Ragusa, M. (2023). Genetics and RNA regulation of Uveal melanoma. *Cancers*, 15(3), 775. <https://doi.org/10.3390/cancers15030775>
- Bauer, J., Büttner, P., Murali, R., Okamoto, I., Kolaitis, N. A., Landi, M. T., Scolyer, R. A., & Bastian, B. C. (2011). BRAF mutations in cutaneous melanoma are independently associated with age, anatomic site of the primary tumor, and the degree of solar elastosis

- at the primary tumor site. *Pigment Cell & Melanoma Research*, 24(2), 345–351. <https://doi.org/10.1111/j.1755-148x.2011.00837.x>
- Bos, J. (1989). ras oncogenes in human cancer: a review. *PubMed*, 49(17), 4682–4689. <https://pubmed.ncbi.nlm.nih.gov/2547513>
- Boulton, T. G., Nye, S. H., Robbins, D. J., Ip, N. Y., Radzilewska, E., Morgenbesser, S. D., DePinho, R. A., Panayotatos, N., Cobb, M. H., & Yancopoulos, G. D. (1991). ERKs: A family of protein-serine/threonine kinases that are activated and tyrosine phosphorylated in response to insulin and NGF. *Cell*, 65(4), 663–675. [https://doi.org/10.1016/0092-8674\(91\)90098-j](https://doi.org/10.1016/0092-8674(91)90098-j)
- Bradley, S. D., Chen, Z., Melendez, B., Talukder, A. H., Khalili, J. S., Rodriguez-Cruz, T., Liu, S., Whittington, M., Deng, W., Li, F., Bernatchez, C., Radvanyi, L. G., Davies, M. A., Hwu, P., & Lizee, G. (2015). BRAFV600E co-opts a conserved MHC Class I internalization pathway to diminish antigen presentation and CD8+ T-cell recognition of melanoma. *Cancer Immunology Research*, 3(6), 602–609. <https://doi.org/10.1158/2326-6066.cir-15-0030>
- Brănișteanu, D., Bogdănici, C. M., Brănișteanu, D., Mărănducă, M. A., Zemba, M., Baltă, F., Branisteanu, C. I., & Moraru, A. (2021). Uveal melanoma diagnosis and current treatment options (Review). *Experimental and Therapeutic Medicine*, 22(6). <https://doi.org/10.3892/etm.2021.10863>
- Burd, C. E., Liu, W., Huynh, M. V., Waqas, M. A., Gillahan, J. E., Clark, K. S., Fu, K., Martin, B. L., Jeck, W. R., Souroullas, G. P., Darr, D. B., Zedek, D. C., Miley, M. J., Baguley, B. C., Campbell, S. L., & Sharpless, N. E. (2014). Mutation-Specific RAS oncogenicity explains NRAS Codon 61 selection in melanoma. *Cancer Discovery*, 4(12), 1418–1429. <https://doi.org/10.1158/2159-8290.cd-14-0729>
- Callender, G. R. (1931). Malignant melanotic tumors of the eye. A study of histologic types in 111 cases. *Transactions of the American Ophthalmological Society*.

- Carvajal, R. D., Piperno-Neumann, S., Kapiteijn, E., Chapman, P. B., Frank, S. J., Joshua, A. M., Piulats, J. M., Wolter, P., Cocquyt, V., Chmielowski, B., Evans, T. J., Gastaud, L., Linette, G. P., Berking, C., Schachter, J., Rodrigues, M., Shoushtari, A. N., Clemett, D., Ghiorghiu, D., . . . Nathan, P. (2018). Selumetinib in combination with dacarbazine in patients with metastatic uveal melanoma: a phase III, multicenter, randomized trial (SUMIT). *Journal of Clinical Oncology*, *36*(12), 1232–1239. <https://doi.org/10.1200/jco.2017.74.1090>
- Carvajal, R. D., Sosman, J. A., Quevedo, J. F., Milhem, M., Joshua, A. M., Kudchadkar, R. R., Linette, G. P., Gajewski, T. F., Lutzky, J., Lawson, D. H., Lao, C. D., Flynn, P. J., Albertini, M. R., Sato, T., Lewis, K. D., Doyle, A., Ancell, K. K., Panageas, K. S., Bluth, M. J., . . . Schwartz, G. K. (2014). Effect of Selumetinib vs Chemotherapy on Progression-Free Survival in Uveal Melanoma. *JAMA*, *311*(23), 2397. <https://doi.org/10.1001/jama.2014.6096>
- Caunt, C. J., Sale, M. J., Smith, P. D., & Cook, S. J. (2015). MEK1 and MEK2 inhibitors and cancer therapy: the long and winding road. *Nature Reviews Cancer*, *15*(10), 577–592. <https://doi.org/10.1038/nrc4000>
- Ceol, C. J., Houvras, Y., Jané-Valbuena, J., Bilodeau, S., Orlando, D. A., Battisti, V., Fritsch, L., Lin, W. M., Hollmann, T. J., Ferrè, F., Bourque, C., Burke, C. J., Turner, L., Uong, A., Johnson, L. A., Beroukhim, R., Mermel, C. H., Loda, M., Ait-Si-Ali, S., . . . Zon, L. I. (2011). The histone methyltransferase SETDB1 is recurrently amplified in melanoma and accelerates its onset. *Nature*, *471*(7339), 513–517. <https://doi.org/10.1038/nature09806>
- Chapman, P. B., Hauschild, A., Robert, C., Haanen, J. B., Ascierto, P. A., Larkin, J., Dummer, R., Garbe, C., Testori, A., Maio, M., Hogg, D., Lorigan, P., Lebbe, C., Jouary, T., Schadendorf, D., Ribas, A., O'Day, S., Sosman, J. A., Kirkwood, J. M., . . . McArthur, G. A. (2011). Improved Survival with Vemurafenib in Melanoma with BRAF V600E Mutation. *The New England Journal of Medicine*, *364*(26), 2507–2516. <https://doi.org/10.1056/nejmoa1103782>

- Chapman, P. B., Robert, C., Larkin, J., Haanen, J. B., Ribas, A., Hogg, D., Hamid, O., Ascierto, P. A., Testori, A., Lorigan, P., Dummer, R., Sosman, J. A., Flaherty, K. T., Chang, I., Coleman, S., Caro, I., Hauschild, A., & McArthur, G. A. (2017). Vemurafenib in patients with BRAFV600 mutation-positive metastatic melanoma: final overall survival results of the randomized BRIM-3 study. *Annals of Oncology*, 28(10), 2581–2587. <https://doi.org/10.1093/annonc/mdx339>
- Chen, P. W., Murray, T. G., Uno, T., Salgaller, M. L., Reddy, R., & Ksander, B. R. (1997). Expression of MAGE genes in ocular melanoma during progression from primary to metastatic disease. *Clinical & Experimental Metastasis*, 15(5), 509–518. <https://doi.org/10.1023/a:1018479011340>
- Chen, X., Wu, Q., Depeille, P., Chen, P., Thornton, S., Kalirai, H., Coupland, S. E., Roose, J. P., & Bastian, B. C. (2017). RASGRP3 mediates MAPK pathway activation in GNAQ mutant uveal melanoma. *Cancer Cell*, 31(5), 685-696.e6. <https://doi.org/10.1016/j.ccell.2017.04.002>
- Chen, X., Wu, Q., Tan, L., Porter, D., Jager, M. J., Emery, C. M., & Bastian, B. C. (2013). Combined PKC and MEK inhibition in uveal melanoma with GNAQ and GNA11 mutations. *Oncogene*, 33(39), 4724–4734. <https://doi.org/10.1038/onc.2013.418>
- Cheng, H., Terai, M., Kageyama, K., Ozaki, S., McCue, P. A., Sato, T., & Aplin, A. E. (2015). Paracrine effect of NRG1 and HGF drives resistance to MEK inhibitors in metastatic uveal melanoma. *Cancer Research*, 75(13), 2737–2748. <https://doi.org/10.1158/0008-5472.can-15-0370>
- Curtin, J. A., Fridlyand, J., Kageshita, T., Patel, H., Busam, K. J., Kutzner, H., Cho, K. H., Aiba, S., Bröcker, E. B., LeBoit, P. E., Pinkel, D., & Bastian, B. C. (2005). Distinct sets of genetic alterations in melanoma. *The New England Journal of Medicine*, 353(20), 2135–2147. <https://doi.org/10.1056/nejmoa050092>
- Dai, X., She, P., Chi, F., Chen, Z., Liu, H., Jin, D., Zhao, Y., Guo, X., Jiang, D., Guan, K. L., Zhong, T., & Zhao, B. (2013). Phosphorylation of angiominin by IGF1R inhibits

- F-actin binding, cell migration, and angiogenesis. *Journal of Biological Chemistry*, 288(47), 34041–34051. <https://doi.org/10.1074/jbc.m113.518019>
- Davies, H., Bignell, G. R., Cox, C. E., Stephens, P. J., Edkins, S., Clegg, S., Teague, J. W., Woffendin, H., Garnett, M. J., Bottomley, W., Davis, N. M., Dicks, E., Ewing, R., Floyd, Y., Gray, K., Hall, S., Hawes, R., Hughes, J., Kosmidou, V., . . . Futreal, P. A. (2002). Mutations of the BRAF gene in human cancer. *Nature*, 417(6892), 949–954. <https://doi.org/10.1038/nature00766>
- De Waard-Siebinga, I., Blom, D., Griffioen, M., Schrier, P. I., Hoogendoorn, E., Beverstock, G. C., Danen, E. H., & Jager, M. J. (1995). Establishment and characterization of an uveal-melanoma cell line. *International Journal of Cancer*, 62(2), 155–161. <https://doi.org/10.1002/ijc.2910620208>
- Feng, X., Arang, N., Rigracciolo, D. C., Lee, J. S., Yeerna, H., Wang, Z., Lubrano, S., Kishore, A., Pachter, J. A., König, G. M., Maggiolini, M., Kostenis, E., Schlaepfer, D. D., Tamayo, P., Chen, Q., Ruppin, E., & Gutkind, J. S. (2019). A Platform of Synthetic Lethal Gene Interaction Networks Reveals that the GNAQ Uveal Melanoma Oncogene Controls the Hippo Pathway through FAK. *Cancer Cell*, 35(3), 457-472.e5. <https://doi.org/10.1016/j.ccell.2019.01.009>
- Feng, X., Degese, M. S., Iglesias-Bartolome, R., Vaque, J. P., Molinolo, A. A., Rodrigues, M., Zaidi, M. R., Ksander, B. R., Merlino, G., Sodhi, A., Chen, Q., & Gutkind, J. S. (2014). Hippo-Independent Activation of YAP by the GNAQ Uveal Melanoma Oncogene through a Trio-Regulated Rho GTPase Signaling Circuitry. *Cancer Cell*, 25(6), 831–845. <https://doi.org/10.1016/j.ccr.2014.04.016>
- Freeman, A. K., & Morrison, D. K. (2011). 14-3-3 Proteins: Diverse functions in cell proliferation and cancer progression. *Seminars in Cell & Developmental Biology*, 22(7), 681–687. <https://doi.org/10.1016/j.semcd.2011.08.009>
- Giunta, E. F., De Falco, V., Napolitano, S., Argenziano, G., Brancaccio, G., Moscarella, E., Ciardiello, D., Ciardiello, F., & Troiani, T. (2020). Optimal treatment strategy for

- metastatic melanoma patients harboring BRAF-V600 mutations. *Therapeutic Advances in Medical Oncology*, 12, 175883592092521. <https://doi.org/10.1177/1758835920925219>
- Goldsmith, Z. G., & Dhanasekaran, D. N. (2007). G Protein regulation of MAPK networks. *Oncogene*, 26(22), 3122–3142. <https://doi.org/10.1038/sj.onc.1210407>
- Gordon, D., Resio, B. J., & Pellman, D. (2012). Causes and consequences of aneuploidy in cancer. *Nature Reviews Genetics*, 13(3), 189–203. <https://doi.org/10.1038/nrg3123>
- Griewank, K. G., Yu, X., Khalili, J. S., Sozen, M., Stempke-Hale, K., Bernatchez, C., Wardell, S., Bastian, B. C., & Woodman, S. E. (2012). Genetic and molecular characterization of uveal melanoma cell lines. *Pigment Cell & Melanoma Research*, 25(2), 182–187. <https://doi.org/10.1111/j.1755-148x.2012.00971.x>
- Guo, Y., Pan, W., Liu, S., Shen, Z., Xu, Y., & Hu, L. (2020). ERK/MAPK signalling pathway and tumorigenesis (Review). *Experimental and Therapeutic Medicine*. <https://doi.org/10.3892/etm.2020.8454>
- Harbour, J. W. (2012). The genetics of uveal melanoma: an emerging framework for targeted therapy. *Pigment Cell & Melanoma Research*, 25(2), 171–181. <https://doi.org/10.1111/j.1755-148x.2012.00979.x>
- Harbour, J. W., Onken, M. D., Roberson, E. D., Duan, S., Cao, L., Worley, L. A., Matatall, K. A., Helms, C., & Bowcock, A. M. (2010). Frequent Mutation of BAP1 in Metastasizing Uveal Melanomas. *Science*, 330(6009), 1410–1413. <https://doi.org/10.1126/science.1194472>
- Horsman, D. E., & White, V. A. (1993). Cytogenetic analysis of uveal melanoma consistent occurrence of monosomy 3 and trisomy 8q. *Cancer*, 71(3), 811–819. [https://doi.org/10.1002/1097-0142\(19930201\)71:3](https://doi.org/10.1002/1097-0142(19930201)71:3)
- Huang, J. L., Urtatiz, O., & Van Raamsdonk, C. D. (2015). Oncogenic G protein GNAQ induces uveal melanoma and intravasation in mice. *Cancer Research*, 75(16), 3384–3397. <https://doi.org/10.1158/0008-5472.can-14-3229>



- Huang, J., Wu, S., Barrera, J., Matthews, K. A., & Pan, D. (2005). The hippo signaling pathway coordinately regulates cell proliferation and apoptosis by inactivating Yorkie, the drosophila homolog of YAP. *Cell*, *122*(3), 421–434. <https://doi.org/10.1016/j.cell.2005.06.007>
- Hurks, H. M. H., Valter, M. M., Wilson, L., Hilgert, I., Van Den Elsen, P. J., & Jager, M. J. (2001). Uveal melanoma: no expression of HLA-G. *PubMed*, *42*(13), 3081–3084. <https://pubmed.ncbi.nlm.nih.gov/11726606>
- Istrate, M., Vlaicu, B., Poenaru, M., Hasbei-Popa, M., Salavat, M. C., & Iliescu, D. A. (2020). Photoprotection role of melanin in the human retinal pigment epithelium. Imaging techniques for retinal melanin. *Romanian Journal of Ophtalmology*, *64*(2), 100–104. <https://doi.org/10.22336/rjo.2020.20>
- Iwamoto, T. (1972, November 1). *Ultrastructural comparison of Spindle A, Spindle B, and Epithelioid-Type cells in Uveal malignant melanoma*. <https://iovs.arvojournals.org/article.aspx?articleid=2122248>
- Jager, M. J., Magner, J., Ksander, B. R., & Dubovy, S. R. (2016). Uveal Melanoma Cell Lines: Where do they come from? (An American Ophthalmological Society Thesis). *PubMed*, *114*, T5. <https://pubmed.ncbi.nlm.nih.gov/28018010>
- Jager, M. J., Shields, C. L., Cebulla, C. M., Abdel-Rahman, M. H., Grossniklaus, H. E., Stern, M., Carvajal, R. D., Belfort, R., Jia, R., Shields, J. A., & Damato, B. (2020). Uveal melanoma. *Nature Reviews Disease Primers*, *6*(1). <https://doi.org/10.1038/s41572-020-0158-0>
- Jang, J., Kim, M., & Bae, S. (2018). Reciprocal regulation of YAP/TAZ by the Hippo pathway and the Small GTPase pathway. *Small GTPases*, *11*(4), 280–288. <https://doi.org/10.1080/21541248.2018.1435986>
- Johansson, P., Aoude, L. G., Wadt, K., Glasson, W., Warriar, S., Hewitt, A. W., Kiilgaard, J. F., Heegaard, S., Isaacs, T., Franchina, M., Ingvar, C., Vermeulen, T., Whitehead, K. J., Schmidt, C., Palmer, J. M., Symmons, J., Gerdes, A., Jönsson, G., & Hayward, N. K.

- (2015). Deep sequencing of uveal melanoma identifies a recurrent mutation in PLCB4. *Oncotarget*, 7(4), 4624–4631. <https://doi.org/10.18632/oncotarget.6614>
- Johnson, D. B., & Dahlman, K. B. (2018). Class Matters: Sensitivity of BRAF-Mutant melanoma to MAPK inhibition. *Clinical Cancer Research*, 24(24), 6107–6109. <https://doi.org/10.1158/1078-0432.ccr-18-1795>
- Kadamur, G., & Ross, E. M. (2013). Mammalian phospholipase C. *Annual Review of Physiology*, 75(1), 127–154. <https://doi.org/10.1146/annurev-physiol-030212-183750>
- Kageyama, K., Ohara, M., Saito, K., Ozaki, S., Terai, M., Mastrangelo, M. J., Fortina, P., Aplin, A. E., & Sato, T. (2017). Establishment of an orthotopic patient-derived xenograft mouse model using uveal melanoma hepatic metastasis. *Journal of Translational Medicine*, 15(1). <https://doi.org/10.1186/s12967-017-1247-z>
- Kahlon, N., Doddi, S., Yousif, R., Najib, S., Sheikh, T., Abuhelwa, Z., Burmeister, C., & Hamouda, D. (2022). Melanoma Treatments and mortality rate Trends in the US, 1975 to 2019. *JAMA Network Open*, 5(12), e2245269. <https://doi.org/10.1001/jamanetworkopen.2022.45269>
- Kaliki, S., Shields, C., (2017) Uveal melanoma: relatively rare but deadly cancer. *Eye*, 31(2), 241-257. <https://doi.org/10.1038/eye.2016.275>
- Kanai, F., Marignani, P. A., Sarbassova, D., Yagi, R., Hall, R. A., Donowitz, M., Hisaminato, A., Fujiwara, T., Ito, Y., Cantley, L. C., & Yaffe, M. B. (2000). TAZ: a novel transcriptional co-activator regulated by interactions with 14-3-3 and PDZ domain proteins. *The EMBO Journal*, 19(24), 6778–6791. <https://doi.org/10.1093/emboj/19.24.6778>
- Kan-Mitchell, J., Mitchell, M. S., Rao, N., & Liggett, P. E. (1989). Characterization of uveal melanoma cell lines that grow as xenografts in rabbit eyes. *PubMed*, 30(5), 829–834. <https://pubmed.ncbi.nlm.nih.gov/2722439>
- Kaplan, F. M., Shao, Y., Mayberry, M. M., & Aplin, A. E. (2010). Hyperactivation of MEK–ERK1/2 signaling and resistance to apoptosis induced by the oncogenic B-RAF inhibitor,

- PLX4720, in mutant N-RAS melanoma cells. *Oncogene*, 30(3), 366–371. <https://doi.org/10.1038/onc.2010.408>
- Khokhlatchev, A., Canagarajah, B., Wilsbacher, J. L., Robinson, M. J., Atkinson, M. A., Goldsmith, E. J., & Cobb, M. H. (1998). Phosphorylation of the MAP kinase ERK2 promotes its homodimerization and nuclear translocation. *Cell*, 93(4), 605–615. [https://doi.org/10.1016/s0092-8674\(00\)81189-7](https://doi.org/10.1016/s0092-8674(00)81189-7)
- Kirby, D. B. (1929). Tissue culture in ophthalmic research; ocular tumors. *Transactions of the American Ophthalmological Society*, 27, 334–383.
- Kiuru, M., & Busam, K. J. (2017). The NF1 gene in tumor syndromes and melanoma. *Laboratory Investigation*, 97(2), 146–157. <https://doi.org/10.1038/labinvest.2016.142>
- Komuro, A., Nagai, M., Navin, N., & Sudol, M. (2003). WW Domain-containing Protein YAP Associates with ErbB-4 and Acts as a Co-transcriptional Activator for the Carboxyl-terminal Fragment of ErbB-4 That Translocates to the Nucleus. *Journal of Biological Chemistry*, 278(35), 33334–33341. <https://doi.org/10.1074/jbc.m305597200>
- Ksander, B. R., Rubsamen, P. E., Olsen, K. R., Cousins, S. W., & Streilein, J. W. (1991). Studies of tumor-infiltrating lymphocytes from a human choroidal melanoma. *PubMed*, 32(13), 3198–3208. <https://pubmed.ncbi.nlm.nih.gov/1748551>
- Lapadula, D., & Benovic, J. L. (2021). Targeting oncogenic GAQ/11 in uveal melanoma. *Cancers*, 13(24), 6195. <https://doi.org/10.3390/cancers13246195>
- Lapadula, D., Farías, E. F., Randolph, C., Purwin, T. J., McGrath, D., Charpentier, T. H., Zhang, L., Wu, S., Terai, M., Sato, T., Tall, G. G., Zhou, N., Wedegaertner, P., Aplin, A. E., Aguirre-Ghiso, J. A., & Benovic, J. L. (2019). Effects of oncogenic GAQ and GA11 inhibition by FR900359 in Uveal melanoma. *Molecular Cancer Research*, 17(4), 963–973. <https://doi.org/10.1158/1541-7786.mcr-18-0574>
- Larribère, L., & Utikal, J. (2020). Update on GNA Alterations in Cancer: Implications for Uveal melanoma treatment. *Cancers*, 12(6), 1524. <https://doi.org/10.3390/cancers12061524>

- Lee, C., Lee, K., Lee, S. B., Park, D., & Rhee, S. G. (1994). Regulation of phospholipase C-beta 4 by ribonucleotides and the alpha subunit of Gq. *Journal of Biological Chemistry*, 269(41), 25335–25338. [https://doi.org/10.1016/s0021-9258\(18\)47252-3](https://doi.org/10.1016/s0021-9258(18)47252-3)
- Lei, Q., Zhang, H., Zhao, B., Zha, Z., Bai, F., Pei, X., Zhao, S., Xiong, Y., & Guan, K. L. (2008). TAZ promotes cell proliferation and Epithelial-Mesenchymal transition and is inhibited by the hippo pathway. *Molecular and Cellular Biology*, 28(7), 2426–2436. <https://doi.org/10.1128/mcb.01874-07>
- Li, H., Li, Q., Dang, K., Ma, S., Cotton, J. L., Sun, Y., Zhu, L. J., Deng, A., Ip, Y. T., Johnson, R. L., Wu, X., Punzo, C., & Mao, J. (2019). YAP/TAZ Activation drives uveal melanoma initiation and progression. *Cell Reports*, 29(10), 3200-3211.e4. <https://doi.org/10.1016/j.celrep.2019.03.021>
- Li, L., Sabnis, A. J., Chan, E., Olivas, V., Cade, L., Pazarentzos, E., Asthana, S., Neel, D. S., Yan, J., Lu, X., Pham, L., Wang, M. M., Karachaliou, N., Cao, M. G., Manzano, J. L., Ramirez, J. L., Torres, J., Buttitta, F., Rudin, C. M., . . . Bivona, T. G. (2015). The Hippo effector YAP promotes resistance to RAF- and MEK-targeted cancer therapies. *Nature Genetics*, 47(3), 250–256. <https://doi.org/10.1038/ng.3218>
- Long, G. V., Fung, C., Menzies, A. M., Pupo, G. M., Carlino, M. S., Hyman, J., Shahheydari, H., Tembe, V., Thompson, J. F., Saw, R. P., Howle, J. R., Hayward, N. K., Johansson, P., Scolyer, R. A., Kefford, R., & Rizos, H. (2014). Increased MAPK reactivation in early resistance to dabrafenib/trametinib combination therapy of BRAF-mutant metastatic melanoma. *Nature Communications*, 5(1). <https://doi.org/10.1038/ncomms6694>
- Luyten, G. P. M., Naus, N., Mooy, C. M., Hagemeyer, A., Kan-Mitchell, J., Van Drunen, E., Vuzevski, V., De Jong, P. T. V. M., & Luiders, T. M. (1996). Establishment and characterization of primary and metastatic uveal melanoma cell lines. *International Journal of Cancer*, 66(3), 380–387. [https://doi.org/10.1002/\(sici\)1097-0215\(19960503\)66:3](https://doi.org/10.1002/(sici)1097-0215(19960503)66:3)

- Mahoney, W. M., Hong, J. H., Yaffe, M. B., & Farrance, I. K. (2005). The transcriptional co-activator TAZ interacts differentially with transcriptional enhancer factor-1 (TEF-1) family members. *Biochemical Journal*, *388*(1), 217–225. <https://doi.org/10.1042/bj20041434>
- Maldonado, J. L., Fridlyand, J., Patel, H., Jain, A. N., Busam, K. J., Kageshita, T., Ono, T., Albertson, D. G., Pinkel, D., & Bastian, B. C. (2003). Determinants of BRAF mutations in primary melanomas. *JNCI: Journal of the National Cancer Institute*, *95*(24), 1878–1890. <https://doi.org/10.1093/jnci/djg123>
- Mana-Capelli, S., Paramasivam, M., Dutta, S., & McCollum, D. (2014). Angiomotins link F-actin architecture to Hippo pathway signaling. *Molecular Biology of the Cell*, *25*(10), 1676–1685. <https://doi.org/10.1091/mbc.e13-11-0701>
- Mandalà, M., De Logu, F., Merelli, B., Nassini, R., & Massi, D. (2017). Immunomodulating property of MAPK inhibitors: from translational knowledge to clinical implementation. *Laboratory Investigation*, *97*(2), 166–175. <https://doi.org/10.1038/labinvest.2016.132>
- Martin, M., Maßhöfer, L., Temming, P., Rahmann, S., Metz, C. H., Bornfeld, N., Van De Nes, J. A., Klein-Hitpaß, L., Hinnebusch, A. G., Horsthemke, B., Lohmann, D., & Zeschnigk, M. (2013). Exome sequencing identifies recurrent somatic mutations in EIF1AX and SF3B1 in uveal melanoma with disomy 3. *Nature Genetics*, *45*(8), 933–936. <https://doi.org/10.1038/ng.2674>
- McCubrey, J. A., Steelman, L. S., Chappell, W. H., Abrams, S. L., Wong, E. W., Chang, F., Lehmann, B. D., Terrian, D. M., Milella, M., Tafuri, A., Stivala, F., Libra, M., Bäsecke, J., Evangelisti, C., Martelli, A. M., & Franklin, R. A. (2007). Roles of the Raf/MEK/ERK pathway in cell growth, malignant transformation and drug resistance. *Biochimica Et Biophysica Acta (BBA) - Molecular Cell Research*, *1773*(8), 1263–1284. <https://doi.org/10.1016/j.bbamcr.2006.10.001>

*Melanoma of the skin - Cancer Stat Facts.* (n.d.).

SEER. <https://seer.cancer.gov/statfacts/html/melan.html>

*Melanoma treatment.* (2023, June 30). National Cancer

Institute. <https://www.cancer.gov/types/skin/patient/melanoma-treatment-pdq>

Moore, A. R., Ceraudo, E., Sher, J., Guan, Y., Shoushtari, A. N., Chang, M. T., Zhang, J. Q., Walczak, E., Kazmi, M. A., Taylor, B. S., Huber, T., Chi, P., Sakmar, T. P., & Chen, Y. (2016). Recurrent activating mutations of G-protein-coupled receptor CYSLTR2 in uveal melanoma. *Nature Genetics*, *48*(6), 675–680. <https://doi.org/10.1038/ng.3549>

Moore, A. R., Ran, L., Guan, Y., Sher, J., Hitchman, T. D., Zhang, J. Q., Hwang, C., Walczak, E. G., Shoushtari, A. N., Monette, S., Murali, R., Wiesner, T., Griewank, K. G., Chi, P., & Chen, Y. (2018). GNA11 Q209L mouse model reveals RASGRP3 as an essential signaling node in Uveal melanoma. *Cell Reports*, *22*(9), 2455–2468. <https://doi.org/10.1016/j.celrep.2018.01.081>

Morrison, D. K. (2012). MAP Kinase Pathways. *Cold Spring Harbor Perspectives in Biology*, *4*(11), a011254. <https://doi.org/10.1101/cshperspect.a011254>

Morrison, D. K., & Davis, R. J. (2003). Regulation of MAP kinase signaling modules by scaffold proteins in mammals. *Annual Review of Cell and Developmental Biology*, *19*(1), 91–118. <https://doi.org/10.1146/annurev.cellbio.19.111401.091942>

Nareyeck, G., Zeschnigk, M., Bornfeld, N., & Anastassiou, G. (2009). Novel cell lines derived by Long-Term culture of primary uveal melanomas. *Ophthalmologica*, *223*(3), 196–201. <https://doi.org/10.1159/000201566>

Nasti, T. H., & Timares, L. (2014). MC1R, Eumelanin and pheomelanin: Their role in determining the susceptibility to skin Cancer. *Photochemistry and Photobiology*, *91*(1), 188–200. <https://doi.org/10.1111/php.12335>

Nguyen, L. K., Kholodenko, B. N., & Von Kriegsheim, A. (2016). Rac1 and RhoA: Networks, loops and bistability. *Small GTPases*, *9*(4), 316–321. <https://doi.org/10.1080/21541248.2016.1224399>

- Nissan, M. H., Pratilas, C. A., Jones, A. M., Ramirez, R., Won, H., Liu, C., Tiwari, S., Kong, L., Hanrahan, A. J., Yao, Z., Merghoub, T., Ribas, A., Chapman, P. B., Yaeger, R., Taylor, B. S., Schultz, N., Berger, M. F., Rosen, N., & Solit, D. B. (2014). Loss of NF1 in Cutaneous Melanoma Is Associated with RAS Activation and MEK Dependence. *Cancer Research*, *74*(8), 2340–2350. <https://doi.org/10.1158/0008-5472.can-13-2625>
- Onken, M. D., Makepeace, C. M., Kaltenbronn, K. M., Choi, J., Hernandez-Aya, L. F., Weilbaecher, K. N., Piggott, K., Rao, P. K., Yuede, C. M., Dixon, A. J., Osei-Owusu, P., Cooper, J. A., & Blumer, K. J. (2021). Targeting primary and metastatic uveal melanoma with a G protein inhibitor. *Journal of Biological Chemistry*, *296*, 100403. <https://doi.org/10.1016/j.jbc.2021.100403>
- Onken, M. D., Makepeace, C. M., Kaltenbronn, K. M., Kanai, S. M., Todd, T. D., Wang, S., Broekelmann, T. J., Rao, P. K., Cooper, J. A., & Blumer, K. J. (2018). Targeting nucleotide exchange to inhibit constitutively active G protein  $\alpha$  subunits in cancer cells. *Science Signaling*, *11*(546). <https://doi.org/10.1126/scisignal.aao6852>
- Onken, M. D., Worley, L. A., & Harbour, J. W. (2010). Association between Gene Expression Profile, Proliferation and Metastasis in Uveal Melanoma. *Current Eye Research*, *35*(9), 857–863. <https://doi.org/10.3109/02713683.2010.493265>
- Ottaviano, M., Giunta, E. F., Tortora, M., Curvietto, M., Attademo, L., Bosso, D., Cardalesi, C., Rosanova, M., De Placido, P., Pietroluongo, E., Riccio, V., Mucci, B., Parola, S., Vitale, M. G., Palmieri, G., Daniele, B., & Simeone, E. (2021). BRAF gene and melanoma: Back to the future. *International Journal of Molecular Sciences*, *22*(7), 3474. <https://doi.org/10.3390/ijms22073474>
- Paraiso, K. H., Xiang, Y., Rebecca, V. W., Abel, E. V., Chen, Y. A., Munko, A. C., Wood, E. R., Fedorenko, I. V., Sondak, V. K., Anderson, A. R., Ribas, A., Palma, M. D., Nathanson, K. L., Koomen, J. M., Messina, J. L., & Smalley, K. S. (2011). PTEN Loss Confers BRAF Inhibitor Resistance to Melanoma Cells through the Suppression of BIM

- Expression. *Cancer Research*, 71(7), 2750–2760. <https://doi.org/10.1158/0008-5472.can-10-2954>
- Parrella, P., Caballero, O. L., Sidransky, D., & Merbs, S. L. (2001). Detection of c-myc amplification in uveal melanoma by fluorescent in situ hybridization. *PubMed*, 42(8), 1679–1684. <https://pubmed.ncbi.nlm.nih.gov/11431428>
- Perez, D. E., Henle, A. M., Amsterdam, A., Hagen, H. R., & Lees, J. A. (2018). Uveal melanoma driver mutations in GNAQ/11 yield numerous changes in melanocyte biology. *Pigment Cell & Melanoma Research*, 31(5), 604–613. <https://doi.org/10.1111/pcmr.12700>
- Phan, H. T., Kim, N. H., Wei, W., Tall, G. G., & Smrcka, A. V. (2021). Uveal melanoma-associated mutations in PLC $\beta$ 4 are constitutively activating and promote melanocyte proliferation and tumorigenesis. *Science Signaling*, 14(713). <https://doi.org/10.1126/scisignal.abj4243>
- Phelps, G. B., Amsterdam, A., Hagen, H. R., García, N. Z., & Lees, J. A. (2022). MITF deficiency and oncogenic GNAQ each promote proliferation programs in zebrafish melanocyte lineage cells. *Pigment Cell & Melanoma Research*, 35(5), 539–547. <https://doi.org/10.1111/pcmr.13057>
- Phelps, G. B., Hagen, H. R., Amsterdam, A., & Lees, J. A. (2022). MITF deficiency accelerates GNAQ-driven uveal melanoma. *Proceedings of the National Academy of Sciences of the United States of America*, 119(19). <https://doi.org/10.1073/pnas.2107006119>
- Piccolo, S., Dupont, S., & Cordenonsi, M. (2014). The Biology of YAP/TAZ: Hippo Signaling and Beyond. *Physiological Reviews*, 94(4), 1287–1312. <https://doi.org/10.1152/physrev.00005.2014>
- Price, E., & Fisher, D. E. (2001). Sensorineural deafness and pigmentation genes. *Neuron*, 30(1), 15–18. [https://doi.org/10.1016/s0896-6273\(01\)00259-8](https://doi.org/10.1016/s0896-6273(01)00259-8)
- Prior, I. A., Lewis, P. D., & Mattos, C. (2012). A comprehensive survey of RAS mutations in cancer. *Cancer Research*, 72(10), 2457–2467. <https://doi.org/10.1158/0008-5472.can-11-2612>



- Reggiani, F., Gobbi, G., Ciarrocchi, A., & Sancisi, V. (2021). YAP and TAZ Are Not Identical Twins. *Trends in Biochemical Sciences*, *46*(2), 154–168. <https://doi.org/10.1016/j.tibs.2020.08.012>
- Richards, J. R., Yoo, J. H., Shin, D., & Odelberg, S. J. (2020). Mouse models of uveal melanoma: Strengths, weaknesses, and future directions. *Pigment Cell & Melanoma Research*, *33*(2), 264–278. <https://doi.org/10.1111/pcmr.12853>
- Rimoldi, D., Salvi, S., Liénard, D., Lejeune, F. J., Speiser, D. E., Zografos, L., & Cerottini, J. (2003). Lack of BRAF mutations in uveal melanoma. *PubMed*, *63*(18), 5712–5715. <https://pubmed.ncbi.nlm.nih.gov/14522889>
- Robertson, A. G., Shih, J., Yau, C., Gibb, E. A., Oba, J., Mungall, K., Hess, J. M., Uzunangelov, V., Walter, V., Danilova, L., Lichtenberg, T. M., Kucherlapati, M., Kimes, P. K., Tang, M., Penson, A., Babur, Ö., Akbani, R., Bristow, C. A., Hoadley, K. A., . . . Zmuda, E. (2017). Integrative analysis identifies four molecular and clinical subsets in uveal melanoma. *Cancer Cell*, *32*(2), 204–220.e15. <https://doi.org/10.1016/j.ccell.2017.07.003>
- Sanz-Moreno, V., Gadéa, G., Ahn, J., Paterson, H., Marra, P., Pinner, S., Sahai, E., & Marshall, C. J. (2008). RAC activation and inactivation control Plasticity of tumor cell movement. *Cell*, *135*(3), 510–523. <https://doi.org/10.1016/j.cell.2008.09.043>
- Sanz-Moreno, V., & Marshall, C. J. (2009). Rho-GTPase signaling drives melanoma cell plasticity. *Cell Cycle*, *8*(10), 1484–1487. <https://doi.org/10.4161/cc.8.10.8490>
- Scatena, C., Murtas, D., & Tomei, S. (2021). Cutaneous Melanoma Classification: The importance of High-Throughput Genomic Technologies. *Frontiers in Oncology*, *11*. <https://doi.org/10.3389/fonc.2021.635488>
- Schadendorf, D., Fisher, D. E., Garbe, C., Gershenwald, J. E., Grob, J., Halpern, A. C., Herlyn, M., Marchetti, M. A., McArthur, G. A., Ribas, A., Roesch, A., & Hauschild, A. (2015). Melanoma. *Nature Reviews Disease Primers*, *1*(1). <https://doi.org/10.1038/nrdp.2015.3>

- Schadendorf, D., Van Akkooi, A. C. J., Berking, C., Griewank, K. G., Gutzmer, R., Hauschild, A., Stang, A., Roesch, A., & Ugurel, S. (2018). Melanoma. *The Lancet*, *392*(10151), 971–984. [https://doi.org/10.1016/s0140-6736\(18\)31559-9](https://doi.org/10.1016/s0140-6736(18)31559-9)
- Schaub, F. X., Dhankani, V., Berger, A. C., Trivedi, M., Richardson, A. B., Shaw, R., Zhao, W., Zhang, X., Ventura, A., Liu, Y., Ayer, D. E., Hurlin, P. J., Cherniack, A. D., Eisenman, R. N., Bernard, B., Grandori, C., Caesar-Johnson, S. J., Demchok, J. A., Felau, I., . . . Mariamidze, A. (2018). Pan-cancer Alterations of the MYC Oncogene and Its Proximal Network across the Cancer Genome Atlas. *Cell Systems*, *6*(3), 282-300.e2. <https://doi.org/10.1016/j.cels.2018.03.003>
- Schrage, R., Schmitz, A. L., Gaffal, E., Annala, S., Kehraus, S., Wenzel, D., Büllsbach, K. M., Bald, T., Inoue, A., Shinjo, Y., Galandrin, S., Shridhar, N., Hesse, M., Grundmann, M., Merten, N., Charpentier, T. H., Martz, M., Butcher, A. J., Slodczyk, T., . . . Kostenis, E. (2015). The experimental power of FR900359 to study Gq-regulated biological processes. *Nature Communications*, *6*(1). <https://doi.org/10.1038/ncomms10156>
- Shain, A. H., Bagger, M., Yu, R., Chang, D., Liu, S., Vemula, S., Weier, J. F., Wadt, K., Heegaard, S., Bastian, B. C., & Kiilgaard, J. F. (2019). The genetic evolution of metastatic uveal melanoma. *Nature Genetics*, *51*(7), 1123–1130. <https://doi.org/10.1038/s41588-019-0440-9>
- Silva-Rodríguez, P., Fernández-Díaz, D., Bande, M. F., Pardo, M. L., Loidi, L., & Blanco-Teijeiro, M. J. (2022). GNAQ and GNA11 Genes: A Comprehensive Review on oncogenesis, Prognosis and therapeutic opportunities in Uveal Melanoma. *Cancers*, *14*(13), 3066. <https://doi.org/10.3390/cancers14133066>
- Smoot, R. L., Werneburg, N. W., Sugihara, T., Hernandez, M. C., Yang, L., Mehner, C., Graham, R. P., Bronk, S. F., Truty, M. J., & Gores, G. J. (2017). Platelet-derived growth factor regulates YAP transcriptional activity via Src family kinase dependent tyrosine phosphorylation. *Journal of Cellular Biochemistry*, *119*(1), 824–836. <https://doi.org/10.1002/jcb.26246>

- Strano, S., Munarriz, E., Rossi, M., Castagnoli, L., Shaul, Y., Sacchi, A., Oren, M., Sudol, M., Cesareni, G., & Blandino, G. (2001). Physical Interaction with Yes-associated Protein Enhances p73 Transcriptional Activity. *Journal of Biological Chemistry*, 276(18), 15164–15173. <https://doi.org/10.1074/jbc.m010484200>
- Sugase, T., Lam, B., Danielson, M., Terai, M., Aplin, A. E., Gutkind, J. S., & Sato, T. (2020). Development and optimization of orthotopic liver metastasis xenograft mouse models in uveal melanoma. *Journal of Translational Medicine*, 18(1). <https://doi.org/10.1186/s12967-020-02377-x>
- Terai, M., Kageyama, K., Sugase, T., Lam, B., Alexeev, V., & Sato, T. (2021). Orthotopic human metastatic uveal melanoma Xenograft mouse models: Applications for understanding the pathophysiology and therapeutic management of metastatic uveal melanoma. *Current Protocols*, 1(4). <https://doi.org/10.1002/cpz1.110>
- Thomas, A. J., & Erickson, C. A. (2008). The making of a melanocyte: the specification of melanoblasts from the neural crest. *Pigment Cell & Melanoma Research*, 21(6), 598–610. <https://doi.org/10.1111/j.1755-148x.2008.00506.x>
- Trinh, P., Li, S., & Sarin, K. Y. (2022). Neurofibromatosis type 1 and risk of skin cancer. *JAMA Dermatology*, 158(10), 1214. <https://doi.org/10.1001/jamadermatol.2022.3083>
- Uner, O. E., Gandrakota, N., Azarcon, C. P., & Grossniklaus, H. E. (2022). Animal models of uveal melanoma. *Annals of Eye Science*, 7, 7. <https://doi.org/10.21037/aes-21-30>
- Van Allen, E. M., Wagle, N., Sucker, A., Treacy, D. J., Johannessen, C. M., Goetz, E. M., Place, C. S., Taylor-Weiner, A., Whittaker, S. R., Kryukov, G. V., Hodis, E., Rosenberg, M., McKenna, A., Cibulskis, K., Farlow, D. N., Zimmer, L., Hillen, U., Gutzmer, R., Goldinger, S. M., . . . Schadendorf, D. (2014). The genetic landscape of clinical resistance to RAF inhibition in metastatic melanoma. *Cancer Discovery*, 4(1), 94–109. <https://doi.org/10.1158/2159-8290.cd-13-0617>
- Van Der Ent, W., Burrello, C., Teunisse, A. F., Ksander, B. R., Van Der Velden, P. A., Jager, M. J., Jochemsen, A. G., & Snaar-Jagalska, B. E. (2014). Modeling of human uveal

- melanoma in zebrafish xenograft embryos. *Investigative Ophthalmology & Visual Science*, 55(10), 6612. <https://doi.org/10.1167/iovs.14-15202>
- Van Raamsdonk, C. D., Bezrookove, V., Green, G., Bauer, J., Gaugler, L., O'Brien, J. M., Simpson, E. M., Barsh, G. S., & Bastian, B. C. (2008). Frequent somatic mutations of GNAQ in uveal melanoma and blue naevi. *Nature*, 457(7229), 599–602. <https://doi.org/10.1038/nature07586>
- Van Raamsdonk, C. D., Griewank, K. G., Crosby, M. E., Garrido, M. C., Vemula, S., Wiesner, T., Obenaus, A. C., Wackernagel, W., Green, G., Bouvier, N., Sozen, M., Baimukanova, G., Roy, R., Heguy, A., Dolgalev, I., Khanin, R., Busam, K. J., Speicher, M. R., O'Brien, J. M., & Bastian, B. C. (2010). Mutations InGNA11in uveal melanoma. *The New England Journal of Medicine*, 363(23), 2191–2199. <https://doi.org/10.1056/nejmoa1000584>
- Vassilev, A., Kaneko, K. J., Shu, H., Zhao, Y., & DePamphilis, M. L. (2001). TEAD/TEF transcription factors utilize the activation domain of YAP65, a Src/Yes-associated protein localized in the cytoplasm. *Genes & Development*, 15(10), 1229–1241. <https://doi.org/10.1101/gad.888601>
- Ventii, K., Devi, N. S., Friedrich, K. L., Chernova, T. A., Tighiouart, M., Van Meir, E. G., & Wilkinson, K. D. (2008). BRCA1-Associated Protein-1 Is a Tumor Suppressor that Requires Deubiquitinating Activity and Nuclear Localization. *Cancer Research*, 68(17), 6953–6962. <https://doi.org/10.1158/0008-5472.can-08-0365>
- Walker, T. M., Van Ginkel, P. R., Gee, R. L., Ahmadi, H., Subramanian, L., Ksander, B. R., Meisner, L. F., Albert, D. M., & Polans, A. S. (2002). Expression of angiogenic factors CYR61 and tissue factor in uveal melanoma. *Archives of Ophthalmology*, 120(12), 1719. <https://doi.org/10.1001/archopht.120.12.1719>
- Wan, P., Garnett, M. J., Roe, S. M., Lee, S., Niculescu-Duvaz, D., Good, V. M., Genome, C., Jones, C., Marshall, C. J., Springer, C. J., Barford, D., & Marais, R. (2004). Mechanism

- of activation of the RAF-ERK signaling pathway by oncogenic mutations of B-RAF. *Cell*, 116(6), 855–867. [https://doi.org/10.1016/s0092-8674\(04\)00215-6](https://doi.org/10.1016/s0092-8674(04)00215-6)
- Wellbrock, C., Rana, S., Paterson, H., Pickersgill, H., Brummelkamp, T. R., & Marais, R. (2008). Oncogenic BRAF Regulates Melanoma Proliferation through the Lineage Specific Factor MITF. *PLOS ONE*, 3(7), e2734. <https://doi.org/10.1371/journal.pone.0002734>
- White, V. A., Chambers, J. D., Courtright, P., Chang, W. Y., & Horsman, D. E. (1998). Correlation of cytogenetic abnormalities with the outcome of patients with uveal melanoma. *Cancer*, 83(2), 354–359. [https://doi.org/10.1002/\(sici\)1097-0142\(19980715\)83:2](https://doi.org/10.1002/(sici)1097-0142(19980715)83:2)
- Yagi, R., Chen, L. F., Shigesada, K., Murakami, Y., & Ito, Y. (1999). A WW domain-containing Yes-associated protein (YAP) is a novel transcriptional co-activator. *The EMBO Journal*, 18(9), 2551–2562. <https://doi.org/10.1093/emboj/18.9.2551>
- Yavuzyiğitoğlu, S., Koopmans, A. E., Verdijk, R. M., Vaarwater, J., Eussen, B., Van Bodegom, A., Paridaens, D., Kılıç, E., & De Klein, A. (2016). Uveal Melanomas with SF3B1 Mutations. *Ophthalmology*, 123(5), 1118–1128. <https://doi.org/10.1016/j.ophtha.2016.01.023>
- Yoshida, M., Selvan, S. R., McCue, P. A., DeAngelis, T., Baserga, R., Fujii, A., Rui, H., Mastrangelo, M. J., & Sato, T. (2014). Expression of insulin-like growth factor-1 receptor in metastatic uveal melanoma and implications for potential autocrine and paracrine tumor cell growth. *Pigment Cell & Melanoma Research*, 27(2), 297–308. <https://doi.org/10.1111/pcmr.12206>
- Zhao, B., Wei, X., Li, W., Udan, R. S., Yang, Q., Kim, J., Xie, J., Ikenoue, T., Yu, J., Li, L., Zheng, P., Ye, K., Chinnaiyan, A. M., Halder, G., Lai, Z. C., & Guan, K. L. (2007). Inactivation of YAP oncoprotein by the Hippo pathway is involved in cell contact inhibition and tissue growth control. *Genes & Development*, 21(21), 2747–2761. <https://doi.org/10.1101/gad.1602907>

Zuidervaart, W., Van Nieuwpoort, F., Stark, M., Dijkman, R., Packer, L., Borgstein, A. M., Pavey, S., Van Der Velden, P., Out, C., Jager, M. J., Hayward, N. K., & Gruis, N. A. (2005). Activation of the MAPK pathway is a common event in uveal melanomas although it rarely occurs through mutation of BRAF or RAS. *British Journal of Cancer*, 92(11), 2032–2038. <https://doi.org/10.1038/sj.bjc.6602598>

## **Chapter II. Either YAP or TAZ is dispensable for Uveal Melanoma, reflecting pathway plasticity**

Authors: Swanny Lamboy Rodríguez, Grace B. Phelps, Adam Amsterdam, Griffin Salus, Nicole Henning, Kevin Gibbons, and Jacqueline Lees

### Contributions:

The zebrafish experiments were conducted by GBP and AA except for the drug response analyses, which were a collaborative effort between SLR, GS and KG.

The human knockout cells were generated by GBP and validated by SLR. SLR conducted all of the *in vitro* characterization of these cells including their drug responses except for the transcriptomic analyses and cell cycle phasing analyses (conducted by AA), and the Mel202 YAP KO trametinib drug experiment and pERK western blot analysis and quantification (conducted by GS).

The *in vivo* tumor analyses were a collaborative effort between SLR, GS, AA and NH.

SLR, GBP and JAL designed the study and wrote the manuscript, with contributions from AA and GS.

## Abstract

Uveal Melanoma (UM) is the primary ocular malignancy in adults. The primary tumor is treatable but 50% of patients develop fatal metastases, predominantly to the liver. Most UM are driven by activating mutations in the heterotrimeric G protein alpha subunits paralogs, *GNAQ* or *GNA11*, whose main downstream effectors are MAPK signaling and the transcriptional activator YAP. Recent zebrafish work established the importance of YAP and de-emphasized the role of MAPK in UM. Here we establish that *yap* and its paralog, *taz*, play functional redundant roles in zebrafish UM; either paralog can drive UM, functioning in a TEAD-dependent manner, and either gene can be deleted without significant effect on the incidence, or kinetics, of *GNAQ*<sup>Q209L</sup>-driven UM. To determine the human relevance, multiple YAP or TAZ-deficient clones were generated for two human UM cell lines, Mel202 and MP41. Deletion of either protein had no consistent deleterious effects on the survival or proliferation properties of these cells *in vitro*. We also assessed the ability of these clones to form liver tumors through cardiac transplant assays. All clones yielded some liver tumors, which displayed nuclear YAP and/or TAZ, as appropriate for their genotype, as well as low-level, heterogenous staining for phospho-ERK. For MP41, YAP or TAZ were fully dispensable for tumorigenesis. For Mel202, TAZ deletion did not reduce tumor burden, but the level of nuclear YAP was high. In contrast, YAP deletion greatly reduced the number and size of liver tumors, without upregulation of TAZ. We conclude that the YAP/TAZ signaling plays a dominant role in both zebrafish and human UM, but most tumors can survive without YAP or TAZ due to their functional redundancy.

## Introduction

UM arises from the melanocytes within the uvea of the eye, which is composed of the choroid, ciliary body, and the iris (Jager et al., 2020). Treatment of the primary tumor consists of localized radiation therapy, or in more severe cases, removal of the eye (enucleation). Nevertheless, approximately 50% of patients will develop metastasis within 10 to 15 years after



diagnosis of the primary lesion (Jager et al., 2020). Of the patients that develop metastasis, ~89% will have liver metastases, followed by 29% to the lungs, and 17% to the bone marrow (Kaliki & Shields 2017). Historically, UM metastasis has been fatal, with the median survival post-diagnosis being only 4-15 months (Augsburger et al., 2009; Carvajal et al 2018). The FDA recently approved a new therapy for metastatic UM (mUM) but only 47% of UM patients qualify, and the lifespan extension is modest (Hua et al., 2022). Thus, there is still a critical need to identify biological programs that represent core vulnerabilities for UM development and progression.

UM's main oncogene is the small alpha subunit of the GTPase *GNAQ*, or its paralog *GNAI1*. Approximately 90% of patients carry a point mutation that renders the resulting  $G\alpha Q/11$  constitutively active. The canonical role of  $G\alpha Q/11$  is to promote activation of the MAPK pathway via interaction with the phospholipase c protein, PLC $\beta$ 4 (Lee et al., 1994). PLC $\beta$ 4 cleaves phosphatidylinositol 4,5-biphosphate (PIP2) into phosphatidylinositol 3,4,5-triphosphate (PIP3) and diacylglycerol (DAG), and the latter binds to PKC and triggers MAPK pathway activation through RASGRP3 (Chen et al., 2017; Kadamur et al., 2013; Moore et al., 2018). The second pathway downstream of  $G\alpha Q/11$  is the YAP pathway.  $G\alpha Q/11$  promotes YAP nuclear localization through a non-canonical mechanism that involves interaction with the Rho-GEF (guanine exchange factor), TRIO (Feng et al., 2014). YAP is a transcription factor that is typically regulated by the Hippo pathway, which adds negative phosphorylation marks at serine residues, such as serine 127 (S127), and leads to cytoplasmic sequestration by 14-3-3 proteins and AMOT (Zhao et al., 2007; Zhao et al., 2010; Zhao et al., 2011). Active YAP translocates to the nucleus and interacts with other transcription factors, primarily as TEADs, to modulate transcription (Johnson & Halder 2014; Regianni et al., 2021). TAZ (gene name, *WWTR1*) is a paralog of YAP (gene name, *YAP1*). These proteins have 40% homology and share many of the same functional domains, regulatory phosphorylation sites and associated transcription factors, including the TEADs (Khan et al., 2017; Li et al 2010; Reggiani et al., 2021). Both YAP and TAZ were shown to be expressed in  $G\alpha q^{Q209L}$

Melan-a cells (Yu et al., 2019). This raises the possibility that Gαq/11 could also regulate TAZ, as it does YAP.

To enable development of viable treatment strategies for UM, we need to identify signaling pathways that drive these tumors and determine whether they represent true vulnerabilities to tumor survival or development. We have previously used a zebrafish model of UM to identify the key signaling pathways. Initially, we generated a zebrafish transgenic model of UM by expressing oncogenic *GNAQ<sup>Q209L</sup>* or *GNAI1<sup>Q209L</sup>* under the control of the promoter for the melanocyte transcription factor, *mitfa* (Perez et al., 2018). These oncogenes yielded tumors very rarely, and with long latency, arguing that at least one cooperating mutation is required. Thus, we generated *Tg(mitfa:GNAQ<sup>Q209L</sup>);tp53<sup>-/-</sup>* and *Tg(mitfa:GNAI1<sup>Q209L</sup>);tp53<sup>-/-</sup>* fish and found that these formed tumors with complete penetrance that recapitulated UM pathology (Perez et al., 2018). This included displaying homogenous high levels of nuclear YAP, which is a hallmark of human UM, as well as heterogenous, and somewhat weak, staining for pERK (Perez et al., 2018; Phelps, et al., 2022a). We also discovered that deletion of *mitfa* enables *GNAQ<sup>Q209L</sup>* single mutant fish to develop UM, indicating that this serves as an alternate cooperating mutation in UM (Phelps et al., 2022a).

Having established that zebrafish can be used to model UM, we modified an existing mosaic transposon integration system (Ceol et al., 2011) to probe the key driving pathways. Specifically, we generated transposon vectors that carried both candidate UM drivers under the control of the *mitfa* promoter and a *mitfa*-GFP reporter gene, injected these into single cell zebrafish embryos that were either *tp53<sup>-/-</sup>* or *tp53<sup>-/-</sup>;mitfa*, and assayed for the formation of GFP positive UM tumors (Phelps et al., 2022a). We confirmed that *mitfa* promoter is active in both contexts (i.e. *Mitfa* expression is not required for *mitfa* promoter activity) and that *GNAQ<sup>Q209L</sup>* works well in this assay, yielding GFP+ UM with complete penetrance (Phelps et al., 2022a). We then tested two rarer UM-derived mutations: *CYSLTR2<sup>L129Q</sup>* (the signaling receptor upstream of GαQ/11) and *PLCβ4<sup>D630Y</sup>* (thought to specifically activate the MAPK pathway), as well as a constitutively active version of YAP, *YAP<sup>S127A;S381A</sup>*, (henceforth referred to as *YAP<sup>AA</sup>*) as YAP is

not mutated in UM, or any other tumor types. *CYSLTR2*<sup>L129Q</sup> also yielded GFP+ tumors with good efficiency when introduced into either *tp53*<sup>-/-</sup> or *tp53*<sup>-/-</sup>;*mitfa*<sup>-/-</sup> mutant embryos (Phelps et al., 2022a). In contrast, *PLCβ4*<sup>D630Y</sup> was essentially non-tumorigenic in *tp53*<sup>-/-</sup> embryos, and yielded tumors in the *tp53*<sup>-/-</sup>;*mitfa*<sup>-/-</sup> mutant background with significantly longer latency and lower frequency than the *GNAQ*<sup>Q209L</sup> positive control (Phelps et al., 2022a). Remarkably, these tumors lacked pERK, but displayed high levels of nuclear Yap, arguing that *PLCβ4*<sup>D630Y</sup> was serving to engage Yap and not MAPK signaling (Phelps, Hagen et al., 2022). Although initially unexpected, there is precedent for YAP nuclear localization in HRAS<sup>V12</sup>-driven and PI3K-driven tumors (Mayrhifer et al., 2017; Y. Zhao et al., 2018). Finally, we found that *YAP*<sup>AA</sup> drove tumors in both *tp53*<sup>-/-</sup> or *tp53*<sup>-/-</sup>;*mitfa*<sup>-/-</sup> backgrounds with significantly reduced latency and increased aggressiveness compared to the *GNAQ*<sup>Q209L</sup> positive control (Phelps, et al., 2022a). Collectively, these data supported the importance of YAP and de-emphasized the role of PLCβ4-MAPK in UM tumorigenesis.

These prior studies show that YAP is sufficient to drive UM tumor formation in zebrafish. However, they do not address its essentiality, which is a key step in understanding the degree to which YAP inhibition might represent a therapeutic vulnerability. In this current study, we took advantage of an existing Yap-deficient zebrafish line (Miesfeld et al., 2015) to assess the requirement for Yap in UM. This led us to discover that *yap* loss has no significant effect on the incidence, or kinetics, of *GNAQ*<sup>Q209L</sup>-driven zebrafish UM. Additional analyses argue that this reflects functionally redundant roles for Yap and its paralog, Taz. Specifically, in a similar manner to Yap, constitutively active TAZ induces UM tumors with high efficiency, but *taz* deletion has no effect on zebrafish UM. Moreover, we confirm that the UM forming ability of both proteins is dependent upon residues that mediate their TEAD interactions. To establish human relevance, we also generated YAP or TAZ deficient human UM cell lines. Single knockout of either YAP or TAZ yielded no consistent impairment of the UM cells' viability or proliferation rate in vitro. Moreover, these cells all retained ability to form liver tumors in transplant assays, with only one

context – YAP deletion in Mel202 cells – showing a clear reduction in tumor burden. The histological staining patterns of the various tumors supports the importance of YAP/TAZ signaling, while de-emphasizing MAPK signaling, in strong agreement with our zebrafish UM studies. Collectively, these results argue that UM cells and tumors display significant plasticity, such that they can easily tolerate loss of either YAP or TAZ, due to redundancy of these two proteins.

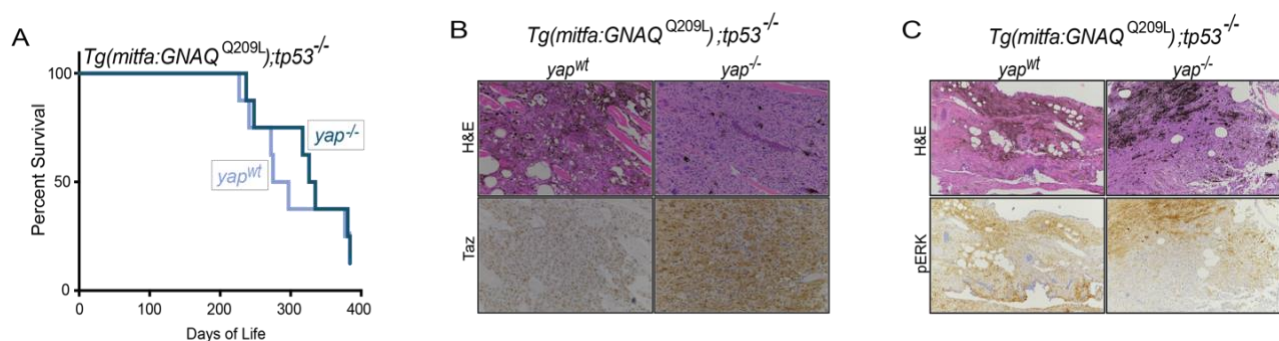
## Results

### Yap is fully dispensable to drive zebrafish UM

Our first goal was to determine whether *yap* was essential for development of UM tumor in zebrafish. For this, we took advantage of an existing *yap* mutant line, *yap<sup>mw48</sup>*, which has a 4-nucleotide deletion within the TEAD binding domain that creates a premature stop codon (Miesfeld et al., 2015). Since *yap<sup>mw48</sup>* is a complete loss of function (Miesfeld et al., 2015), we herein call it *yap<sup>-/-</sup>* for simplicity. *yap<sup>-/-</sup>* zebrafish are semi-viable, with the survivors being typically smaller than wildtypes, but otherwise healthy (Miesfeld et al., 2015). We crossed *yap<sup>-/-</sup>* into our *Tg(mitfa:GNAQ<sup>Q209L</sup>)* line (Perez et al., 2018) and generated control cohorts that were either *Tg(mitfa:GNAQ<sup>Q209L</sup>);tp53<sup>-/-</sup>;yap<sup>-/-</sup>* or *Tg(mitfa:GNAQ<sup>Q209L</sup>);tp53<sup>-/-</sup>;yap<sup>wt</sup>*. Unexpectedly, the *Tg(mitfa:GNAQ<sup>Q209L</sup>);tp53<sup>-/-</sup>;yap<sup>-/-</sup>* cohort had the same reduced lifespan as their *yap<sup>wt</sup>* controls, due to the development of UM (Figure 1A). Thus, we conclude that *yap* is fully dispensable for *GNAQ<sup>Q209L</sup>*-driven tumorigenesis.

We hypothesized that the *yap<sup>-/-</sup>* tumors were relying on alternative pathways. Since *yap<sup>-/-</sup>* embryos were previously reported to express higher protein levels of Taz and nuclear localization (Miesfeld et al., 2015), we screened *yap<sup>wt</sup>* and *yap<sup>-/-</sup>* tumors for differences in Taz. Initially, we used qRT-PCR to quantify *taz* mRNA. This revealed considerable tumor-to-tumor variation in *taz* mRNA levels between tumors of the same genotype (i.e. *yap<sup>-/-</sup>* or *yap<sup>wt</sup>*) but no significant

difference in the mean *taz* mRNA levels in *yap*<sup>-/-</sup> versus *yap*<sup>wt</sup> tumors (Fig S1). We also saw no significant difference in the mean levels of *yap* mRNA between the two genotypes (Fig S1.). We also conducted immunohistochemistry (IHC) on the tumors, to examine Taz protein levels and subcellular localization. We were unable to get the currently available Yap-specific antibodies to work in any zebrafish UM tumors. However, an anti-human YAP/TAZ antibody, which specifically detects Taz and not Yap in zebrafish (Brandt et al., 2020; see also Figure 2G), showed nuclear Taz in the majority of cells for both *Tg(mitfa:GNAQ<sup>Q209L</sup>);tp53<sup>-/-</sup>;yap<sup>wt</sup>* and *Tg(mitfa:GNAQ<sup>Q209L</sup>);tp53<sup>-/-</sup>;yap<sup>-/-</sup>* tumors (Fig 1B). Thus, nuclear Taz exists in *GNAQ<sup>Q209L</sup>*-driven zebrafish UM. We also wondered whether MAPK pathway signaling was altered in the *yap*<sup>-/-</sup> tumors and thus performed IHC for pERK. The pERK signal was highly heterogenous in control *Tg(mitfa:GNAQ<sup>Q209L</sup>);tp53<sup>-/-</sup>;yap<sup>wt</sup>* tumors, with some regions showing high levels of pERK and others showing low or no pERK, consistent with our prior findings (Phelps et al., 2022a) and the *Tg(mitfa:GNAQ<sup>Q209L</sup>);tp53<sup>-/-</sup>;yap<sup>-/-</sup>* tumors showed the same phenotype (Fig. 1C). This is consistent with our prior conclusion that MAPK signaling plays a lesser role in zebrafish UM, and further argues that this is not elevated in compensation for YAP loss.



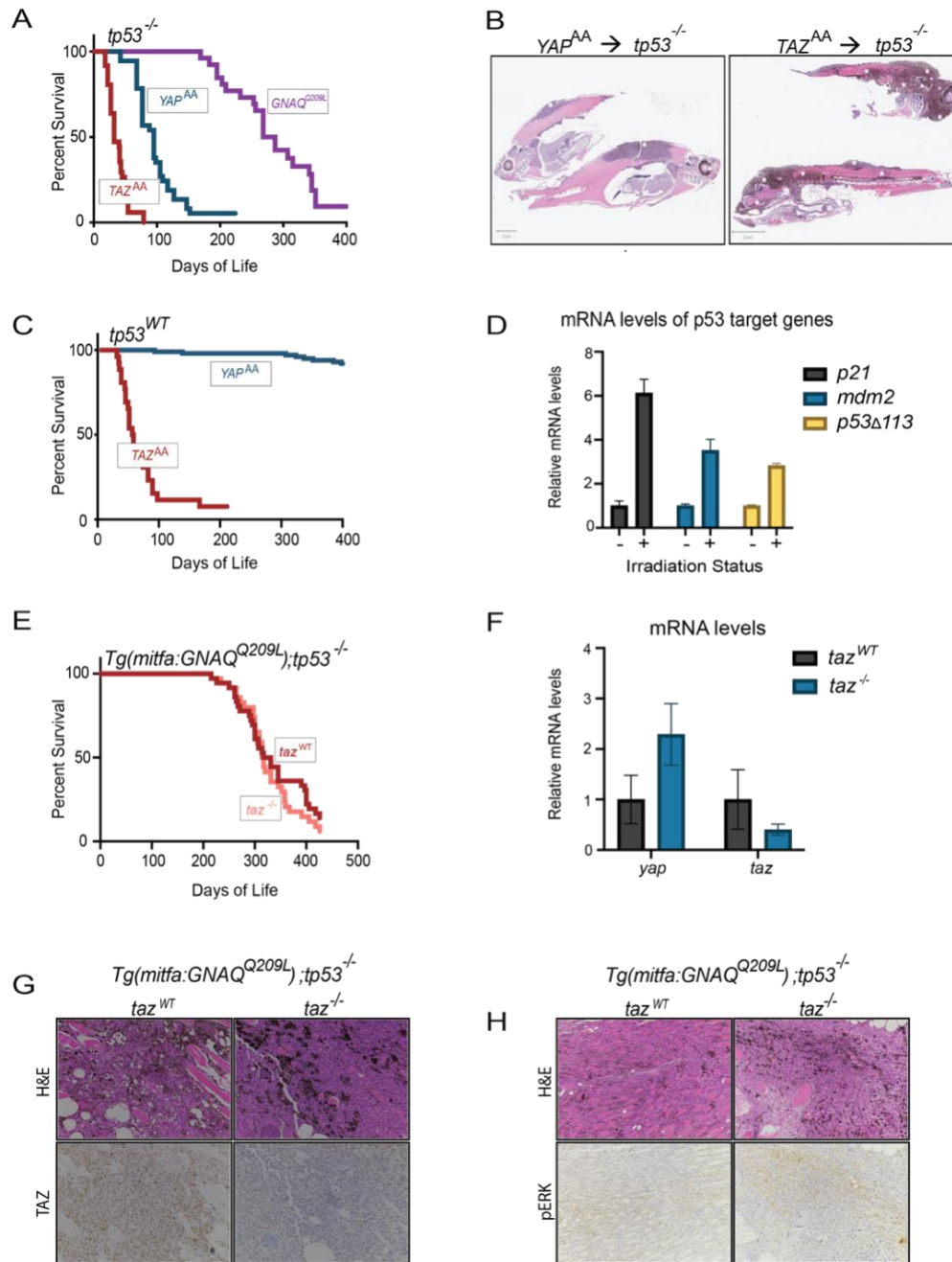
**Figure 1. Yap deletion does not alter the development of *GNAQ<sup>Q209L</sup>*-driven UM in zebrafish.**

Cohorts of *Tg(mitfa:GNAQ<sup>Q209L</sup>);tp53<sup>-/-</sup>* fish that were *yap*<sup>+/+</sup> versus *yap*<sup>-/-</sup> were directly compared. (A) Kaplan-Meier curves show no significant difference in overall survival; *p* = 0.9194 (n.s.) as determined by log-rank test. (B-C) Representative images of IHC (*n* ≥ 3 tumors for each condition) for Taz (40X) and pERK (10X) show: (B) widespread nuclear Taz, and (C) heterogenous pERK staining, in both genotypes.

## Oncogenic TAZ is sufficient to drive UM but endogenous *taz* is dispensible for *GNAQ<sup>Q209L</sup>*-driven tumorigenesis

We wondered if TAZ can drive tumor formation *in vivo*, in a similar manner to YAP. To address this, we used a constitutively active version of human TAZ, *TAZ<sup>AA</sup>*, in which inhibitory phosphorylation sites (S89 and S311) were mutated to alanine (Cordenonsi et al., 2011; Li et al., 2015). We generated a construct that allows co-integration of *mitfa-TAZ<sup>AA</sup>* and the *mitfa-GFP* reporter and injected this into one cell *tp53<sup>-/-</sup>* or *tp53<sup>wt</sup>* zebrafish embryos. *TAZ<sup>AA</sup>* promoted tumors extremely efficiently in the *tp53<sup>-/-</sup>* background, with significantly faster kinetics than *GNAQ<sup>Q209L</sup>* ( $p < 0.0001$ ) or *YAP<sup>AA</sup>* ( $p < 0.0001$ ; Fig 2A). Indeed, *tp53<sup>-/-</sup>* zebrafish with *TAZ<sup>AA</sup>* developed multiple independent tumors and succumbed as early as 18 days of age, in contrast to *YAP<sup>AA</sup>*, which almost always yielded a single tumor (Fig 2B). Furthermore, *TAZ<sup>AA</sup>* successfully induced rapid tumor UM formation in the *tp53<sup>wt</sup>* background, unlike *YAP<sup>AA</sup>* (Fig. 2C) or *GNAQ<sup>Q209L</sup>* (Perez et al., 2018). Collectively, these results raise the possibility that *TAZ<sup>AA</sup>* can yield UM without any cooperating mutation (Fig S2). To address this, we asked whether tumors arising in *TAZ<sup>AA</sup> → tp53<sup>wt</sup>* fish retained *tp53* activity by dissociating the constituent cells, treating them with or without  $\gamma$ -irradiation to activate DNA damage, and performing qRT-PCR for known zebrafish *tp53* target genes, *p21*, *mdm2* and *p53 $\Delta$ 113*.  $\gamma$ -irradiation induced all of these targets (Fig 2D), confirming that *p53* remains active and supporting the notion that *TAZ<sup>AA</sup>* is sufficient to drive UM.

We next asked whether *taz* is necessary for *GNAQ<sup>Q209L</sup>*-driven tumorigenesis. Mirroring our investigation of endogenous *yap*, we obtained the *taz<sup>mw49</sup>* zebrafish line (Miesfeld et al., 2015), which we refer to as *taz<sup>-/-</sup>*, and generated cohorts of *Tg(mitfa:GNAQ<sup>Q209L</sup>);tp53<sup>-/-</sup>* fish that are *taz<sup>-/-</sup>* or *taz<sup>wt</sup>*. Just as we'd seen with *yap* knockout, *taz* status had no effect on survival (Fig 2E). Notably, qRT-PCR showed that the *taz<sup>-/-</sup>* tumors express reduced levels of *taz* mRNA, as well as elevated levels of *yap* mRNA, compared to *taz<sup>wt</sup>* controls (Fig 2F). The anti-human YAP/TAZ antibody gave a strong IHC signal in *taz<sup>wt</sup>* tumors, and no signal in *taz<sup>-/-</sup>* tumors (Fig. 2G), confirming the absence of *taz* (as well as this antibody's specificity for Taz and not Yap in



**Figure 2. Taz is sufficient to drive UM but fully dispensable for GNAQ<sup>Q209L</sup>-driven UM.**

(A) Kaplan-Meier curves of overall survival of mosaic cohorts in which the indicated oncogene, under control of the *mitfa* promoter, was introduced into one cell stage *tp53*<sup>-/-</sup> embryos. *TAZ*<sup>AA</sup>→*tp53*<sup>-/-</sup> drives tumors significantly faster than either *YAP*<sup>AA</sup>→*tp53*<sup>-/-</sup> (*p*<0.0001) or *GNAQ*<sup>Q209L</sup>→*tp53*<sup>-/-</sup> (*p*<0.0001), as determined by log-rank test. (B) Representative H&E staining of *TAZ*<sup>AA</sup>→*tp53*<sup>-/-</sup> versus *YAP*<sup>AA</sup>→*tp53*<sup>-/-</sup> zebrafish (white\* indicates tumor) shows that *TAZ*<sup>AA</sup> yields many tumors, while *YAP*<sup>AA</sup> typically yields only one. *TAZ*<sup>AA</sup> typically results in higher pigmentation. (C) *TAZ*<sup>AA</sup>→*wildtype* shows a significantly reduced survival, versus *YAP*<sup>AA</sup>→*wildtype* (*p*<0.0001 by log-rank test). (D) Cells were dissociated from *TAZ*<sup>AA</sup>→*tp53*<sup>WT</sup> tumors, treated with or without  $\gamma$ -irradiation (*n*=2 per condition) and *tp53* target genes quantified by qRT-PCR. Post-irradiation levels are compared to no irradiation levels, which were set to 1. (E) Kaplan-Meier curves of *Tg(mitfa:GNAQ*<sup>Q209L</sup>*);tp53*<sup>-/-</sup> cohorts that are *taz*<sup>WT</sup> versus *taz*<sup>-/-</sup> show no significant difference in overall survival (*p* = 0.3619 (n.s.) by log-rank test). (F-H) *Tg(mitfa:GNAQ*<sup>Q209L</sup>*);tp53*<sup>-/-</sup> tumors that are *taz*<sup>WT</sup> versus *taz*<sup>-/-</sup> were assayed for: (F) qRT-PCR of *yap* and *taz* mRNA levels (*n*=3 per genotype); or (G-H) H&E staining and either (G) anti-TAZ (both 40X) or (H) anti-pERK (10X) IHC, with representative images shown.

zebrafish). We also observed similar heterogeneous pERK staining in *taz*<sup>-/-</sup> versus *taz*<sup>wt</sup> tumors, indicating that MAPK signaling is not elevated in the *taz*-deficient tumors (Fig. 2H). Collectively, these data show that ectopic expression of constitutively active TAZ is sufficient to drive zebrafish UM, but the endogenous *taz* gene is fully dispensable for *GNAQ*<sup>Q209L</sup>-driven tumorigenesis in concert with upregulation of *yap* mRNA but not MAPK signaling.

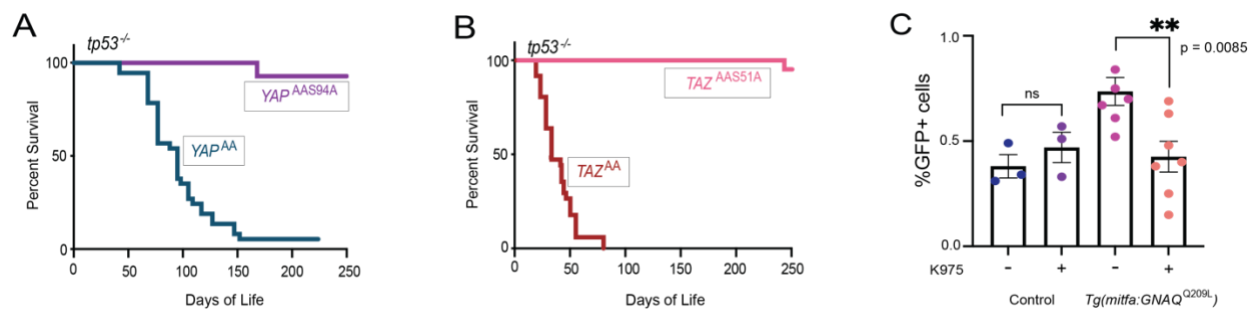
### **TEADs are required for YAP and TAZ to drive UM and for *GNAQ*<sup>Q209L</sup>-driven biology**

The simplest explanation of our findings is functionally redundant roles for Yap and Taz in UM. If true, we expect these proteins to work through a shared mechanism. The transcriptional activity of Yap and Taz depends on their ability to bind to transcription factors, the best-known of which are the TEADs (Zhao et al., 2008). Prior studies have identified point mutations that prevent *YAP* (S94A) and *TAZ* (S51A) from binding TEADs, (Li et al., 2015; Zhao et al., 2008). Thus, we injected *mitfa-YAP*<sup>AAS94A</sup> or *mitfa-TAZ*<sup>AAS51A</sup> constructs into *tp53*<sup>-/-</sup> embryos and found that neither were able to generate UM tumors (Fig 3A and 3B). These fish did eventually develop tumors, but these were all GFP-negative, malignant peripheral nerve-sheath tumors (MPNSTs), which are a hallmark of the *tp53*<sup>-/-</sup> recipient's themselves. We therefore conclude that the TEAD-binding residues are required for YAP/TAZ to drive UM tumors.

We also examined the role of TEAD in the context of *GNAQ*<sup>Q209L</sup> signaling. Previously we've shown that *GNAQ*<sup>Q209L</sup> yields characteristic changes in melanocyte development, including increased representation of melanocytic cells, that is evident as early as 5 days post fertilization (Perez et al., 2018). We've previously leveraged this phenotype to assess the ability of small molecule inhibitors to impact *GNAQ*<sup>Q209L</sup> signaling (Phelps et al., 2022b). Specifically, we isolate developing embryos that carry an *mitfa:eGFP* reporter and are either *Tg(mitfa:GNAQ*<sup>Q209L</sup>*)* or wildtype, incubate them with test drug or vehicle control, and quantify the GFP-positive cells (i.e. the melanocytic lineage) as a percent of the dissociated cell population by flow cytometry (Phelps et al., 2022b). We used this assay to test a TEAD inhibitor (TEADi), K975, previously shown to



disrupt the YAP-TEAD interaction (Kaneda et al., 2020), treating GFP-expressing control or *Tg(mitfa:GNAQ<sup>Q209L</sup>)* embryos with drug or DMSO vehicle from day 2-5 of development. After embryo dissociation, flow cytometry showed that the TEADi significantly decreased the representation of GFP+ cells in the *Tg(mitfa:GNAQ<sup>Q209L</sup>)* embryos, versus the DMSO control, while having no effect on the control embryos (Figure 3C). This establishes that TEADi specifically disrupt the effects of oncogenic *GNAQ<sup>Q209L</sup>* signaling, and not normal melanocytic development, reinforcing our conclusion that the YAP/TAZ-TEAD interaction is important for *GNAQ<sup>Q209L</sup>* driven biology.



**Figure 3. TEAD interaction is necessary for YAP/TAZ driven tumorigenesis** (A-B) Mutation of residues required for TEAD binding within constitutively active: (A) YAP (*YAP<sup>AAS94A</sup>*) or (B) TAZ (*TAZ<sup>AAS51A</sup>*) causes significant extension of lifespan compared to the relevant constitutively active *YAP<sup>AA</sup>* or *TAZ<sup>AA</sup>* positive controls ( $p < 0.0001$  in both cases, as determined by log-rank test). (C) Cohorts of *mitfa:eGFP* alone (control) or *mitfa:eGFP* plus *Tg(mitfa:GNAQ<sup>Q209L</sup>)* zebrafish embryos were treated with DMSO or the TEADi, K975, and the representation of GFP-positive cells, indicating melanocytic lineage cells, quantified by flow cytometry. Each cohort comprised  $\geq 40$  embryos per replicate, which were:  $n = 3$  for control plus DMSO;  $n = 3$  for control plus K975;  $n = 6$  for *Tg(mitfa:GNAQ<sup>Q209L</sup>)* plus DMSO; and  $n = 7$  for *Tg(mitfa:GNAQ<sup>Q209L</sup>)* plus K975. K975 significantly suppressed the increased representation of GFP-positive cells resulting from *GNAQ<sup>Q209L</sup>* expression ( $p = 0.0085$ ) while having no effect on the no-oncogene control embryos.

### **TAZ and YAP are both expressed in human UM, but either one is fully dispensable for UM cell line viability *in vitro*.**

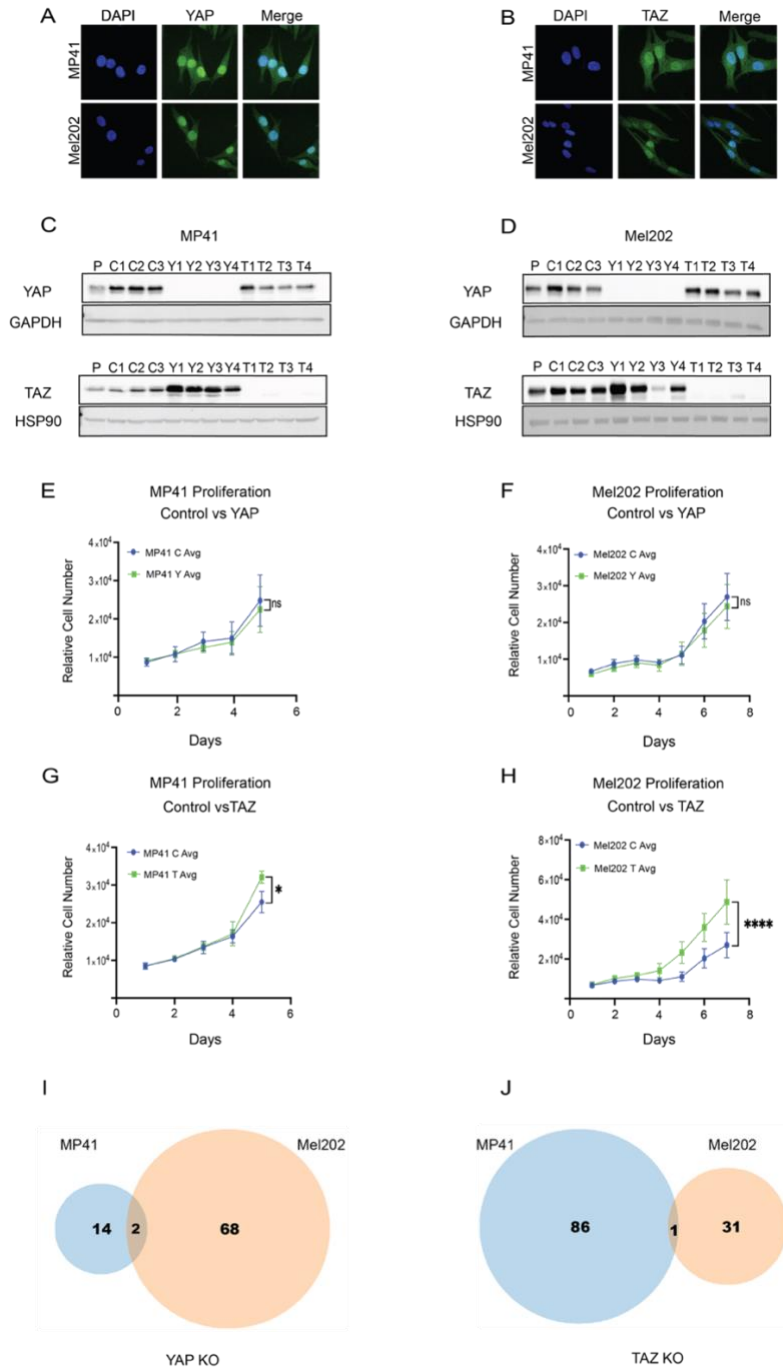
We wanted to extend our analyses of YAP versus TAZ to human UM. Initially, we examined the UM patient data set ( $n=80$  samples) present in The Cancer Genome Atlas (TCGA). Our analyses showed that decreased progression free survival was significantly associated ( $p < 0.0001$ ) with higher levels of *TAZ* mRNA (z score  $> 0.5$ ,  $n = 17$  patients) versus lower levels (z score  $< -0.5$ ,  $n = 31$  patients) (Fig S3A) but did not correlate significantly with higher levels of *YAP* mRNA ( $p = 0.1052$ ; Fig S3B). Furthermore, most patients with monosomy of chromosome

3, a key hallmark of metastatic UM, had higher levels of *TAZ* mRNA (75% of patients, z-score > 0.5; Fig. S3C) and/or *YAP* mRNA (67% of patients, z-score > 0.5; Fig. S3D). This finding is particularly intriguing in the case of *TAZ*, as this gene resides on chromosome 3 and thus the remaining *TAZ* allele must be more actively transcribed and/or the stability of the *TAZ* mRNA increased. Collectively, these results support a link between poor prognosis, monosomy of chromosome 3, and expression of YAP/TAZ in UM.

Having established that *YAP* and *TAZ* mRNAs are present in UM tumors, we turned to human UM cell lines to further probe their roles. We selected two lines, Mel202 and MP41, that carrying activating Q209L mutations in *GNAQ* or *GNA11*, respectively (Amirouchene-Angelozzi et al., 2014; Griewank et al., 2012). Initially, we performed immunofluorescence staining with anti-YAP and anti-TAZ specific antibodies and confirmed both cell lines contain YAP and TAZ proteins, which are predominantly nuclear (Fig. 4A and B).

Prior studies have shown that knock-down of YAP using shRNAs, is detrimental to UM cell viability (Barbosa et al., 2023; Feng et al., 2014; Yu et al., 2014). To directly test whether YAP or TAZ are absolutely required for UM cells, we transduced Mel202 and MP41 cells with retroviral vectors carrying the puromycin resistance gene, Cas9, and sgRNAs targeting *YAP*, *TAZ* or control sequences. After 6 days of drug selection, we plated single cells into 96 well plate, and allowed clones to grow out. For each guide and cell line, we picked many single cell clones and screened them for the presence of YAP and TAZ protein by western blotting. We successfully identified multiple clones for Mel202 and MP41 that had complete knockout of YAP (herein labeled as labeled Y clones) or TAZ (T clones) or carried control guides and continued to express both YAP and TAZ (C clones) (Fig 4C and D).

For both Mel202 and MP41, we selected four each of the Y and T clones, as well as three C clones, for in-depth analyses. First, we compared their levels of YAP and TAZ to those in the parental (P) Mel202 and MP41 lines (Fig 4C and D). Notably, all six of the C lines possess higher



**Figure 4. Active YAP and TAZ exist in human UM cells, but either proteins can be deleted without affecting viability *in vitro*.** (A-B) Immunofluorescence on fixed human UM cell lines, MP41 and Mel202, show that both express nuclear YAP and TAZ. (C-J) Control (labeled C), YAP knockout (Y) and TAZ knockout (T) single cell clones were generated by CRISPR mutagenesis in both MP41 and Mel202 and characterized. (C-D) Western blots for YAP, TAZ, HSP90 or GAPDH in C (n=3), Y (n=4), and T (n=4) clones, compared to parental for (C) MP41 and (D) Mel202. (E-H) Relative average proliferation rates of Y or T (n=4 each), versus C (n=3), clones for MP41 and Mel202, as indicated. Statistical analysis was conducted on the relative cell number at the final timepoint (unpaired t-test): (E) MP41 Y vs C  $p = 0.4063$ , (F) Mel202 Y vs C  $p = 0.3558$ , (G) MP41 T vs C  $p = 0.0197$  (\*), and (H) Mel20 T vs C  $p < 0.0001$ (\*\*\*\*). (G-H) Transcriptomic analyses were conducted on single samples for each of the Y and T clones for MP41 and Mel202, as well as 4 samples of each parental line that were generated on different days. The Venn diagrams indicate the number of differentially expressed genes ( $\geq 2$ -fold difference;  $p < 0.05$ ) and the overlap between the MP41 and Mel202 lines for: (I) Y clones and parental cells or (J) T clones and parental cells.

levels of YAP and TAZ than their relevant P line (Fig 4C and D), suggesting that the single cell clone process selects for cells with higher YAP/TAZ. We then examined the knockout cells. The T clones had no detectable TAZ, and no upregulation of YAP beyond that observed in the C clones (Fig 4C and D). The Y clones all completely lacked YAP and showed differences in TAZ. In the Mel202 Y clones, TAZ showed range of levels; Y1 had more than the C clones, Y3 had less than the P cells, and Y2 and Y4 were similar to the C clones or P cells respectively (Fig. 4D). In contrast, all four of the MP41-Y clones showed further upregulation of TAZ compared to the relevant C clones and considerably higher than the parental MP41 cells (Fig. 4C). Interestingly, it was noticeably harder to generate MP41-Y clones than any of the other clones (as judged by the frequency of generation). Taken together, our data show that UM cell lines can thrive in the absence of either YAP or TAZ but, at least in some contexts, this is accompanied by changes such as the upregulation of TAZ in the MP41 line.

Having shown that *YAP* or *TAZ* knockout UM cells are viable, we asked whether there was any impairment in their properties. First, we used the CyQuant assay (ThermoFisher) to measure their proliferation rates *in vitro* over 5 (MP41) or 7 (Mel202) days. First, we saw that the 5/6 of the C clones showed a higher rate of proliferation than their relevant P cell line, reaching statistical significance in the case of Mel202 clones (Fig. S4A-D). This is consistent with the notion that the single cell cloning is selecting for the fittest cells. We then analyzed the knockout lines. This showed that the Y clones of both cell lines, displayed no significant difference in average proliferation rate compared to their relevant C clones (Fig. 4E and F), and were typically more proliferative than their relevant P line (Fig. S4E and F). In contrast, the T clones showed a significant higher average proliferation rate than the C clones for both Mel202 ( $p < 0.0001$ ) and MP41 ( $p < 0.05$ ; (Fig. 4G and H) and were much faster than the P lines (Fig. S4G and H).

We also examined cell cycle phasing, using EdU/DAPI labeling and FACS to quantify the fraction of cells present in G1, S, or G2/M phases (Fig S5A-D). There was considerable variation in this assay, including for a single cell line from experiment to experiment, except for the Mel202

T lines, which consistently had a higher proportion of cells in S phase (Fig S5B). However, this did not hold true for the MP41 T lines, and the rest of the knockout cells all remained within the range observed for C clones and P lines. Taken together, these data show that the sustained loss of YAP or TAZ can occur without any negatively impact on the proliferative capacity or cell cycle phasing of UM cells *in vitro*.

Given this finding, as well as the observed upregulation of TAZ protein levels in the MP41-Y clones, we speculate that the knockout clones might have undergone adaptive changes during the selection process to compensate for the loss of YAP or TAZ. To address this, we performed RNA-sequencing on each of the *YAP* and *TAZ* knockout cells (single samples of each to serve as biological replicates), as well as four plates of parental cells grown on different days. We found remarkably little variability that could be explained by the absence of YAP or TAZ. In Principal Component Analysis (PCA), the cells did not cluster well by genotype (Fig S4 E and F). Moreover, our analyses identified a relatively modest number of genes that were significantly differentially-expressed (DE,  $\geq 2$ -fold difference and adjusted p value  $< 0.05$ ) between the *YAP* or *TAZ* knockout clones versus their relevant parental line and found only 2 genes for YAP clones and 1 gene for TAZ clones that showed significant differential regulation in both the MP41 and Mel202 cells (Fig 4I and J). Even the canonical YAP and TAZ genes *CCN1* and *CCN2* did not differ in their expression as a response of YAP or TAZ loss in MP41 and Mel202. Taken together, our data suggest the sustained loss of YAP or TAZ in UM cells caused minimal changes in the transcriptional program. Thus, if adaption is required to enable the knockout cells to thrive, it appears to be largely post-transcriptional.

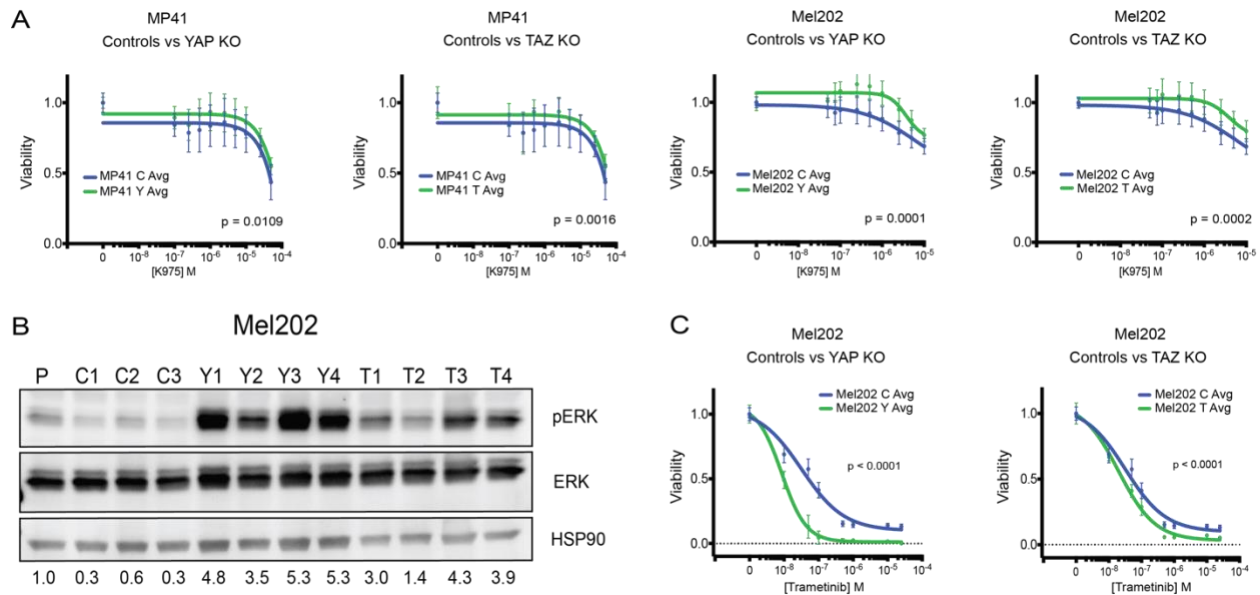
**Sustained absence of YAP or TAZ does not alter the sensitivity of UM cells to TEAD inhibitors but upregulates the levels of, and reliance on, MAPK signaling *in vitro*.**

A key goal of our studies is to identify vulnerabilities in UM cells that might inform therapeutic strategies. Our zebrafish studies showed that TEAD-interacting residues are essential

for YAP/TAZ to drive tumors and that the TEAD inhibitor, K975, suppresses the proliferation of melanocytic cells induced by *GNAQ<sup>Q209L</sup>*. Thus, we hypothesized that human UM cells lacking either YAP or TAZ would show increased sensitivity to K975 compared to controls. To test this, we conducted dose response curves with K975 in the parental UM cell lines, versus our clones, measured cell viability using REAL TIME Glo (Fig. 5A, Fig. S7-10). Consistent with recent reports (Barbosa et al., 2023), the parental MP41 and Mel202 cell lines, as well as their C clones, were relatively insensitive to K975; only half of the cells died at the highest possible K975 dose whether treated for 48 (Fig. 5A) or 74 hours (Fig. S6A). Unexpectedly, the MP41 Y (p=0.01), MP41 T (p=0.0016), Mel202 Y (p=0.0001) and Mel202 T (p=0.0002) clones all showed a modest, but significantly lower, average K975 sensitivity, compared to their relevant C clone controls (Fig. 5A, Fig S7-8). In the case of MP41 (Fig. S9), but not Mel202 (Fig. S10), the C clones were slightly (but not significantly) more sensitive to K975 than their parental lines. Thus, we also compared the KO clones to the parental lines; for MP41 there was no significant differences (Fig. S9), while the Mel202 Y (p=0.001) and T (p=0.0014) clones were less sensitive to K975 than the P cells (Fig. S10). Together, these experiments show that the loss of either YAP or TAZ does not increase the vulnerability of UM cells to TEADi *in vitro*.

We hypothesized that the knockout cells have compensated for the loss of YAP or TAZ by increasing the activity of the remaining YAP/TAZ paralog and/or shifting their dependence to other signaling pathways. Considering the latter possibility, we wondered whether these cells showed increased reliance on the other major GαQ/11 effector pathway, MAPK signaling. We addressed this in two ways. First, we used western blotting to compare the levels of active pERK, as well as total ERK, in all the cell lines. Total ERK levels were relatively constant across all the samples, but pERK levels varied considerably. Thus, we quantified the ratio of pERK to HSP90 (loading control) to allow cross sample comparisons. For Mel202, the pERK/HSP90 ratio was reduced in the three C clones compared to the parental cells (0.39 fold down, Figure 5B) indicating that the single cell cloning process does not select for increased MAPK signaling by default.

Notably, the pERK/HSP90 ratio was increased in all four of the Mel202-T clones (average is 8.2-fold higher than that of the C clones and 3.2-fold higher than P line) and even more upregulated in the four Mel 202-Y clones (avg. 12.2-fold higher than the C clones and 4.7-fold higher than P). For the MP41 parental cells and clones, at a general level pERK was present at much lower levels (Fig S6B). The second way we probed MAPK's contributions was to compare the C, Y and T clones' response to the MEKi, trametinib, over a range of concentrations (0 to 25  $\mu$ M). The highest trametinib drug concentration was very effective, killing 85-90% of the Mel202 (Fig. 5C) and MP41 cells lines (Fig. S11) after 48 or 97 hours respectively. We found that trametinib sensitivity was significantly higher for the Mel202-Y ( $p < 0.0001$ ), Mel202-T ( $p < 0.0001$ ) and MP41-Y ( $p < 0.0001$ ) clones, compared to their relevant C clones controls (Fig. 6C and Fig. S11). The MP41-T clones also trended to higher sensitivity, but this did not reach statistical significance. Collectively, these results support the notion that the UM cells increase their reliance of additional pathways, including MAPK, to adapt to loss of YAP or TAZ in the context of *in vitro* culture.



**Figure 5. Loss of YAP or TAZ in UM cell lines leads to increase sensitivity to MEK inhibition**  
 (A) MP41 and Mel202 control (C, n=3) and KO cell lines (Y or T, n=4) were treated for 48hr with DMSO alone or a range of concentrations of the TEAD inhibitor, K975. Graphs shows viability relative to the DMSO alone samples. Statistical analysis was performed after calculating the area under the curve (AUC) for each individual replicate and conducting unpaired t-testing (see Fig S7 – S10 for more details). (B) Western blot of pERK and ERK in Mel202 cell lines lysates. Numbers at the bottom of the blot show the pERK/HSP90 ratio, relative to that of the parental, which was set to 1. Quantification was done using the Image Studio Lite software. (C) Mel202 control (C, n=3) and KO cell lines (Y or T, n=4) were treated for 48 hr with DMSO alone or a range of concentrations of the MEK inhibitor Trametinib. Graphs show viability relative to the DMSO alone samples. Statistical analysis was performed as in (A) above (see Fig S11- S15 for more details).

### **YAP or TAZ are dispensable for tumor formation *in vivo***

Several prior studies have reported that knockdown of YAP decreases the viability of UM cells and reduces their tumorigenicity in xenograft models, including in the Mel202 line (Barbosa et al 2023; Feng et al 2014; Yu et al 2014). Thus, we directly tested the tumorigenic potential of the P line, as well as two each of the C, Y and T clones, for both MP41 and Mel202. We introduced these cells [75,000 for MP41 and  $10^6$  for Mel202, per recipient (n=4)] into the left ventricle of non-obese diabetic gamma (NOD) mice by ultrasound-guided injection, which causes them to be widely distributed throughout the body and makes most tissues available for colonization. We monitored the recipient's health with regular weighing and euthanized test animals and appropriate controls when the first animals showed evident weight loss. Importantly, autopsy revealed the presence of visible liver tumors in many recipients, recapitulating the overwhelming tendency of human UM to metastasize to liver (Kaliki & Shields 2017). We also observed enlarged adrenal glands in some animals and thus conducted histological analyses on the livers, adrenal glands, and kidneys. H&E-staining showed that all cell lines/genotypes yielded liver tumors, to some degree. To quantify liver tumor burden, we trained the Qu Path program to quantify tumor versus normal cells from one slide (which includes a section with various pieces of liver per mouse) and calculate the percentage of tumor cells (Fig 6a.).

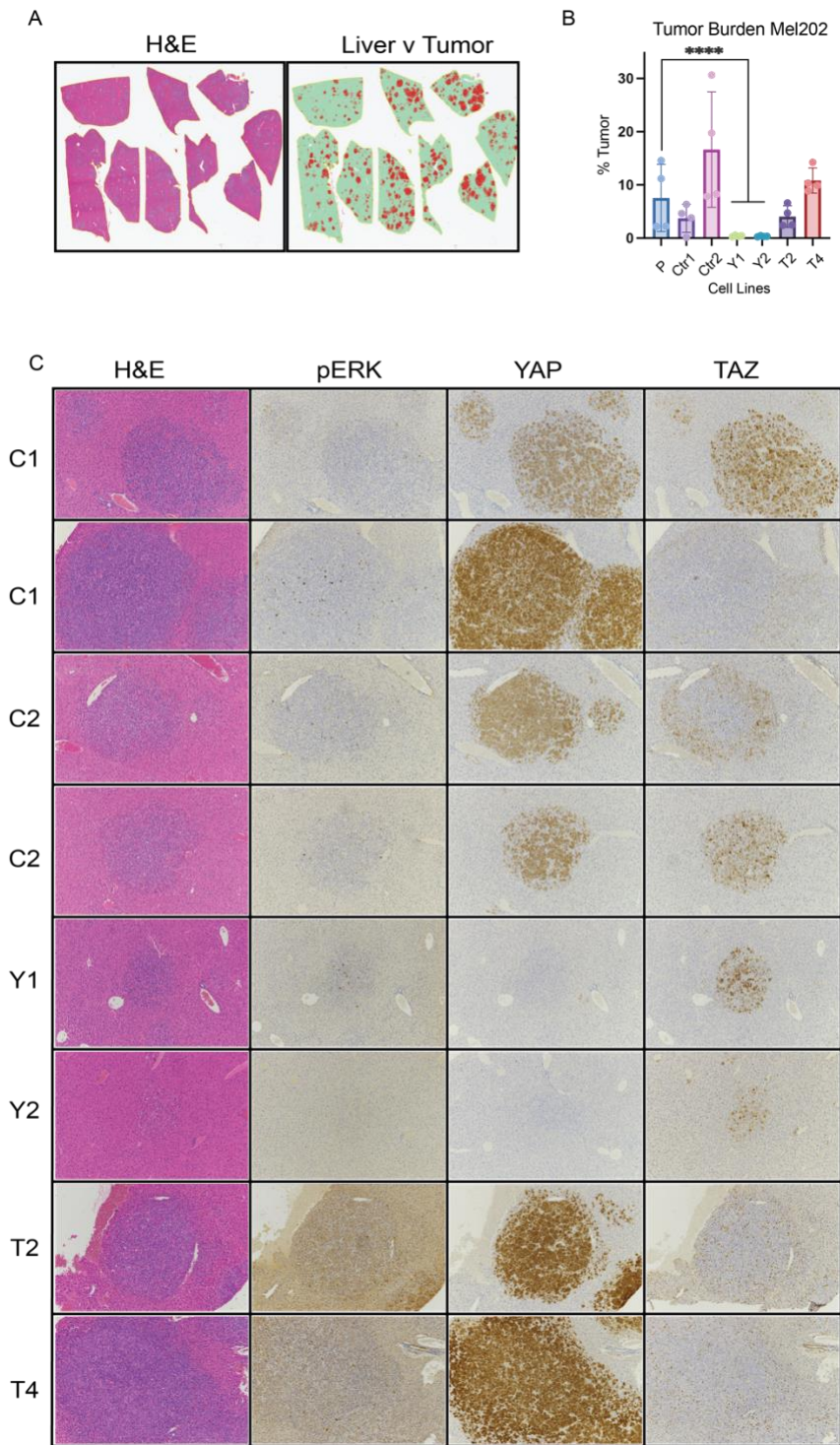
For MP41, a single clone, Y3, resulted in dramatic weight loss by 3 weeks of age and thus we euthanized these animals, along with P, C1 and C2 (n=4) controls. All four Y3 mice had significant liver tumors (average burden = 13%). In contrast, P, C1, and C2, had an average tumor burden of <1% (Fig. S22A). We launched a second MP41 cohort, with all clones except Y3, and harvested this at 4 weeks of age. In this context, the percentage of tumor cells remained <1% for all cell lines (Fig. S22B). C1 exhibited the highest average tumor burden (0.73%), remaining below 1%. C2 and Y1 had the lowest tumor burden, where C2 failed to make tumors in the liver of all mice, and only one mouse for the Y1 cohort yielded liver tumors, with a 0.035% burden. There was variation between the two Y and two T clones, but their tumor burden was within the range of, or higher (for Y3) than, the controls. We conducted IHC for YAP, TAZ and pERK (Fig. S23).



The parental and control lines showed strong, consistent staining for YAP and variable TAZ, while the pERK signal was low and heterogenous. As expected, the YAP- or TAZ-deficient clones completely lacked the deleted protein. The remaining TAZ or YAP stayed within the range of controls, and there was no increase, or broadening, of pERK. Collectively, these data indicate that YAP or TAZ is fully dispensable for the tumorigenicity of MP41, without any obvious increase in the other paralog or the MAPK pathway signaling. These data closely resemble the phenotypes of our zebrafish YAP/TAZ wildtype and knockout UM tumors.

For Mel202, the transplant recipients were euthanized at 6 weeks. There was some variation in the liver tumor burden in the P, C1 and C2 controls, ranging between 3 and 16% (Fig. 6b). The two T clones were well within this control range and there was no statistically significant difference between the P, C and T clones (Fig 6b). In contrast, the Mel202-Y clones yielded considerably lower tumor burden (Fig 6b). This was true for both Y clones, and in all four recipients (Fig. 6b), because the tumors were much fewer and smaller. H&E-staining confirmed the presence of adrenal gland (but never kidney) tumors in some mice, with the prevalence closely matching the liver burden (Fig. S16).

As above, we conducted IHC on the liver tumors (Fig. 6C). The phenotypes of Mel202 controls (P and C) mirrored those of MP41, with the only difference being that nuclear YAP and TAZ showed a somewhat higher degree of variance. For the Mel202-T tumors, TAZ was completely absent, pERK mirrored the heterogeneity of the controls, and nuclear YAP was consistently at the higher end of the range observed for control tumors. The rarer and smaller Y tumors had appropriately lost YAP and mirrored both the heterogenous pERK and range of TAZ levels seen in the controls. The simplistic interpretation of these results is that YAP and TAZ play overlapping roles in promoting Mel202 tumors and deletion of TAZ is well tolerated, in part by selecting for higher normal levels of YAP, while YAP deletion fails to select for higher TAZ levels and impairs, but does not fully suppress, UM tumors.



**Figure 6. YAP or TAZ is dispensable for *in vivo* tumor growth.**  $10^6$  Mel202 parental (P) cells, or representative control (C1 & 2), YAP KO (Y1 & 2) or TAZ KO (T1 & 4) clones were injected into the left ventricle of NSG mice ( $n=4$ /cell type) and euthanized when we observed weight loss in the first animals. (A) Representative images for the QuPATH program that identifies tumor versus normal liver tissue in the H&E images. (B) Bar graph of percent of total tissue identified as tumor for each cell line. Y1 and Y2 were significantly different from parental ( $p<0.0001$ ); all others were n.s. (C) Representative slides of liver sections (10X) from the indicated cell line/clones stained with H&E or IHC for: pERK, YAP, and TAZ.

## Discussion

Previous work, from us and others, has shown that YAP is a key player in UM tumor progression (Feng et al., 2014, Li et al., 2019, Phelps, et al., 2022a, Yu et al., 2014). In this study, we address the requirement for YAP in UM. In the context of zebrafish, we showed that *yap* is fully dispensable for *GNAQ<sup>Q209L</sup>*-driven UM *in vivo*. This led us to discover that *taz* plays a similar role to *yap*: constitutively active forms of either paralog can drive UM in zebrafish, but either *yap* or *taz* can be deleted without altering the course of *GNAQ<sup>Q209L</sup>*-driven UM development. Our analyses further show that the ability of YAP and TAZ to drive UM fully depends on a single residue that is required for TEAD interaction, and that *GNAQ<sup>Q209L</sup>*-driven phenotypes are suppressed by TEADi. The simplest conclusion of these data is that YAP and TAZ play functionally redundant roles in enabling zebrafish UM development in a TEAD-dependent manner.

Our analyses of human UM cells are consistent with redundant function of YAP and TAZ. We find that deletion of either gene does not impair the viability or proliferative response of two different UM cell lines, Mel202 and MP41, *in vitro*. Moreover, it does not prevent either cell line from forming liver tumors in transplant assays. In the case of MP41, there is no detectable impairment in tumorigenesis. Indeed, one the YAP-deficient lines is much more efficient at producing tumors than any of the control lines. The MP41 YAP- and TAZ-deficient tumors show no differences in the levels of the remaining TAZ/YAP paralog or pERK, compared to controls, arguing that these normal levels are entirely sufficient to compensate for the missing YAP or TAZ. In Mel202, the situation is more nuanced. TAZ-deficient UM liver tumors are prevalent, but clearly display levels of nuclear YAP at the higher end of the normal spectrum. Even more striking, YAP-deficiency does not prevent tumor formation, but it greatly reduces both the number and size of liver tumors, without detectable upregulation of TAZ or pERK. These observations, suggest a shared role for YAP/TAZ, and particularly YAP, in driving Mel202 *in vivo*. Importantly, the

phenotypes of the human UM transplant tumors, and the conclusion of functional redundant roles for YAP and TAZ, mirrors our zebrafish tumor studies.

The consistency of these *in vivo* results serves to highlight our finding that the human knockout cells display clear differences *in vitro* versus *in vivo*. The most striking is that the Mel202 Y have no proliferation defects *in vitro*, but show a profound reduction in tumor burden *in vivo*. Additionally, we see differences in the contribution of MAPK pathway signaling. Specifically, the knockout clones show evidence of increased dependence on MAPK pathway signaling *in vitro*, including upregulation of pERK and/or heightened sensitivity to MEKi, while the *in vivo* tumors all show low level and heterogenous pERK staining, irrespective of genotype. We hypothesize that these *in vitro* versus *in vivo* differences result from adaption events during the single cell cloning process, together with context-dependent differences in growth factor availability. Specifically, we speculate that the knockout clones, and particularly the Mel202 Y clones, increase use of the MAPK pathway to compensate for YAP/TAZ loss, which is enabled by the presence of growth factors in the culture media. However, transplantation involves removal from serum, reducing pERK signaling and offering a fairer assessment of the impact of YAP or TAZ loss.

Interestingly, various prior studies have investigated YAP's requirement in human UM cell lines and arrived at opposing conclusions; some use knockdown approaches and reporting a critical role (Barbosa et al., 2023; Brouwer et al., 2021; Feng et al., 2014; Yu et al., 2014) and others, using either knockdown (Kim et al., 2020) or CRISPR mutagenesis (Ma et al., 2020), conclude that YAP is dispensable. We presume that these varying results reflect context dependent differences in the ease of cellular plasticity, which could be due to different cell lines or a consequence of acute versus sustained inactivation of YAP at the time of analyses.

We believe that the observed *in vitro* versus *in vivo* discrepancies have critical implications for consideration of therapeutic strategies for UM. Prior studies have shown that numerous UM cell lines are responsive to MAPK inhibitors *in vitro* (Amirouchene-Angelozzi et al., 2014; Faiao-Flores et al., 2019). In contrast, MAPK pathway inhibitors were found to be largely ineffective in

a genetic mouse model of UM (Moore et al., 2018) and, most importantly, in human UM patients. Additionally, we saw a relatively weak response of both Mel202 and MP41 lines to TEADi *in vitro*, which was not altered by YAP- or TAZ-deficiency. *In vitro* studies in a panel of UM cell lines also reported poor responsiveness to TEADi (Barbosa et al., 2023). In contrast, in the *in vivo* context of zebrafish, we found that YAP/TAZ drive UM in a TEAD-dependent manner, and TEADi successfully suppress *GNAQ*<sup>209L</sup>-induced embryo phenotypes. Given these findings, we are concerned that the *in vitro* culture context does not appropriately model the efficacy of small inhibitors on UM, because it over-emphasizes MAPK signaling and thus underestimates YAP/TAZ-TEAD biology. Consequently, we believe it is crucial that inhibitors are tested in *in vivo* context models, and think our zebrafish embryo assay offers a relatively tractable approach (Phelps et al., 2022b). Finally, we think it would be fascinating to assess the consequences of deleting *yap* or *taz* in existing UM tumors, to see if they can survive, and whether this involves the MAPK pathway or other signaling mechanisms.

## Materials & Methods

### Zebrafish lines

Zebrafish were maintained using protocols approved by the Committee on Animal Care at MIT. Experiments were performed in the AB/Tübingen (TAB5/14) genetic background. The *yap<sup>mw48/+</sup>* zebrafish described in Miesfeld et al., 2015 were obtained from Dr. Wolfram Goessling (Brigham and Women's) and Brian Link (Medical College of Wisconsin). The *ta<sup>z</sup><sup>mw49/+</sup>* zebrafish were obtained from Dr. Brian Link (Medical College of Wisconsin). *Tg(mitfa:GNAQ<sup>Q209L</sup>);tp53<sup>-/-</sup>* zebrafish are the Q-1 transgenic line from Perez et al., 2018. Zebrafish were euthanized upon moribund tumor burden for Kaplan-Meier curves.

### Plasmids

Gibson assembly was used to insert the following into the EcoRI site of the GOI-GFP vector: TAZ<sup>S89A;S311A</sup> (generated via Gibson PCR and assembly to mutate c.311AG>GC on a TAZ<sup>S89A</sup> plasmid (MSCV-TAZ<sup>S89A</sup>, provided by R. Hynes, MIT)), TAZ<sup>S89A;S311A;S51A</sup> (generated via Gibson PCR and assembly to mutate c.51T>G on the GOI-GFP TAZ<sup>S89A;S311A</sup> plasmid), YAP<sup>S127A;S381A;S94A</sup> (generated via Gibson PCR and assembly to mutate c.94T>G on the GOI-GFP YAP<sup>S127A;S381A;S94A</sup> plasmid), zebrafish codon-optimized Cas9 (Ablain et al., 2015) (Addgene #63155).

### Zebrafish Histopathology & Immunohistochemistry

Zebrafish were fixed in formalin, de-calcified with EDTA, bisected, embedded in paraffin, and ultimately sectioned (4µm thick) at multiple steps throughout the fish. One slide per step was stained with hematoxylin and eosin (H&E), and sequential unstained slides were used for immunohistochemistry (IHC). Immunohistochemistry (IHC) analyses and imaging were carried out as previously described (Perez et al., 2018). Primary antibodies were: phospho-ERK1/2 (1:200; #4370 Cell Signaling), and YAP/TAZ (1:200; #8418 Cell Signaling). The YAP/TAZ antibody specifically recognizes TAZ in zebrafish – see Sup Fig 4 in the Brandt et al., Development. 2020.

### qRT-PCR

Zebrafish tumor RNA was reverse transcribed using SuperScript III Reverse Transcriptase (Thermo Fisher). Real-time PCR reactions were performed in triplicate using FAST-SYBR Green on a StepOnePlus Real-Time PCR System (Applied Biosystems). Data were analyzed using the  $\Delta\Delta C_T$  method and relative messenger RNA (mRNA) levels were normalized to *actb2* (Beta Actin 2) levels and average average gene expression in wild type controls.

## **Chemical Inhibitor Assays in Zebrafish**

*Tg(mitfa:EGFP)* zebrafish were crossed to either control or homozygous *Tg(mitfa:GNAQ<sup>Q209L</sup>)* and 60-80 embryos were collected of each genotype per sample (DMSO or Drug). These were kept in petri dishes and, after removing the chorion, drug was dissolved in DMSO and directly added to zebrafish water, 30 hours post-fertilization. For this experiment we used K975 (MedChemExpress #HY- HY-138565). 5 days post fertilization, GFP+ cell population was quantified using the dissociation and flow cytometry analysis protocols detailed in Phelps, Amsterdam et al., 2022. FlowJo Software was used to analyze data.

## **Human cell lines**

Mel202 was obtained from Sigma Aldrich (13012457) and MP41 was obtained from ATCC (CRL-3297). Cells were cultured on tissue-culture treated plates in RPMI 1640 with L-glutamine (Thomas Scientific B003K46) supplemented with 10% fetal bovine serum and 1% penicillin/streptomycin and incubated at 37°C with 5% CO<sub>2</sub>.

CRISPR mutagenesis was performed using the lentiCRISPRv2 (Addgene #52961) lentivirus system (expressing an sgRNA against YAP: [5' - GGACTCGGAGACCGACCTGG] or TAZ: [5' – GCAAGTGATCCACGTCACGC, or scrambled sgRNA], cloned as described in Sanjana et al., 2014; Shalem et al., 2014. Transfection was performed using TransIT-LT1 Transfection Reagent (MIR 2305) per manufacturer's instructions and selected with puromycin at 2.5 µg/mL for MP41 or 5 µg/mL for Mel202 for 6 days. Cells were plated in multiple 96-well plates at an average of 0.5 cells/well and later screened for singular colony formation, and resulting single-cell clones were scaled up for characterization.

## **Immunofluorescence**

125,000 Mel202 cells or 75,000 MP41 cells were plated in a 6-well plate with coverslips. Cells were fixed with 4% PFA for 10min upon reaching 60% confluence and immunofluorescence was carried out as previously described (Wilson et al., 2021). Primary antibodies: YAP (1:100; Cell Signaling #14074) or TAZ (1:100; Cell Signaling #83669). Secondary antibody: Goat-anti Rabbit 488 (1:500; Thermo Scientific #A-11008). Stained with DAPI 1:1000. Coverslips were imaged on an Olympus FV1200 Laser Scanning Confocal Microscope and processed using Fiji Image J.

## **Viability assays**

Viability was measured using RealTime-Glo MT Cell Viability Assay (Promega, G9712). Uveal melanoma cell lines were plated on 96-well white-walled, flat clear-bottom plates. Cell lines were plated at 500 cells/well. Two K975 (MedChemExpress #HY-138565) experiments were designed, one with all cell lines (Ps, Cs, Ys, Ts) of both MP41 and Mel202 treated with drug for 48hrs. The

second set of K975 experiment consisted of only parental MP41 and Mel202 cell lines treated for 74.5hrs. 24 hours after plating, K-975, dissolved in DMSO, was added at the appropriate concentration to each well in triplicate. K975 dose range for MP41 and the 74.5hrs experiment was from 0 to 50uM, while the 48hr Mel202 range went from 0 to 10uM. RealTime-Glo was added after 24hrs in drug and luminescence was measured every 12 hours until final timepoint using a Tecan M200 Pro. Normalized viability data from dose-response curves was fit to a 4-parameter hill curve as previously described (Mueller et al., 2021).

For Trametinib (MedChemExpress #HY-10999) experiment, cell lines were plated on 96-well white-walled, flat clear-bottom plates. Mel202 cells were plated at 500 cells/well, while MP41 were plated at 100 cells/well. Mel202 cells were treated with trametinib, dissolved in DMSO, for up to 48hrs, and MP41 cells were treated until 97hrs. Dose range went from 0 to 25uM. RealTime-Glo, readings and normalization of viability data were performed as described above.

### **Western blots**

Cells were washed with PBS, pelleted and frozen at -80°C, and resuspended in 100µL radioimmunoprecipitation assay (RIPA) lysis buffer [50 mM Tris [pH 8.0], 150 mM NaCl, 1% Nonidet P-40, 0.5% sodium deoxycholate, and 0.1% sodium dodecyl sulfate (SDS)] supplemented with protease inhibitor mixture (MilliporeSigma 11697498001), and lysed on ice for 30 minutes with intermittent vortexing every 10 minutes. Debris was pelleted at 4°C and protein supernatant quantified using the BCA Protein Assay Kit (Thermo Fisher 23225). A total of 40µg of protein was used for YAP and TAZ western blots, while 30µg of protein was used for the pERK and total ERK western blots. Western blots were performed as previously described (Mueller et al., 2021). Primary antibodies: YAP (1:1000; Cell Signaling #14074), TAZ (1:1000; Cell Signaling #83669), pERK (1:1,000; Cell Signaling, #8544), ERK (1:1,000; Cell Signaling, #4696), HSP90 (1:2000; BD Biosciences, #610418), or GAPDH (1:5000, sc-365062 Santa Cruz Biotechnology), overnight at 4°C. Secondary antibodies: anti-Rabbit (1:10000, LI-COR BioScience #925-68073) or anti-Mouse 700 (1:10000, LI-COR BioScience #925-68072). Blots were imaged using the BIO-RAD ChemiDoc Imaging System.

### **RNA-Sequencing and Differential Gene Expression Analysis**

One 10 cm plate of cells at 40-50% confluence was collected from each cell line for RNA extraction. Cells were trypsinized, pelleted, resuspended in TRIZOL (Invitrogen 15596026), and frozen at -80°C. RNA was purified from thawed lysates following manufacturer's instructions and resuspended in RNase-free water.

RNA quality was confirmed using the Fragment Analyzer (Agilent Technologies) and RNAseq libraries were prepared from 2-10ng of total RNA using the NEBNext Poly(A) mRNA magnetic isolation module (New England Biolabs E7490) and NEBNext UltraII RNA library prep kit for Illumina (New England Biolabs E7770). Libraries were prepared following the manufacturer's



recommended protocol using 12 cycles of PCR using unique dual indexes. Libraries were validated by sizing using the Fragment Analyzer and quantified by qPCR. Libraries were sequenced as a single end 75nt read on an Illumina NextSeq550 using a 75nt high output kit. RTA version 2.4.11, NextSeq control software version 2.2.0.4.

RNA-seq data was used to quantify transcripts from the hg38 mouse assembly with the Ensembl version 106 annotation using Salmon version 1.6.0 (Patro et al. 2017). Gene level summaries were prepared using tximport version 1.24.0 (Soneson, Love, and Robinson 2015) running under R version 4.2.1 (R Core Team 2021). Differential expression analysis was done with DESeq2 version 1.36.0 (Love, Huber, and Anders 2014; Anders and Huber 2010) and differentially expressed genes were defined as those having an absolute  $\log_2$  fold change greater than 1 and an adjusted p-value less than 0.05. Data parsing and clustering was done using Tibco Spotfire Analyst 7.6.1. Preranked Gene Set Enrichment Analysis (Mootha et al. 2003) was done using javaGSEA version 4.3.2 with msigDb version v2022.1 (Subramanian et al. 2005) gene sets.

### **Patient Data (TCGA) analysis**

RNA-sequencing of primary tumors and corresponding survival data were obtained from The Cancer Genome Atlas (TCGA) PanCancer Atlas database of uveal melanoma (UVM; n = 80 patients). Z-scores were calculated for each queried gene across each patient in the mRNA expression, RSEM, batch normalized from Illumina HiSeq\_RNAseqV2 RNA-seq dataset. Chromosome 3 aneuploidy was obtained from patient sample data.

### **Mouse and ultrasound intracardiac injection of human cell lines**

Animal studies were approved by the Committee for Animal Care at MIT. Nod Scid Gamma (NSG) female mice were purchased from Jackson Laboratory (Stock #005557). Mice were kept in clean housing to avoid exposure to contaminants that could compromise their health. Injections were carried out as detailed in Henning et al., 2024. Procedure does not require post-op care with NSAIDs or heat. Mice recovered immediately and remained under observation with weekly weight measurements until euthanasia.

### **Euthanasia, tissue harvest, and fixation**

Euthanasia was carried out according to humane practices. CO2 chamber was used followed by cervical dislocation before autopsy. Liver and kidneys were removed and immediately placed in formaldehyde (%) for 48hrs, then removed and kept in 70% ethanol. Afterwards, different lobes from the liver of each mouse were sectioned and sent for paraffin embedding. The kidneys were cut longitudinally and sent for paraffin embedding.

## **Mouse H&E and Immunohistochemistry**

4 $\mu$ M sections were mounted onto slides from the paraffin embedded liver or kidney tissues. One slide was stained with hematoxylin & eosin and unstained slides were obtained for immunohistochemistry (IHC). IHC was performed using the following primary antibodies: TAZ (Cell Signaling #83669), pERK (Cell Signaling #4370), ERK (Cell Signaling 4696) and YAP (Abcam #52771). Secondary antibodies were biotinylated Anti-rabbit Vector BA-1000 and, specifically for ERK staining, biotinylated Anti-mouse Vector BA-1000. Images were captured using the Leica Aperio Slide Scanner and Aperio eSlide Manager or the Nikon Eclipse Ci and NIS Elements Software. Immunohistochemistry (IHC) analyses and imaging were carried out as previously described (Perez et al., 2018) with a minor change in the developing kits used. DAB solution with the Vector Laboratories DAB substrate (HRP) kit (SK-4100) was used for YAP or the Eprdia DAB Quanto Detection System (TA-060-QHDX) for TAZ and pERK.

## **Edu/DAPI labeling for Cell Cycle Analysis**

Cells were plated at  $2 \times 10^5$  cells per 10 cm dish (MP41) or  $4 \times 10^5$  cells per 10 cm dish (Mel202) and allowed to grow for 3 days. Cells were then pulsed with 10 $\mu$ M EdU in media for 45 minutes, washed with PBS, trypsinized, and fixed for 15 minutes in 4% formaldehyde. After fixation, cells were washed once in PBS, then incubated for 5 minutes in PBS + 1% BSA, followed by an incubation of 15 minutes in PBS + 1% BSA, 0.5% TritonX-100, then incubated for an additional 30 minutes in PBS + 100mM ascorbic acid, 1mM CuSO<sub>4</sub>, plus 1 $\mu$ M AlexaFluor 488 Azide for cell labeling. Afterwards, cells were washed once in PBS + 1% BSA, 0.5% TritonX-100, then incubated in PBS + 1% BSA, 0.5% TritonX-100, 100 $\mu$ g/ml RNase, 1 $\mu$ g/ml DAPI for 1 hour prior to Flowcytometry Analysis. Cells were gated as 2N or 4N by DAPI and gated as EdU+ by comparison to control lacking Alexa stain. Cells were then assigned as G1=2N, Edu-; S=2N-4N, Edu+; G2/M=4N, Edu-

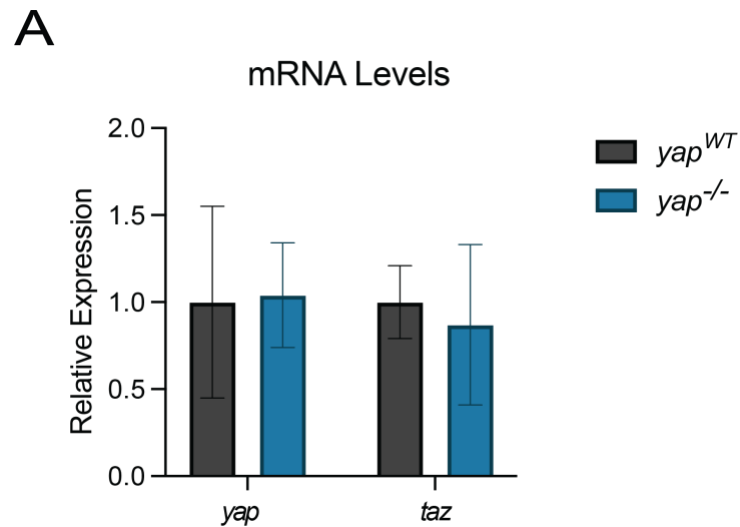
## **Statistical analyses**

Prism software was used to analyze data, draw graphs, and perform statistical analyses. Zebrafish and human Kaplan Meier/survival statistics determined by log-rank test.

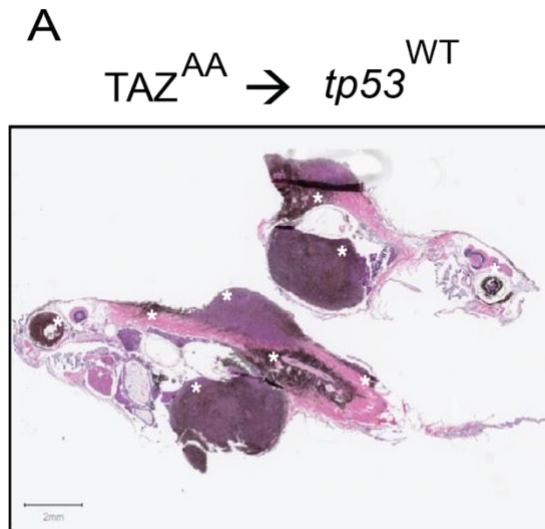
## **Acknowledgements**

This work was supported in part by the Koch Institute Support(core) Grant P30-CA14051 from the National Cancer Institute (NCI). We want to thank the Koch's Institute's Robert A. Swanson (1969) Biotechnology Center for technical support, specifically: the Barbara K. Ostrom (1978) Bioinformatics and Computing Core Facility, Hope Babette Tang (1983) Histology Facility, Preclinical Modeling, Imaging & Testing Core, Nanowell Cytometry Platform, and Zebrafish Facility.

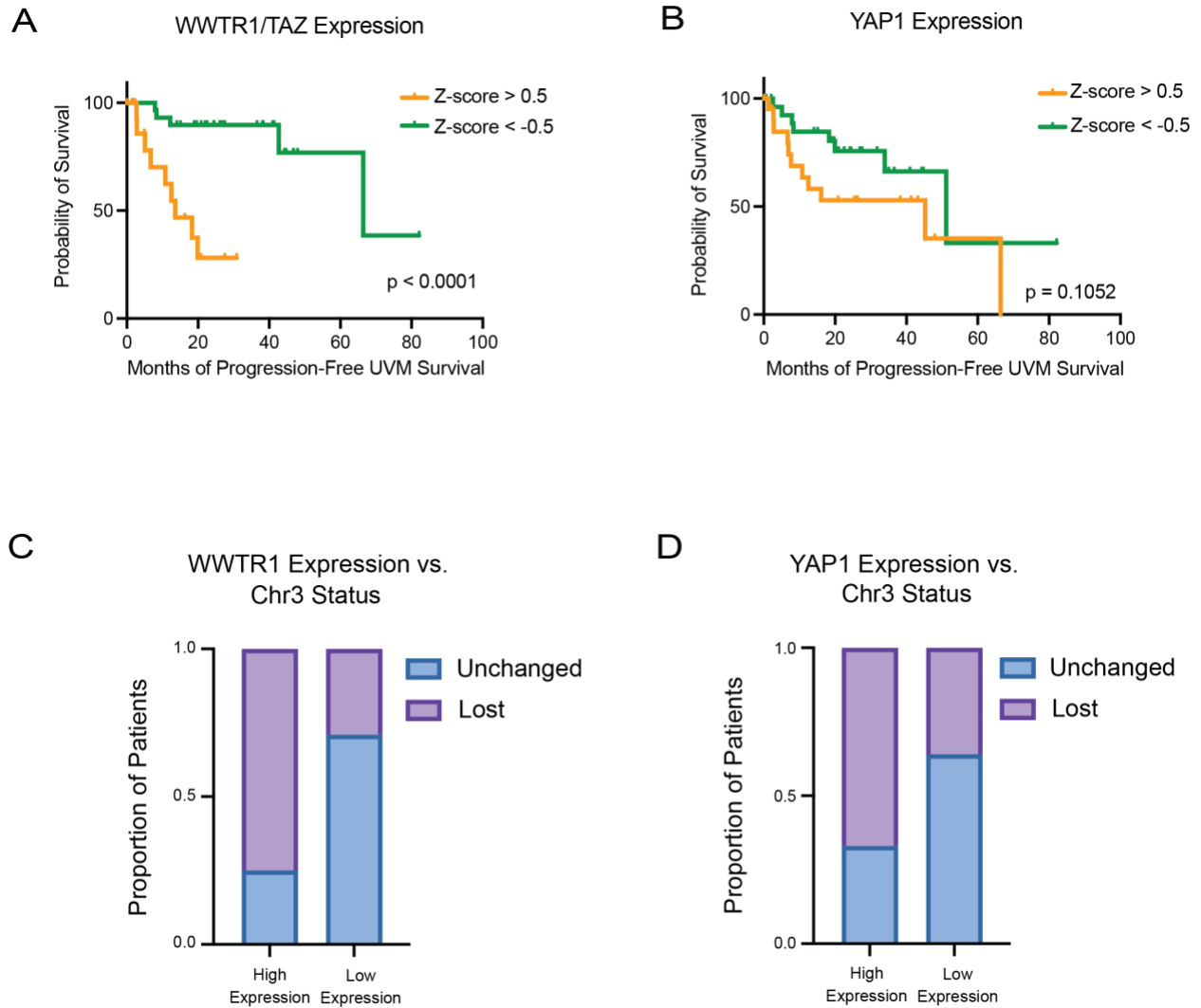
## Supplementary Figures



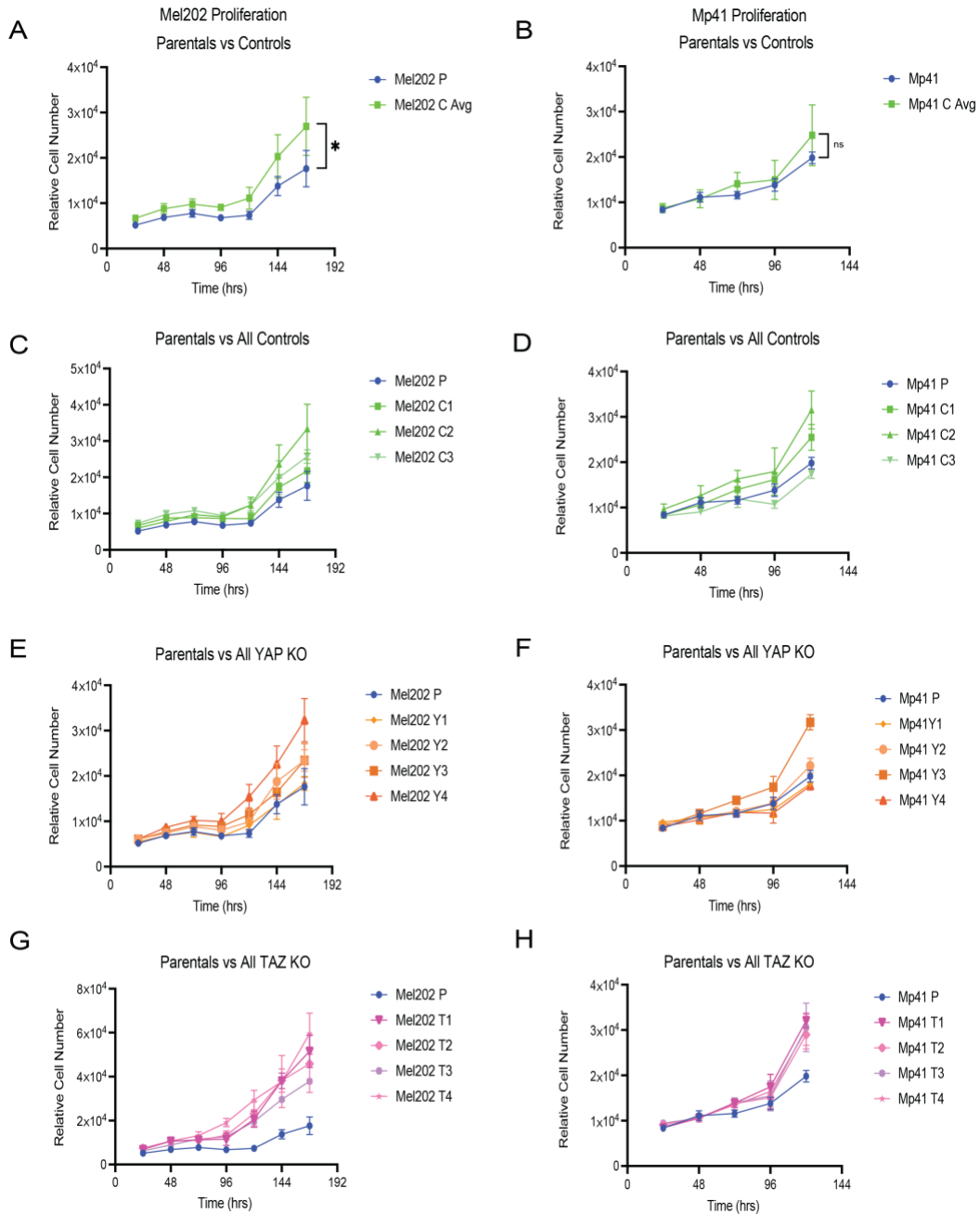
**Figure S1. *yap*<sup>-/-</sup> tumors express the same mRNA levels of YAP and TAZ as *yap*<sup>WT</sup> tumors (A)** Graph shows qRT-PCR results from zebrafish tumors. mRNA expression levels are relative to gene expression levels in *yap*<sup>WT</sup> tumors.



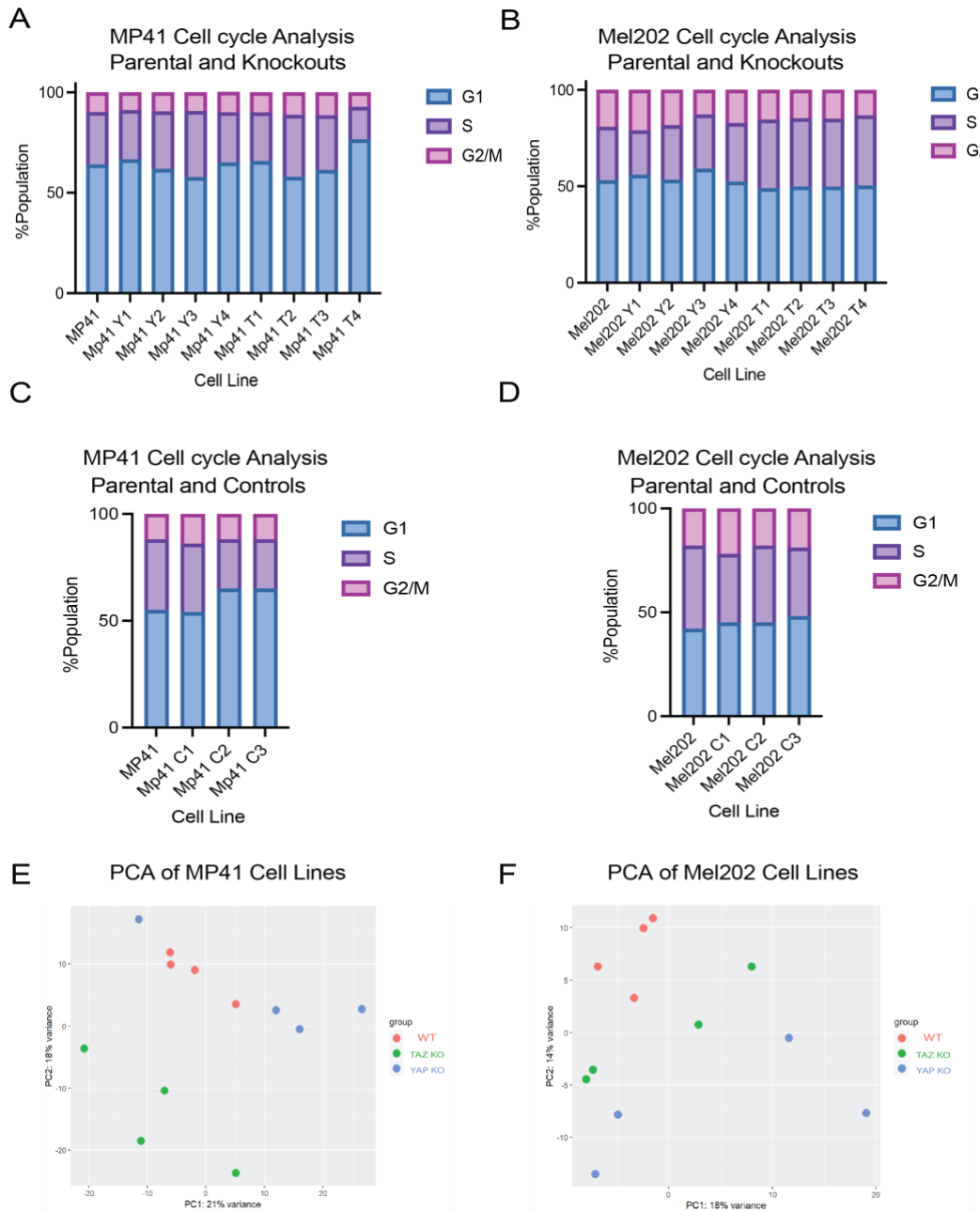
**Figure S2. *TAZ*<sup>AA</sup> generates multifocal tumors across the animal in a wildtype background (A)**  $TAZ^{AA} \rightarrow tp53^{WT}$  generated multiple tumors (denoted by \*) across the body of the zebrafish, similar to  $TAZ^{AA} \rightarrow tp53^{-/-}$ .



**Figure S3. Higher TAZ/WWTR1 expression correlates with poor prognosis.** (A) Higher WWTR1/TAZ mRNA expression (Z-score > 0.5, n = 17 patients) significantly correlates with decreased progression-free UVM survival, compared to lower WWTR1/TAZ expression (Z-score < -0.5, n = 31 patients) ( $p < 0.0001$ , determined by log-rank test). (B) Higher YAP1 mRNA expression (Z-score > 0.5, n = 22 patients) does not significantly correlate with progression-free UVM survival compared to lower YAP1 expression (Z-score < -0.5, n = 28 patients) ( $p = 0.1052$  n.s.), but higher YAP1 expression trends towards lower progression-free UVM survival. (C-D) Proportion of UM patients with monosomy, or unchanged status, of chromosome 3 possessing high versus low levels of: (C) TAZ mRNA or (D) YAP mRNA.

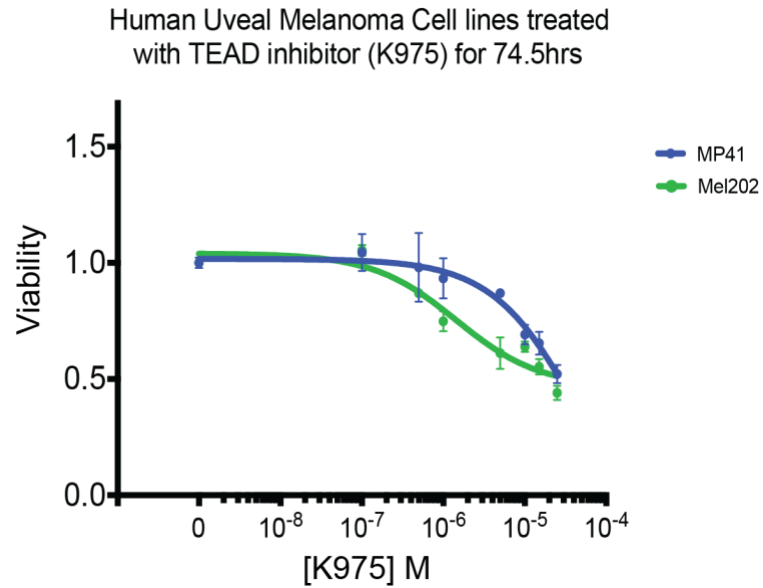


**Figure S4. Relative proliferation of control, YAP knockout and TAZ knockout clones, compared to their parental UM cell lines.** (A) Relative proliferation of Mel202 parental and control (Cs) cell lines average (n =3) show a significant difference in proliferative capacity of the controls relative to parental (p = 0.0422). (B) Relative proliferation of Mp41 parental and control (Cs) cell lines average (n =3) shows no significant difference in proliferative capacity of the controls relative to parental. (C-H) Shows all individual control, YAP KO and TAZ KO, cell lines' relative proliferation for Mel202 and Mp41.



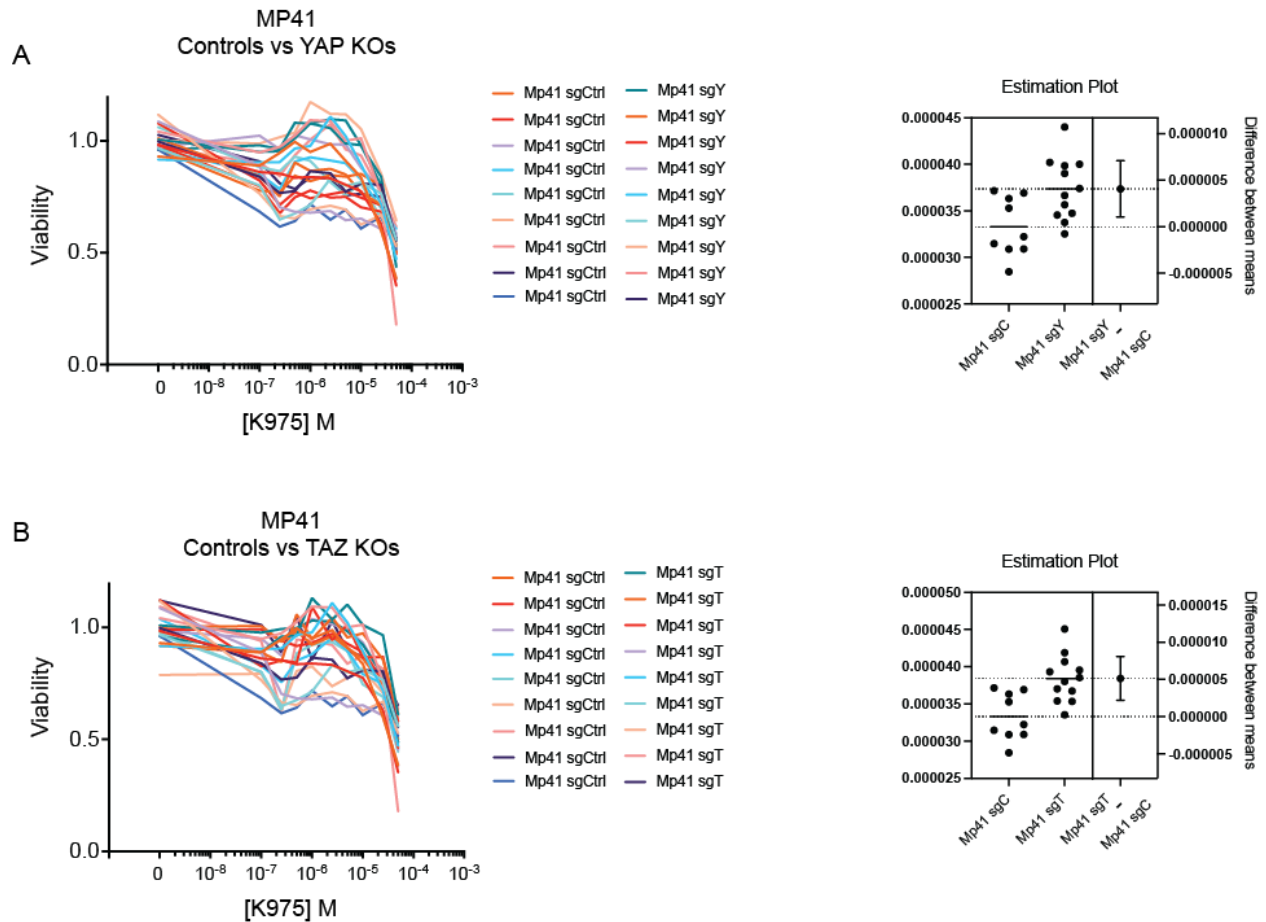
**Figure S5. Cell cycle analysis and PCA show very little overlap in variability across UM cell lines in response to YAP or TAZ loss** (A-B) Cell Cycle analysis of Mp41 or Mel202 parental cell lines with their YAP (Y1-4) or TAZ (T1-T4) KO counterparts. (C-D) Cell Cycle analysis of Mp41 or Mel202 parental cell lines with their control (C1-C3) counterparts. n = 3 for all cell lines. (E-F) PCA of MP41 or Mel202 where WT denotes parental cell line, WWTR1mut denotes TAZ KO, and YAP1mut denotes YAP KO cell line.

A

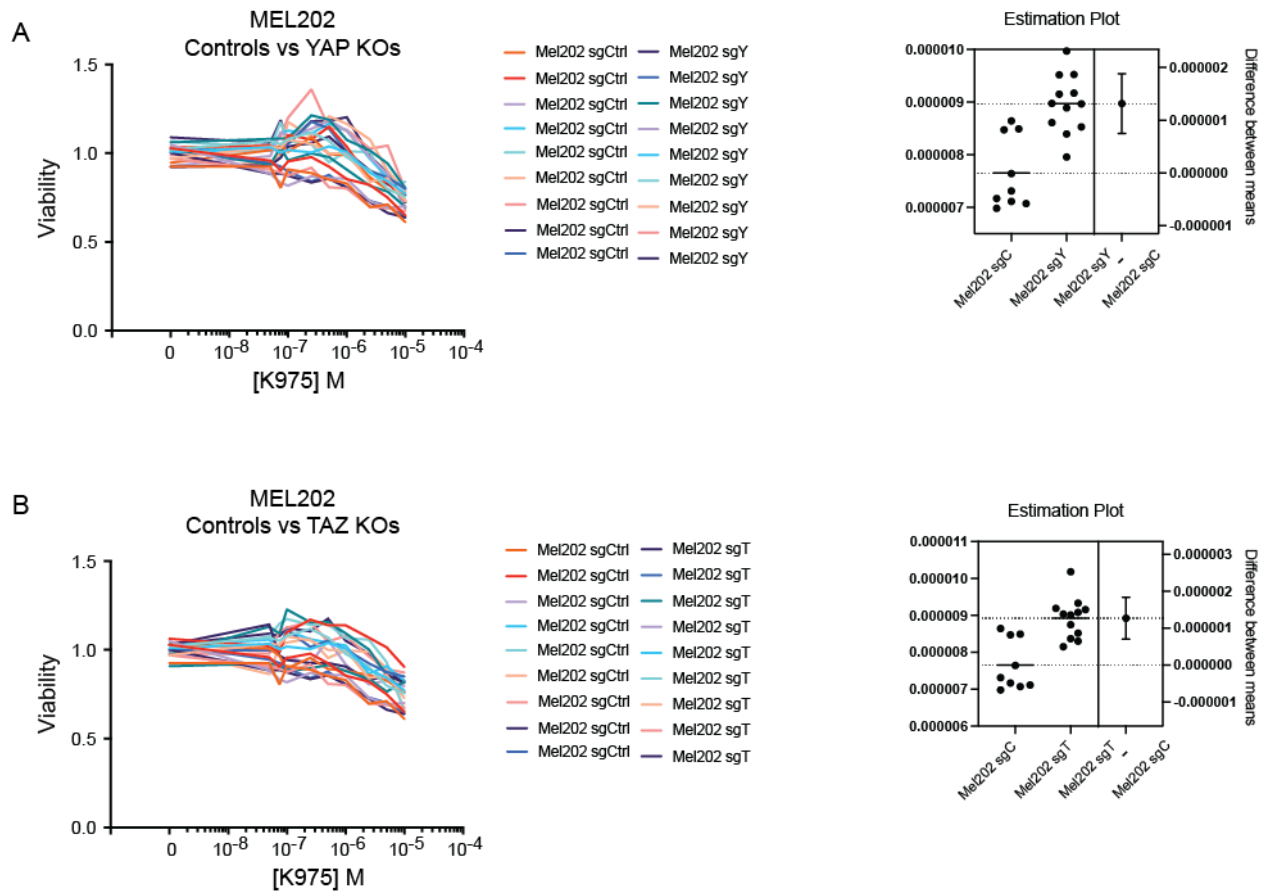


**Figure S6. Response of parental UM cell lines, MP41 and Mel202, to TEAD inhibitor, K975.** (A) UM cell lines were treated with K975 (TEADi) for up to 74.5 hours and viability was measured. Viability did not decrease past 50% even at the high dose of 50 $\mu$ M.

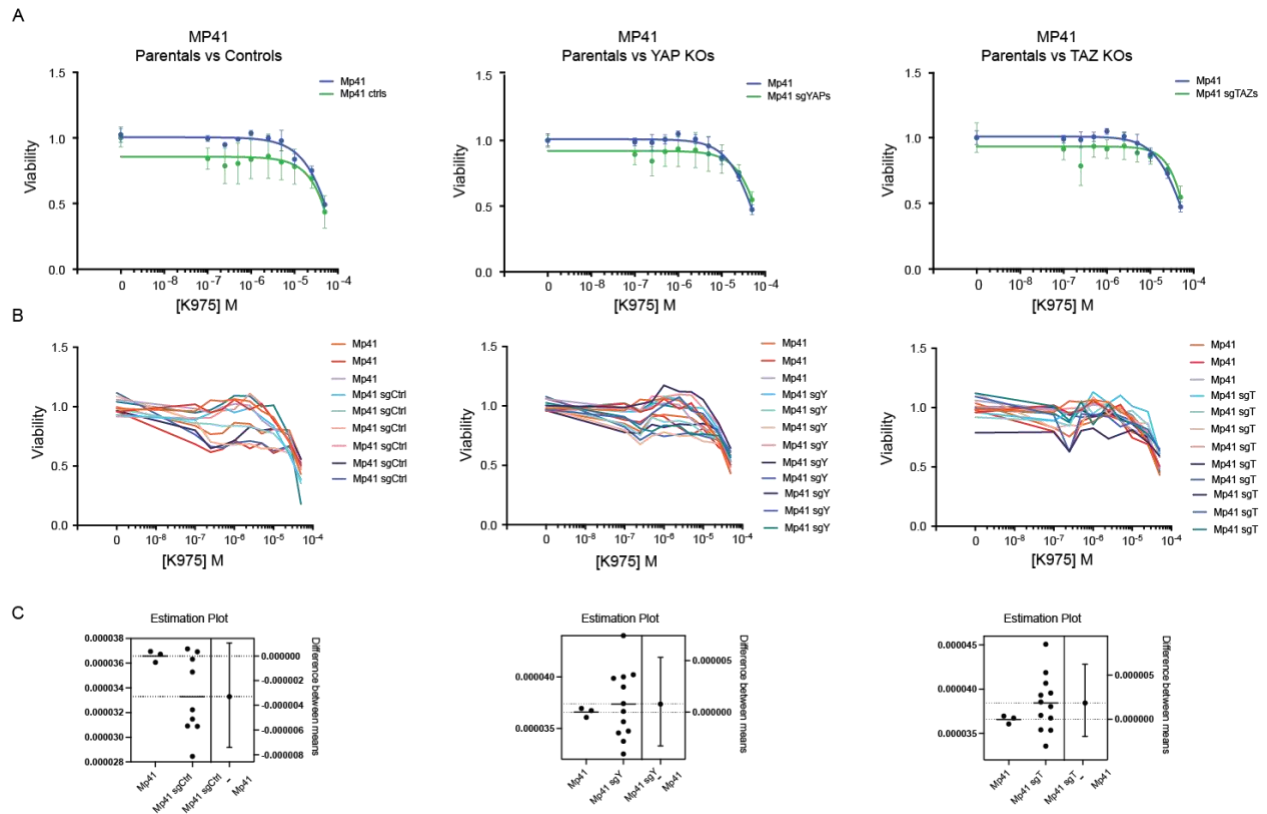




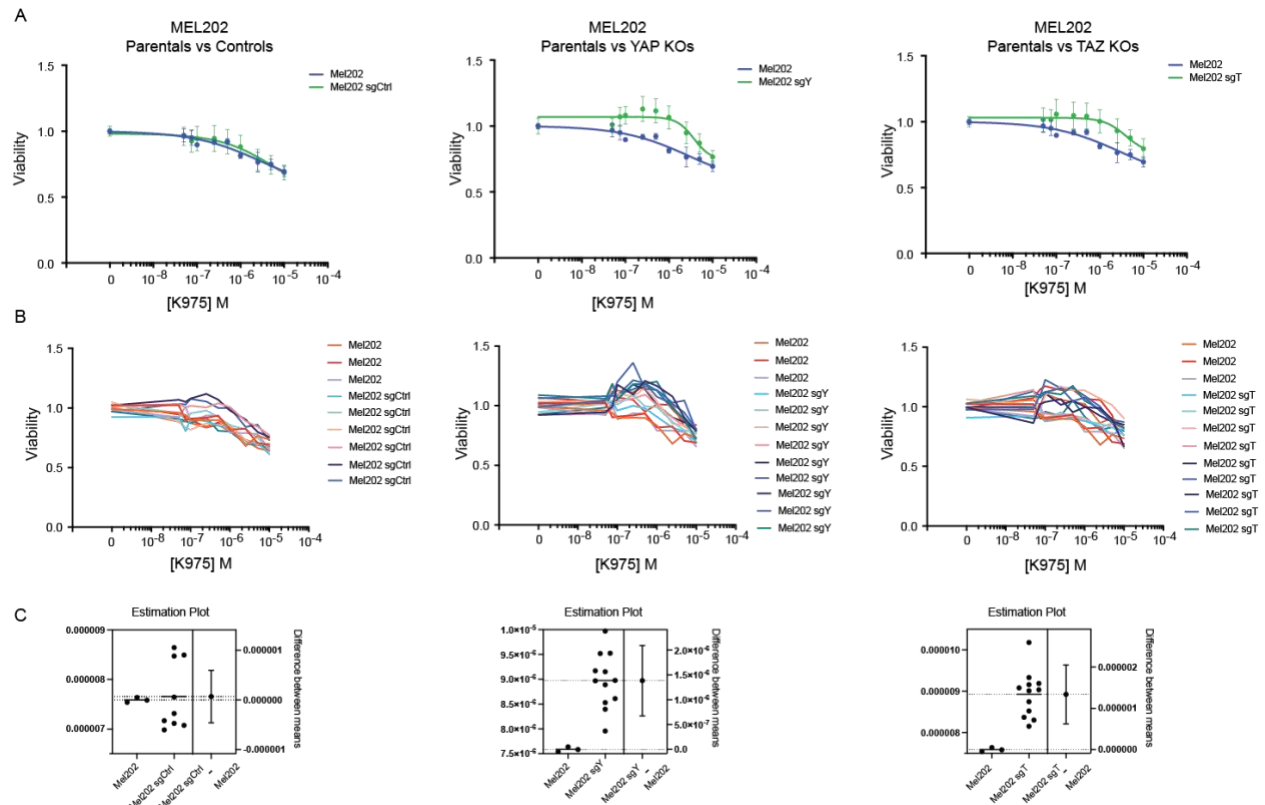
**Figure S7. All replicates of MP41 cell lines treated with TEADi.** (A) Graph shows viability relative to DMSO, of individual control or YAP KO samples, which were used to determine the AUC for each replicate. The estimation plot shows the difference between the means of the AUC values of control or YAP KO lines. On the right, the bar represents the 95% confidence interval ( $p=0.0109$ ). (B) Graph shows viability, relative to DMSO, of individual control or TAZ KO samples. The estimation plot shows the difference between the means of the AUC values of control or TAZ KO lines. On the right, the bar represents the 95% confidence interval ( $p = 0.0016$ ).



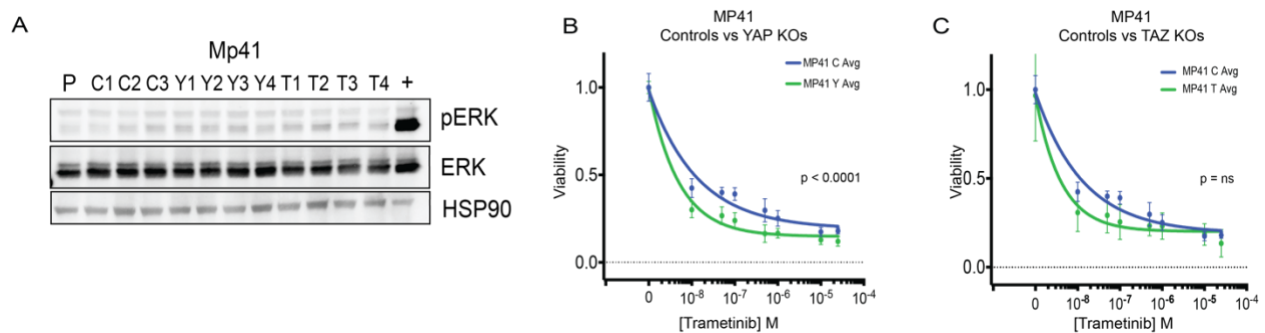
**Figure S8. All replicates of Mel202 cell lines treated with TEADi.** (A) Graph shows viability, relative to DMSO, of individual control or YAP KO samples, which were used to determine the AUC for each. The estimation plot shows the difference between the means of the AUC values of control or YAP KO lines. On the right, the bar represents the 95% confidence interval ( $p=0.0001$ ). (B) Graph shows viability, relative to DMSO, of individual control or TAZ KO samples. The estimation plot shows the difference between the means of the AUC values of control or TAZ KO lines. On the right, the bar represents the 95% confidence interval ( $p = 0.0002$ ).



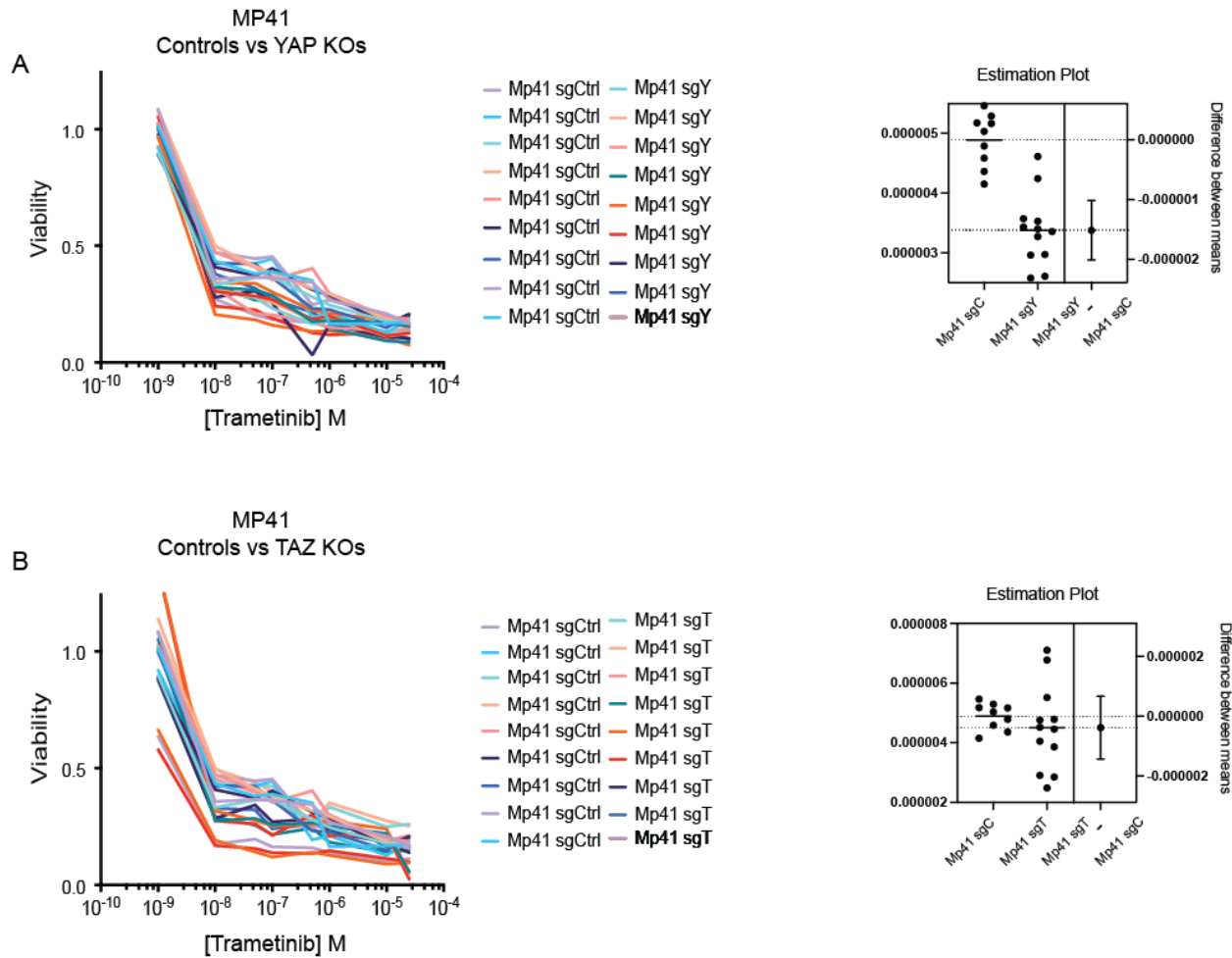
**Figure S9. MP41 P cells versus C, Y, and T lines treated with TEADi.** (A) Graph shows viability, relative to DMSO, of cell lines treated for 48hr with TEAD inhibitor, K975. (B) All individual replicates of the treated cell lines from which AUC is determined. (C) Estimation plots for AUCs of P vs Ctrl (p=ns), P vs YAP KO (p=ns), and P vs TAZ KO (p=ns).



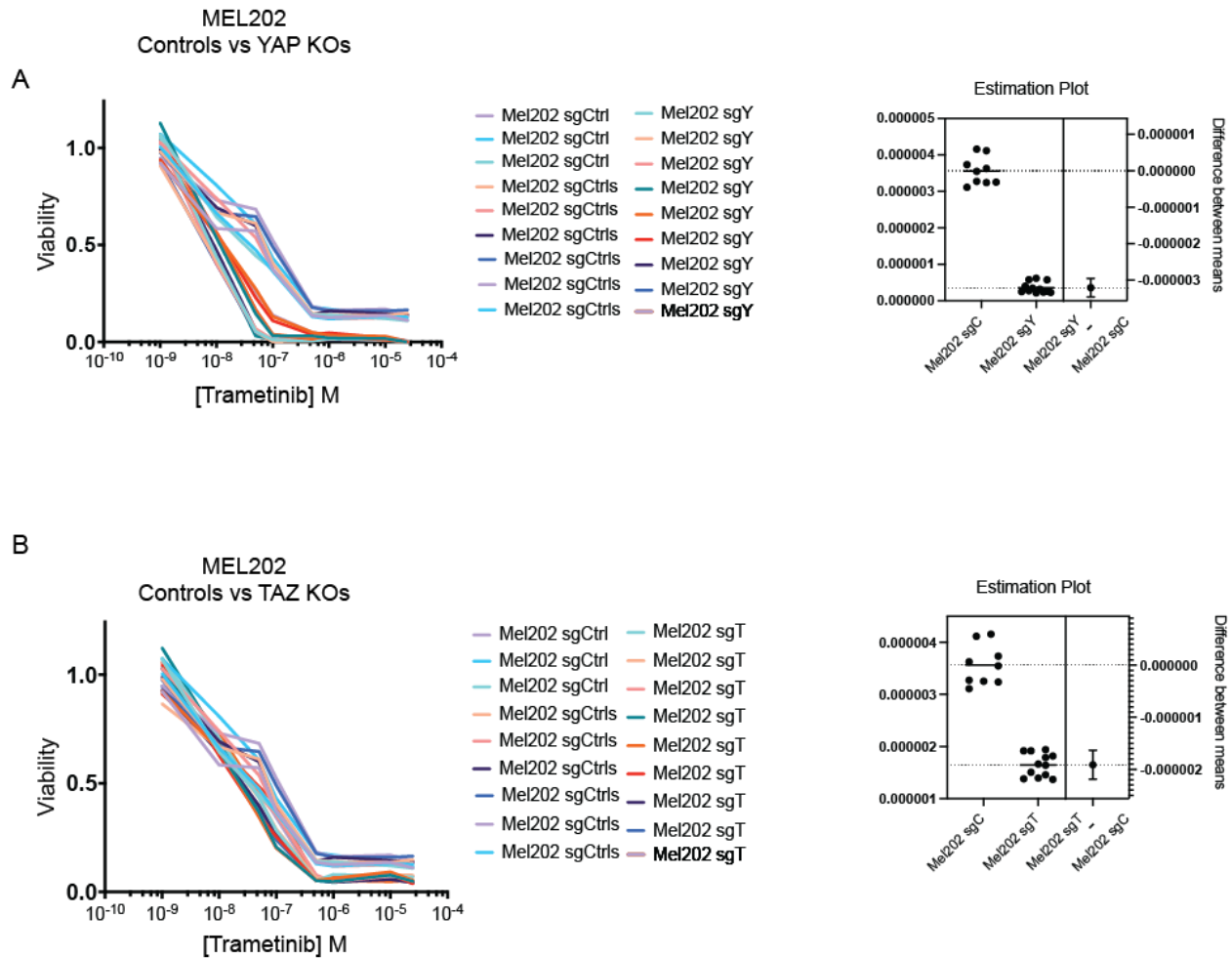
**Figure S10. MEL202 P cells versus C, Y, and T lines treated with TEADi.** (A) Graph shows viability, relative to DMSO, of cell lines treated for 48hr with TEAD inhibitor, K975. (B) All individual replicates of the treated cell lines from which AUC is determined. (C) Estimation plots for AUCs of P vs Ctrl ( $p=ns$ ), P vs YAP KO ( $p=0.0010$ ), and P vs TAZ KO ( $p=0.0014$ ), bar on the right represents 95% confidence interval.



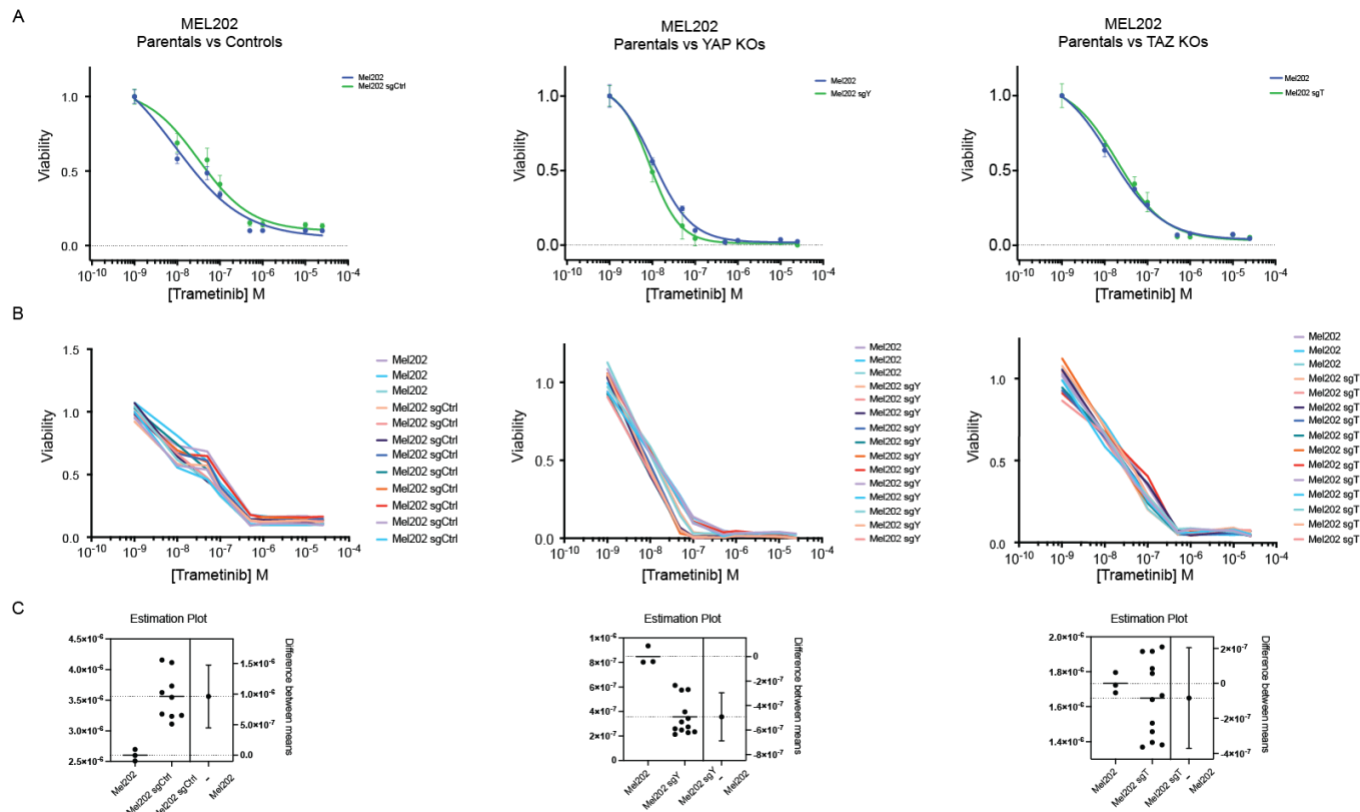
**Figure S11. Response of parental UM cell lines, MP41 and Mel202, to MEK inhibition.** (A) Western blot for pERK & ERK in MP41 clones. Last column shows the results for the positive control cell line, SKMe128<sup>BRAFV600E</sup> (+). (B-C) MP41 control (C,  $n=3$ ) and KO cell lines (Y or T,  $n=4$ ) treated with DMSO or a range of concentrations of the MEK inhibitor, trametinib. Graphs show viability relative to the DMSO alone samples. Statistical analysis was performed after calculating each individual replicate's area under the curve (AUC) and then applying unpaired t-test analysis.



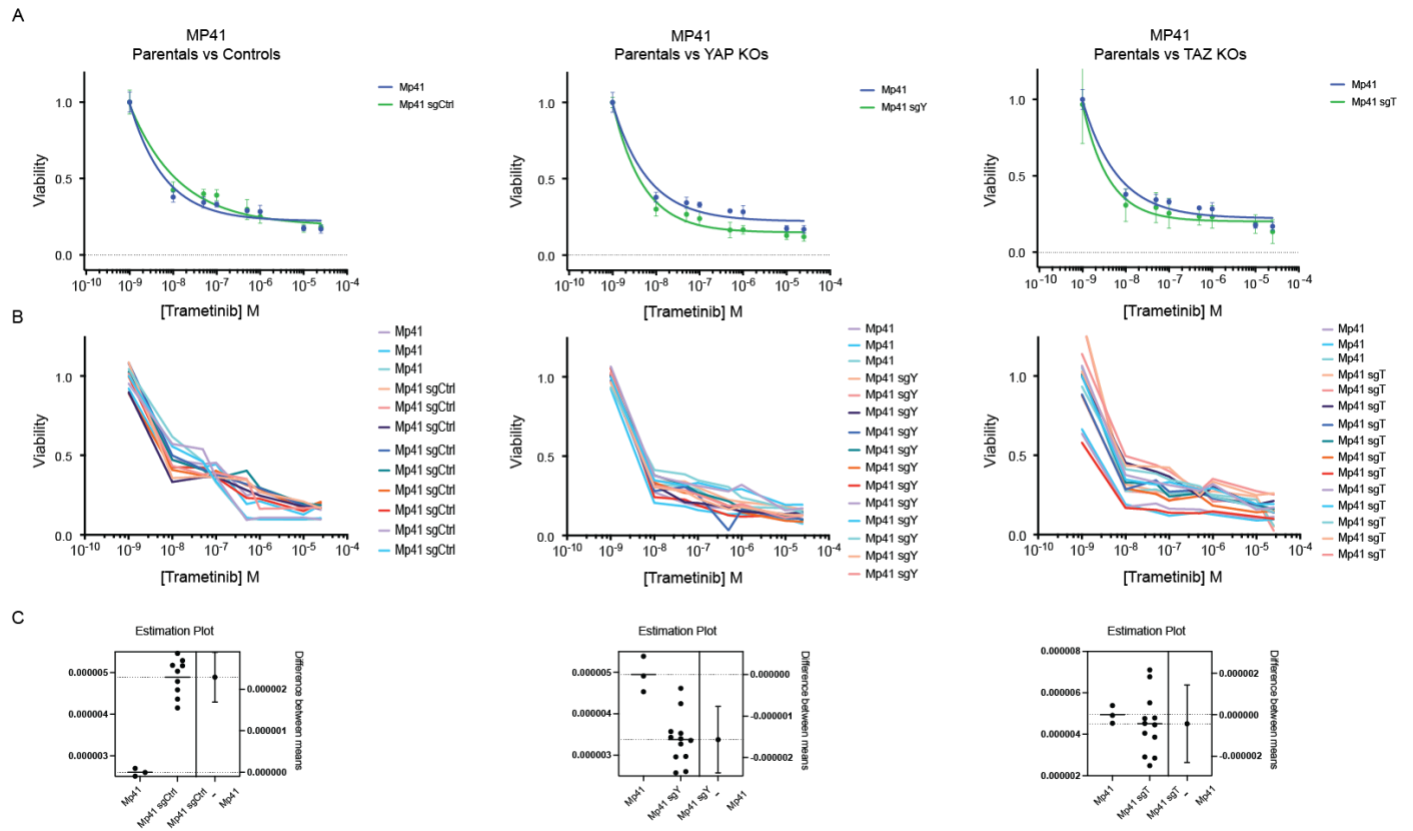
**Figure S12. All replicates of MP41 cell lines treated with MEKi** (A) Graph shows viability, relative to DMSO, of all individual replicates of control or YAP KO lines treated with MEKi, trametinib, for 97hrs. These are used to determine the AUC for each replicate of each cell line. The estimation plot shows the difference between the means of the AUC values of control or YAP KO lines. On the right, the bar represents the 95% confidence interval ( $p < 0.0001$ ) (B) Graph shows viability relative to DMSO, of all individual replicates of control or TAZ KO lines treated with MEKi. The estimation plot shows the difference between the means of the AUC values of control or TAZ KO lines. On the right, the bar represents the 95% confidence interval ( $p = ns$ ).



**Figure S13. All replicates of Mel202 cell lines treated with MEKi.** (A) Graph shows viability, relative to DMSO, of all individual replicates of control or YAP KO lines treated with MEKi, trametinib, treated for 48hrs. These are used to determine the AUC for each replicate of each cell line. The estimation plot shows the difference between the means of the AUC values of control or YAP KO lines. On the right, the bar represents the 95% confidence interval ( $p < 0.0001$ ) (B) Graph shows viability relative to DMSO, of all individual replicates of control or TAZ KO lines treated with MEKi. The estimation plot shows the difference between the means of the AUC values of control or TAZ KO lines. On the right, the bar represents the 95% confidence interval ( $p < 0.0001$ )

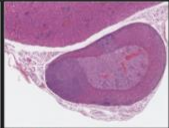
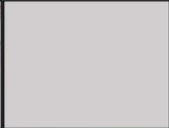
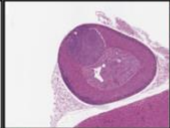
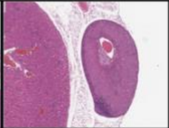

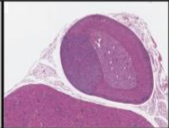
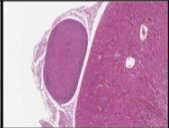
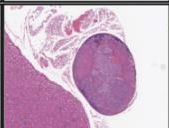
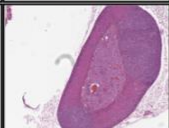
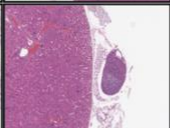
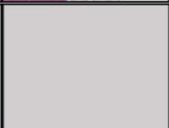
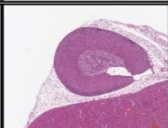
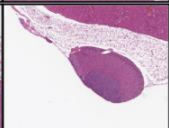
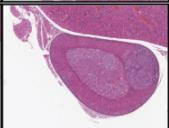
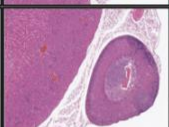
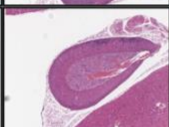
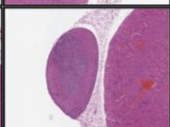
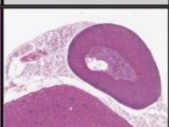

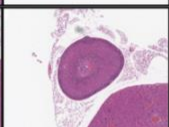

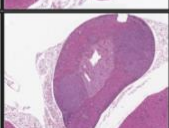
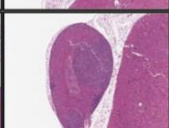
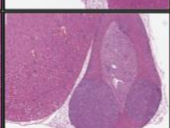
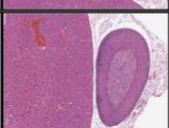
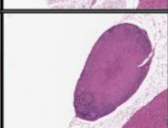
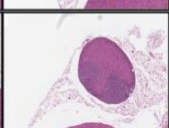
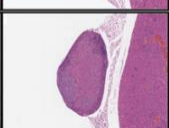


**Figure S14. MEL202 P cells versus C, Y, and T lines treated with MEKi.** (A) Graph shows viability, relative to DMSO, of cell lines treated for 48hr with MEK inhibitor, trametinib. (B) All individual replicates of the treated cell lines from which AUC is determined. (C) Estimation plots for AUCs of P vs Ctrl ( $p=0.0019$ ), P vs YAP KO ( $p=0.0001$ ), and P vs TAZ KO ( $p=ns$ ), bar on the right represents 95% confidence interval.

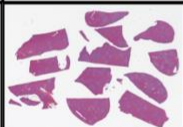









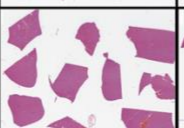



















**Figure S15. MP41 P cells versus C, Y, and T lines treated with MEKi.** (A) Graph shows viability, relative to DMSO, of cell lines treated for 48hr with MEK inhibitor, trametinib. (B) All individual replicates of the treated cell lines from which AUC is determined. (C) Estimation plots for AUCs of P vs Ctrl ( $p < 0.0001$ ), P vs YAP KOs ( $p = 0.0010$ ), and P vs TAZ KOs ( $p = ns$ ), bar on the right represents 95% confidence interval.

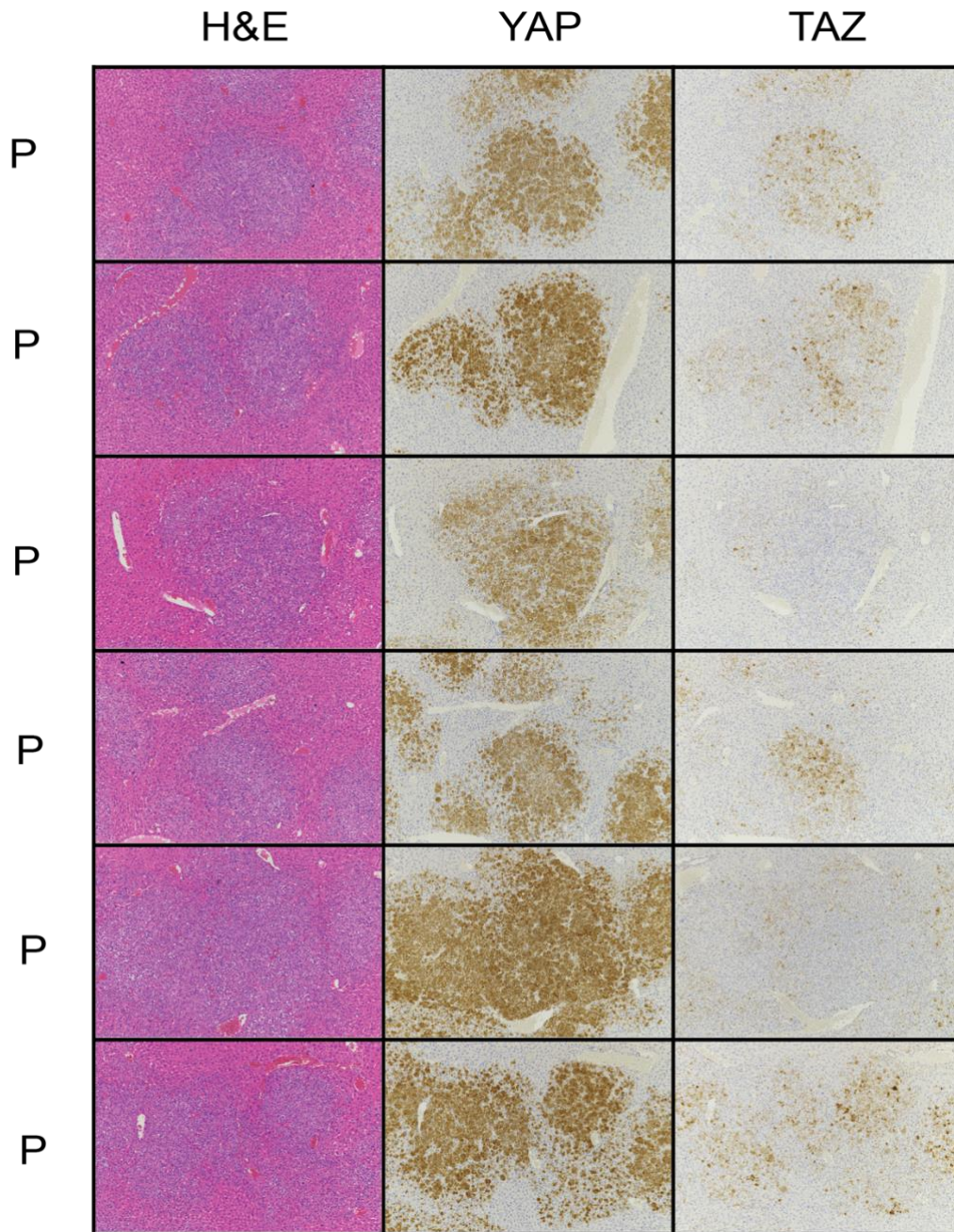


Cell Line	Mel202 P	Mel202 C1	Mel202 C2	Mel202 Y1	Mel202 Y2	Mel202 T1	Mel202 T4
Mice with AG Tumor	4/4	2/4	4/4	0/4	2/4	4/4	4/4
4x							
4x							
4x							
4x							

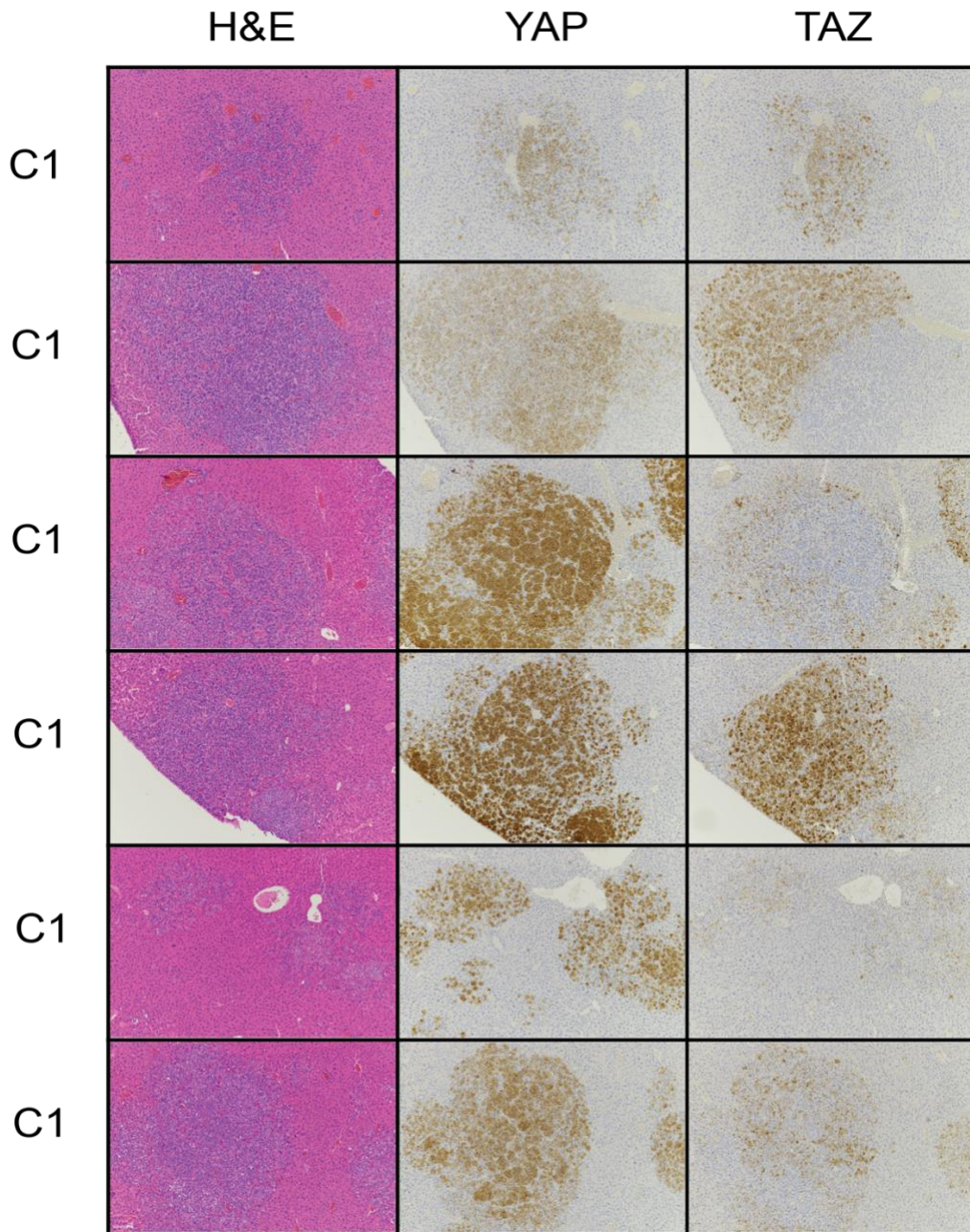
**Figure S16. Mel202 cell lines gave rise to tumors in the adrenal glands** (A) Adrenal gland sections of MEL202 injected NSG mice, stained with H&E and at 4X magnification. Imaged using eSlide manager software from Leica.

Cell Line	Mel202 P	Mel202 C1	Mel202 C2	Mel202 Y1	Mel202 Y2	Mel202 T1	Mel202 T4
							
							
							
							

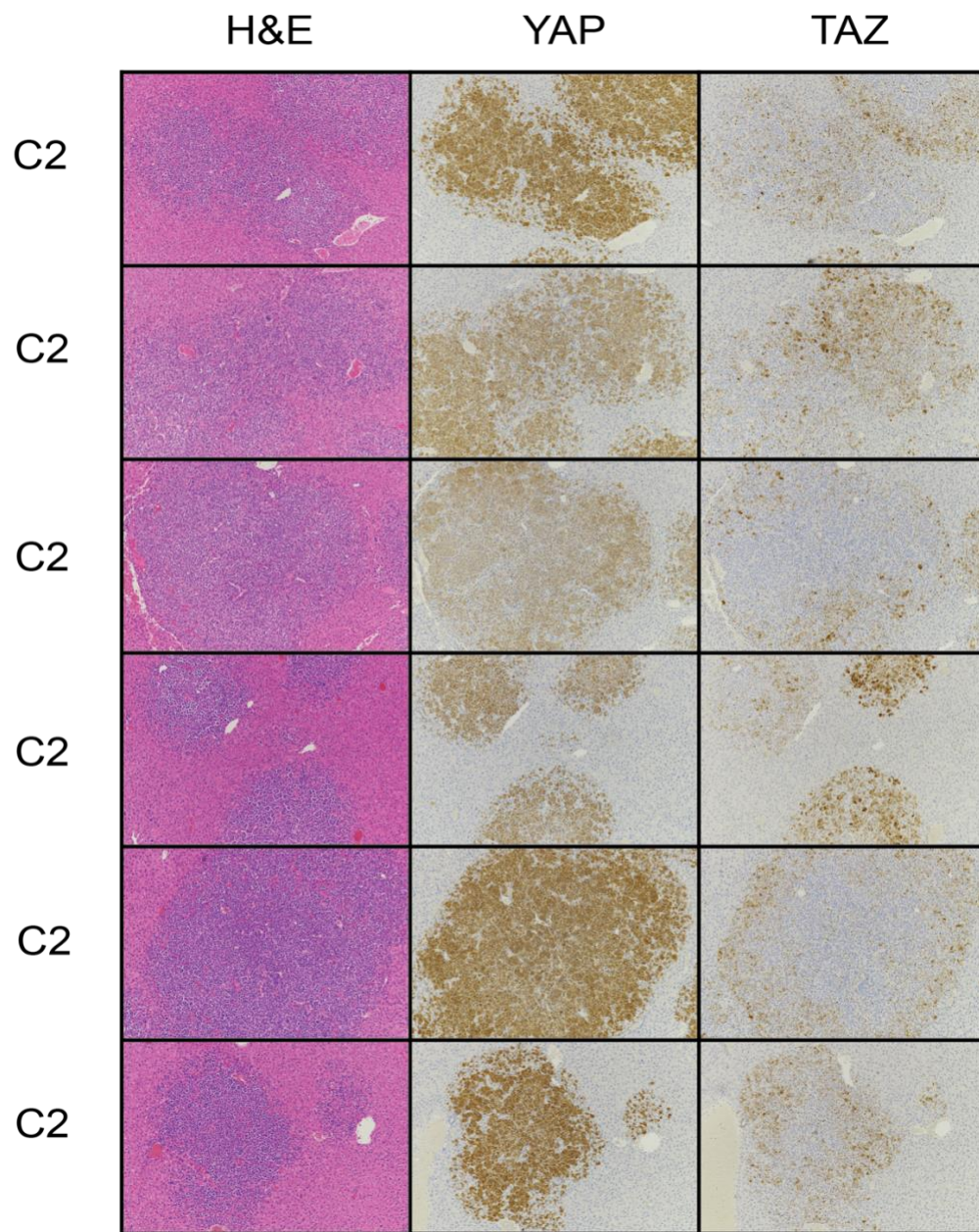
**Figure S17. Whole Slide scans of liver tumor sections from Mel202 injection** (A) Collection of liver sections from all mouse replicates injected with each cell line and stained with H&E. Imaged using eSlide manager software from Leica. These images were studied to determine the qualitative tumor burden value assign to each cell line.



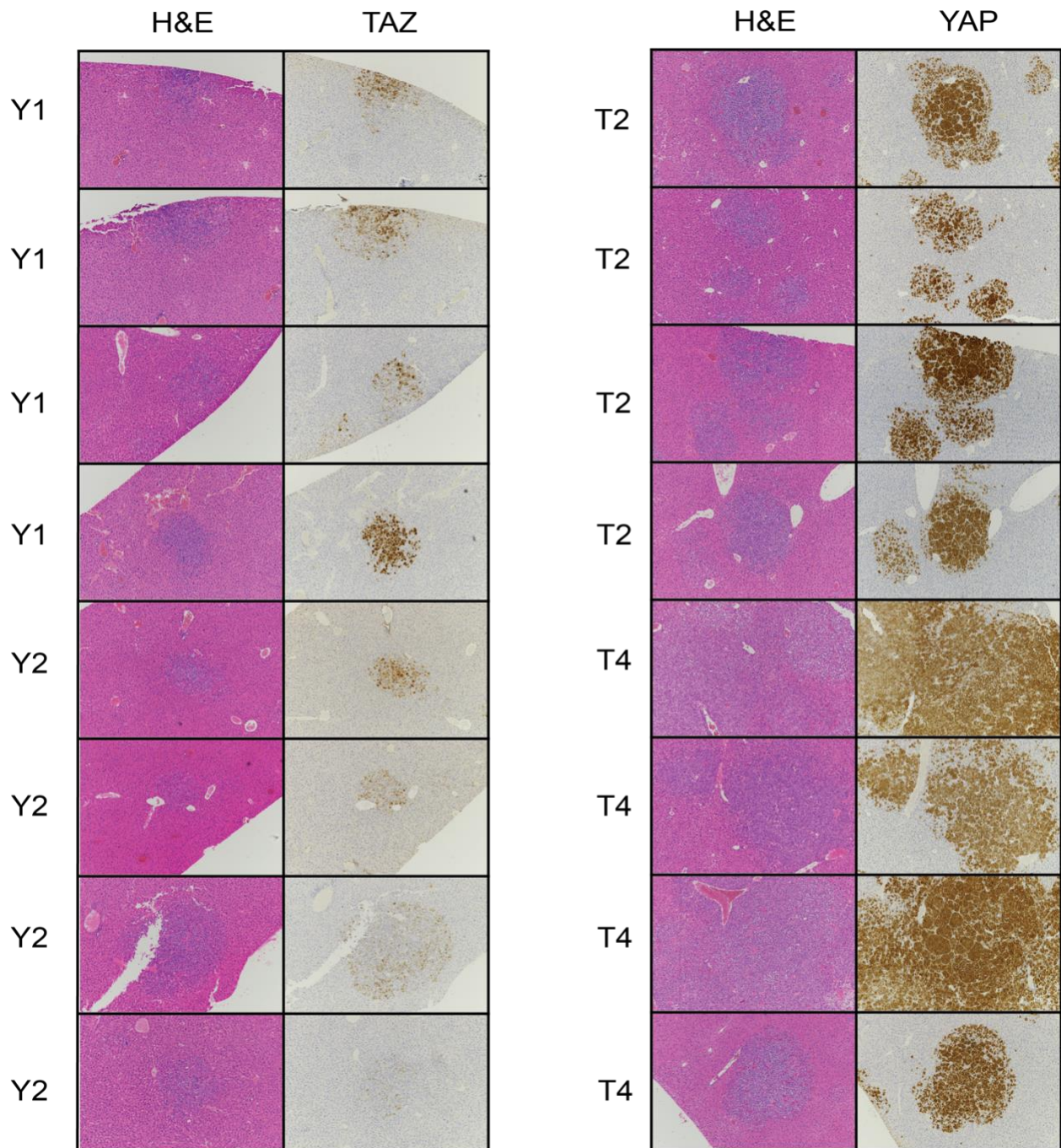
**Fig S18. Mel202 parental line expression of YAP and TAZ in tumors (A)** Table shows the H&E, YAP and TAZ staining of liver tumors from a single mouse injected with Mel202 parental cell line, highlighting the high degree of variability in YAP and TAZ staining across tumors.



**Fig S19. Mel202 control 1 expression of YAP and TAZ (A)** Table shows the H&E, YAP and TAZ staining of liver tumors from the Mel202 C1 cell line. The top three tumors arise in one mouse and the bottom three samples were from a different mouse. All from the same experiment.

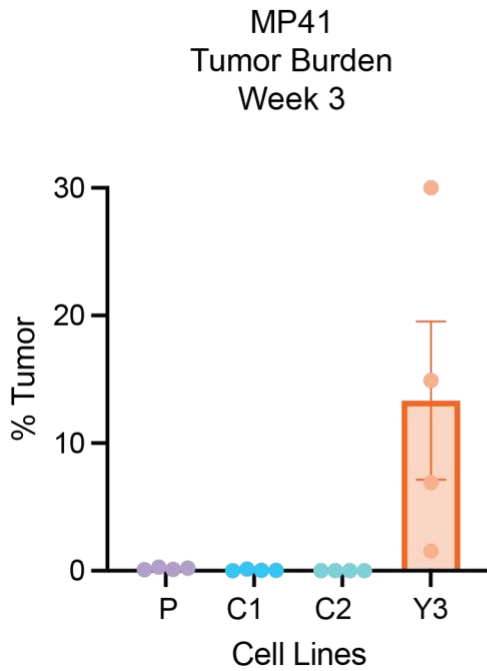


**Fig S20. MEL202 Control 2 YAP and TAZ expression** (A) Table shows the H&E, YAP and TAZ staining of liver tumors from the Mel202 C2 cell line. The top three tumors arise in one mouse and the bottom three samples were from a different mouse. All from the same experiment.

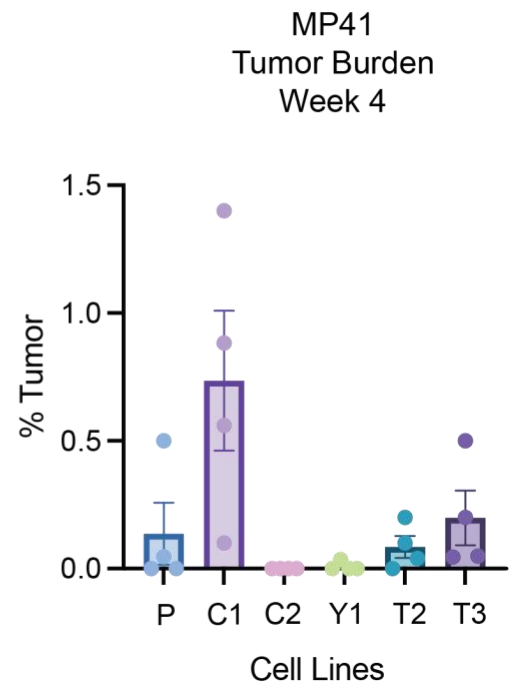


**Fig S21. MEL202 YAP or TAZ knockout clones IHC of respective paralog** (A) Table shows the H&E TAZ staining of liver tumors from the Mel202 YAP KO cell lines injected into mice. TAZ staining has great variability, within and across each Y cell line. All Y1 samples are from the mouse 1, the top two Y2 tumors are from mouse 1, while the bottom two Y2 tumors are from mouse 2. (B) Table shows the H&E TAZ staining of liver tumors from the Mel202 TAZ KO cell lines injected into mice. YAP staining is consistently high across all T cell lines and tumors. All T2 samples represent tumors from the mouse 1, the top two T4 are tumors from mouse 1, but the bottom two T4 samples are from mouse 2. Each cell line was injected into 4 mice cohorts.

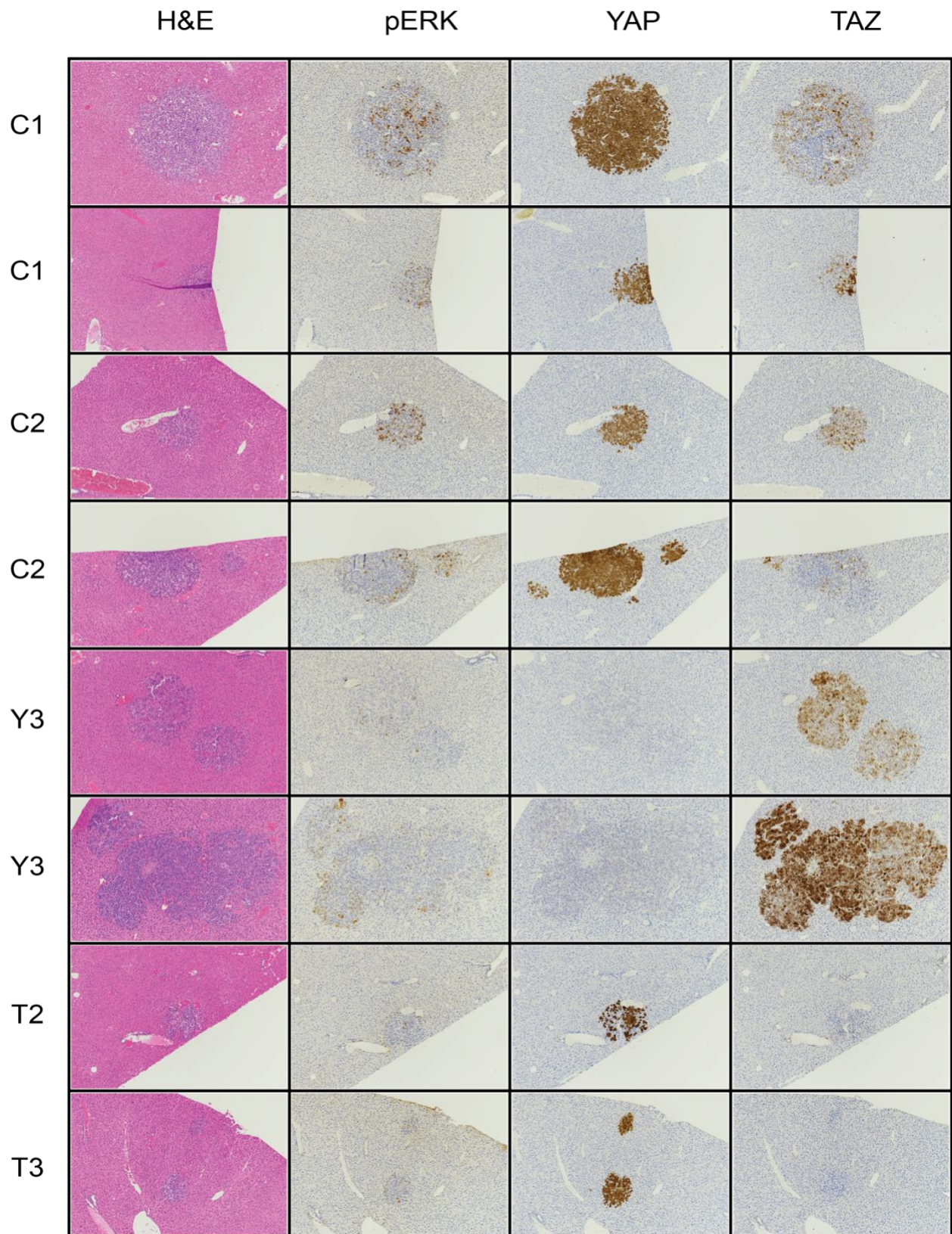
A



B



**Fig S22. Tumor burden from MP41 intracardiac injection.** (A) Graph shows the percent of tumor in liver tissue sections from the intracardiac injection of each cell line. The mice were euthanized, and tissue was harvested at 3 weeks after the injection. (B) Graph shows the percent of tumor in liver tissue sections from the intracardiac injection of each cell line. The mice were euthanized, and tissue was harvested at 4 weeks after the injection.



**Fig S23. MP41 IHC of main UM pathways.** (A) Table shows the H&E, pERK, YAP and TAZ staining of liver tumors from the MP41 cell lines injected intracardially into mice.

## References

- Amirouchene-Angelozzi, N., Némati, F., Gentien, D., André, N., Agathe, D., Carita, G., Camonis, J., Desjardins, L., Cassoux, N., Piperno-Neumann, S., Mariani, P., Sastre, X., Decaudin, D., & Roman-Roman, S. (2014). Establishment of novel cell lines recapitulating the genetic landscape of uveal melanoma and preclinical validation of mTOR as a therapeutic target. *Molecular Oncology*, *8*(8), 1508–1520. <https://doi.org/10.1016/j.molonc.2014.06.004>
- Anders, S., & Huber, W. (2010). Differential expression analysis for sequence count data. *Genome Biology*, *11*(10). <https://doi.org/10.1186/gb-2010-11-10-r106>
- Augsburger, J. J., Corrêa, Z. M., & Shaikh, A. H. (2009). Effectiveness of treatments for metastatic uveal melanoma. *American Journal of Ophthalmology*, *148*(1), 119–127. <https://doi.org/10.1016/j.ajo.2009.01.023>
- Barbosa, I., Gopalakrishnan, R., Mercan, Ş., Mourikis, T. P., Martin, T., Wengert, S., Sheng, C., Ji, F., Lopes, R., Knehr, J., Altorfer, M., Lindeman, A., Russ, C., Naumann, U., Golji, J., Sprouffske, K., Barys, L., Tordella, L., Schübeler, D., . . . Galli, G. (2023). Cancer lineage-specific regulation of YAP responsive elements revealed through large-scale functional epigenomic screens. *Nature Communications*, *14*(1). <https://doi.org/10.1038/s41467-023-39527-w>
- Brandt, Z. J., Echert, A. E., Bostrom, J. R., North, P., & Link, B. A. (2020). Core Hippo pathway components act as a brake on Yap/Taz in the development and maintenance of the biliary network. *Development*. <https://doi.org/10.1242/dev.184242>
- Brouwer, N. J., Konstantinou, E. K., Gragoudas, E. S., Marinković, M., Luyten, G. P. M., Kim, I. K., Jager, M. J., & Vavvas, D. G. (2021). Targeting the YAP/TAZ pathway in Uveal and conjunctival melanoma with verteporfin. *Investigative Ophthalmology & Visual Science*, *62*(4), 3. <https://doi.org/10.1167/iovs.62.4.3>
- Carvajal, R. D., Piperno-Neumann, S., Kapiteijn, E., Chapman, P. B., Frank, S. J., Joshua, A. M., Piulats, J. M., Wolter, P., Cocquyt, V., Chmielowski, B., Evans, T. J., Gastaud, L., Linette, G. P., Berking, C., Schachter, J., Rodrigues, M., Shoushtari, A. N., Clemett, D., Ghiorghiu, D., . . .



- Nathan, P. (2018). Selumetinib in combination with dacarbazine in patients with metastatic uveal melanoma: a phase III, multicenter, randomized trial (SUMIT). *Journal of Clinical Oncology*, 36(12), 1232–1239. <https://doi.org/10.1200/jco.2017.74.1090>
- Ceol, C. J., Houvras, Y., Jané-Valbuena, J., Bilodeau, S., Orlando, D. A., Battisti, V., Fritsch, L., Lin, W. M., Hollmann, T. J., Ferré, F., Bourque, C., Burke, C. J., Turner, L., Uong, A., Johnson, L. A., Beroukhi, R., Mermel, C. H., Loda, M., Ait-Si-Ali, S., . . . Zon, L. I. (2011). The histone methyltransferase SETDB1 is recurrently amplified in melanoma and accelerates its onset. *Nature*, 471(7339), 513–517. <https://doi.org/10.1038/nature09806>
- Chen, X., Wu, Q., Depeille, P., Chen, P., Thornton, S., Kalirai, H., Coupland, S. E., Roose, J. P., & Bastian, B. C. (2017). RASGRP3 mediates MAPK pathway activation in GNAQ mutant uveal melanoma. *Cancer Cell*, 31(5), 685–696.e6. <https://doi.org/10.1016/j.ccell.2017.04.002>
- Cordenonsi, M., Zanconato, F., Azzolin, L., Forcato, M., Rosato, A., Frasson, C., Inui, M., Montagner, M., Parenti, A., Poletti, A., Daidone, M. G., Dupont, S., Basso, G., Bicciato, S., & Piccolo, S. (2011). The Hippo transducer TAZ confers cancer stem Cell-Related traits on breast cancer cells. *Cell*, 147(4), 759–772. <https://doi.org/10.1016/j.cell.2011.09.048>
- Core Team, R. & R Foundation for Statistical Computing. (2021). *R: A Language and Environment for Statistical Computing*. <https://www.R-project.org>.
- Di Agostino, S., Sorrentino, G., Ingallina, E., Valenti, F., Ferraiuolo, M., Bicciato, S., Piazza, S., Strano, S., Del Sal, G., & Blandino, G. (2015). YAP enhances the pro-proliferative transcriptional activity of mutant p53 proteins. *EMBO Reports*, 17(2), 188–201. <https://doi.org/10.15252/embr.201540488>
- Feng, X., Degese, M. S., Iglesias-Bartolomé, R., Vaqué, J. P., Molinolo, A. A., Rodrigues, M., Zaidi, M. R., Ksander, B. R., Merlino, G., Sodhi, A., Chen, Q., & Gutkind, J. S. (2014). Hippo-Independent Activation of YAP by the GNAQ Uveal Melanoma Oncogene through a Trio-Regulated Rho GTPase Signaling Circuitry. *Cancer Cell*, 25(6), 831–845. <https://doi.org/10.1016/j.ccr.2014.04.016>

- Griewank, K. G., Yu, X., Khalili, J. S., Sozen, M., Stempke-Hale, K., Bernatchez, C., Wardell, S., Bastian, B. C., & Woodman, S. E. (2012). Genetic and molecular characterization of uveal melanoma cell lines. *Pigment Cell & Melanoma Research*, 25(2), 182–187. <https://doi.org/10.1111/j.1755-148x.2012.00971.x>
- Harbour, J. W. (2012). The genetics of uveal melanoma: an emerging framework for targeted therapy. *Pigment Cell & Melanoma Research*, 25(2), 171–181. <https://doi.org/10.1111/j.1755-148x.2012.00979.x>
- Henning, N., Roberts, F.F., Fowler, C., & Spanoudaki, V. (2024). Ultrasound guided injection into the left ventricle of the mouse. *Protocol Exchange*. <https://doi.org/10.21203/rs.3.pex-2336/v1>
- Hua, G., Carlson, D. L., & Starr, J. R. (2022). Tebentafusp-tebn: A novel Bispecific T-Cell engager for Metastatic uveal melanoma. *Journal of the Advanced Practitioner in Oncology*, 13(7), 717–723. <https://doi.org/10.6004/jadpro.2022.13.7.8>
- Johnson, R. L., & Halder, G. (2013). The two faces of Hippo: targeting the Hippo pathway for regenerative medicine and cancer treatment. *Nature Reviews Drug Discovery*, 13(1), 63–79. <https://doi.org/10.1038/nrd4161>
- Kaan, H. Y. K., Chan, S. W., Tan, S. K. J., Guo, F., Lim, C. J., Hong, W., & Song, H. (2017). Crystal structure of TAZ-TEAD complex reveals a distinct interaction mode from that of YAP-TEAD complex. *Scientific Reports*, 7(1). <https://doi.org/10.1038/s41598-017-02219-9>
- Kadamur, G., & Ross, E. M. (2013). Mammalian phospholipase C. *Annual Review of Physiology*, 75(1), 127–154. <https://doi.org/10.1146/annurev-physiol-030212-183750>
- Kaliki, S., & Shields, C. L. (2016). Uveal melanoma: relatively rare but deadly cancer. *Eye*, 31(2), 241–257. <https://doi.org/10.1038/eye.2016.275>
- Kanai, F., Marignani, P. A., Sarbassova, D., Yagi, R., Hall, R. A., Donowitz, M., Hisaminato, A., Fujiwara, T., Ito, Y., Cantley, L. C., & Yaffe, M. B. (2000). TAZ: a novel transcriptional co-activator regulated by interactions with 14-3-3 and PDZ domain proteins. *The EMBO Journal*, 19(24), 6778–6791. <https://doi.org/10.1093/emboj/19.24.6778>

- Kaneda, A., Seike, T., Danjo, T., Nakajima, T., Otsubo, N., Yamaguchi, D., Tsuji, Y., Hamaguchi, K., Yasunaga, M., Nishiya, Y., Suzuki, M., Saito, J., Yatsunami, R., Nakamura, S., Sekido, Y., & Mori, K. (2020). The novel potent TEAD inhibitor, K-975, inhibits YAP1/TAZ-TEAD protein-protein interactions and exerts an anti-tumor effect on malignant pleural mesothelioma. *American Journal of Cancer Research*, *10*(12), 4399–4415. <https://europepmc.org/article/MED/33415007>
- Kim, Y. J., Lee, S. C., Kim, S. E., Kim, S. H., Kim, S. K., & Lee, C. S. (2020). YAP Activity is Not Associated with Survival of Uveal Melanoma Patients and Cell Lines. *Scientific Reports*, *10*(1). <https://doi.org/10.1038/s41598-020-63391-z>
- Lee, C., Lee, K., Lee, S. B., Park, D., & Rhee, S. G. (1994). Regulation of phospholipase C-beta 4 by ribonucleotides and the alpha subunit of Gq. *Journal of Biological Chemistry*, *269*(41), 25335–25338. [https://doi.org/10.1016/s0021-9258\(18\)47252-3](https://doi.org/10.1016/s0021-9258(18)47252-3)
- Li, H., Li, Q., Dang, K., Ma, S., Cotton, J. L., Sun, Y., Zhu, L. J., Deng, A., Ip, Y. T., Johnson, R. L., Wu, X., Punzo, C., & Mao, J. (2019). YAP/TAZ Activation drives uveal melanoma initiation and progression. *Cell Reports*, *29*(10), 3200-3211.e4. <https://doi.org/10.1016/j.celrep.2019.03.021>
- Li, Y., Shen, H., Frangou, C., Yang, N., Guo, J., Xu, B., Bshara, W., Shepherd, L., Zhu, Q., Wang, J., Hu, Q., Liu, S., Morrison, C., Sun, P., & Zhang, J. (2015). Characterization of TAZ domains important for the induction of breast cancer stem cell properties and tumorigenesis. *Cell Cycle*, *14*(1), 146–156. <https://doi.org/10.4161/15384101.2014.967106>
- Li, Z., Zhao, B., Wang, P., Chen, F. X., Dong, Z., Yang, H., Guan, K., & Xu, Y. (2010). Structural insights into the YAP and TEAD complex. *Genes & Development*, *24*(3), 235–240. <https://doi.org/10.1101/gad.1865810>
- Love, M. I., Huber, W., & Anders, S. (2014). Moderated estimation of fold change and dispersion for RNA-seq data with DESeq2. *Genome Biology*, *15*(12). [https://doi.org/10.1186/s13059-014-0550-](https://doi.org/10.1186/s13059-014-0550-8)

- Ma, J., Weng, L., Bastian, B. C., & Chen, X. (2020). Functional characterization of uveal melanoma oncogenes. *Oncogene*, *40*(4), 806–820. <https://doi.org/10.1038/s41388-020-01569-5>
- Mayrhofer, M., Gourain, V., Reischl, M., Affaticati, P., Jenett, A., Joly, J. S., Benelli, M., Demichelis, F., Poliani, P. L., Sieger, D., & Mione, M. (2017). A novel brain tumour model in zebrafish reveals the role of YAP activation in MAPK/PI3K induced malignant growth. *Disease Models & Mechanisms*. <https://doi.org/10.1242/dmm.026500>
- Miesfeld, J. B., Gestri, G., Clark, B. S., Flinn, M. A., Poole, R. J., Bader, J. R., Besharse, J. C., Wilson, S. W., & Link, B. A. (2015). Yap and Taz regulate retinal pigment epithelial cell fate. *Development*. <https://doi.org/10.1242/dev.119008>
- Moore, A. R., Ran, L., Guan, Y., Sher, J., Hitchman, T. D., Zhang, J. Q., Hwang, C., Walzak, E. G., Shoushtari, A. N., Monette, S., Murali, R., Wiesner, T., Griewank, K. G., Chi, P., & Chen, Y. (2018). GNA11 Q209L mouse model reveals RASGRP3 as an essential signaling node in Uveal melanoma. *Cell Reports*, *22*(9), 2455–2468. <https://doi.org/10.1016/j.celrep.2018.01.081>
- Mootha, V. K., Lindgren, C. M., Eriksson, K., Subramanian, A., Sihag, S., Lehár, J., Puigserver, P., Carlsson, E., Ridderstråle, M., Laurila, E., Houstis, N. E., Daly, M. J., Patterson, N., Mesirov, J. P., Golub, T. R., Tamayo, P., Spiegelman, B. M., Lander, E. S., Hirschhorn, J. N., . . . Groop, L. (2003). PGC-1 $\alpha$ -responsive genes involved in oxidative phosphorylation are coordinately downregulated in human diabetes. *Nature Genetics*, *34*(3), 267–273. <https://doi.org/10.1038/ng1180>
- Mueller, H. S., Fowler, C. E., Dalin, S., Moiso, E., Udomlumleart, T., Garg, S., Hemann, M. T., & Lees, J. A. (2021). Acquired resistance to PRMT5 inhibition induces concomitant collateral sensitivity to paclitaxel. *Proceedings of the National Academy of Sciences of the United States of America*, *118*(34). <https://doi.org/10.1073/pnas.2024055118>
- Patro, R., Duggal, G., Love, M. I., Irizarry, R. A., & Kingsford, C. (2017). Salmon provides fast and bias-aware quantification of transcript expression. *Nature Methods*, *14*(4), 417–419. <https://doi.org/10.1038/nmeth.4197>

- Perez, D. E., Henle, A. M., Amsterdam, A., Hagen, H. R., & Lees, J. A. (2018). Uveal melanoma driver mutations in GNAQ/11 yield numerous changes in melanocyte biology. *Pigment Cell & Melanoma Research*, 31(5), 604–613. <https://doi.org/10.1111/pcmr.12700>
- Phelps, G. B., Hagen, H. R., Amsterdam, A., & Lees, J. A. (2022a). MITF deficiency accelerates GNAQ-driven uveal melanoma. *Proceedings of the National Academy of Sciences of the United States of America*, 119(19). <https://doi.org/10.1073/pnas.2107006119>
- Phelps, G. B., Amsterdam, A., Hagen, H. R., García, N. Z., & Lees, J. A. (2022b). MITF deficiency and oncogenic GNAQ each promote proliferation programs in zebrafish melanocyte lineage cells. *Pigment Cell & Melanoma Research*, 35(5), 539–547. <https://doi.org/10.1111/pcmr.13057>
- Reggiani, F., Gobbi, G., Ciarrocchi, A., & Sancisi, V. (2021). YAP and TAZ Are Not Identical Twins. *Trends in Biochemical Sciences*, 46(2), 154–168. <https://doi.org/10.1016/j.tibs.2020.08.012>
- Research, C. F. D. E. A. (2022, January 26). *FDA approves tebentafusp-tebn for unresectable or metastatic uveal melanoma*. U.S. Food And Drug Administration. <https://www.fda.gov/drugs/resources-information-approved-drugs/fda-approves-tebentafusp-tebn-unresectable-or-metastatic-uveal-melanoma>
- Soneson, C., Love, M. I., & Robinson, M. D. (2015). Differential analyses for RNA-seq: transcript-level estimates improve gene-level inferences. *F1000Research*, 4, 1521. <https://doi.org/10.12688/f1000research.7563.1>
- Subramanian, A., Tamayo, P., Mootha, V. K., Mukherjee, S., Ebert, B. L., Gillette, M. A., Paulovich, A. G., Pomeroy, S. L., Golub, T. R., Lander, E. S., & Mesirov, J. P. (2005). Gene set enrichment analysis: A knowledge-based approach for interpreting genome-wide expression profiles. *Proceedings of the National Academy of Sciences of the United States of America*, 102(43), 15545–15550. <https://doi.org/10.1073/pnas.0506580102>
- Yu, F., Luo, J., Mo, J., Liu, G., Kim, Y. C., Meng, Z., Zhao, L., Peyman, G. A., Ouyang, H., Jiang, W., Zhao, J., Chen, X., Zhang, L., Wang, C., Bastian, B. C., Zhang, K., & Guan, K. (2014). Mutant

- GQ/11 promote uveal melanoma tumorigenesis by activating YAP. *Cancer Cell*, 25(6), 822–830. <https://doi.org/10.1016/j.ccr.2014.04.017>
- Zhang, W., Gao, Y., Li, F., Tong, X., Ren, Y., Han, X., Yao, S., Long, F., Yang, Z., Fan, H., Zhang, L., & Ji, H. (2015). YAP Promotes Malignant Progression of Lkb1-Deficient Lung Adenocarcinoma through Downstream Regulation of Survivin. *Cancer Research*, 75(21), 4450–4457. <https://doi.org/10.1158/0008-5472.can-14-3396>
- Zhao, B., Li, L., Lü, Q., Wang, L. H., Liu, C., Lei, Q., & Guan, K. (2011). Angiomotin is a novel Hippo pathway component that inhibits YAP oncoprotein. *Genes & Development*, 25(1), 51–63. <https://doi.org/10.1101/gad.2000111>
- Zhao, B., Li, L., Tumaneng, K., Wang, C., & Guan, K. (2010). A coordinated phosphorylation by Lats and CK1 regulates YAP stability through SCF $\beta$ -TRCP. *Genes & Development*, 24(1), 72–85. <https://doi.org/10.1101/gad.1843810>
- Zhao, B., Wei, X., Li, W., Udan, R. S., Yang, Q., Kim, J., Xie, J., Ikenoue, T., Yu, J., Li, L., Zheng, P., Ye, K., Chinnaiyan, A. M., Halder, G., Lai, Z. C., & Guan, K. L. (2007). Inactivation of YAP oncoprotein by the Hippo pathway is involved in cell contact inhibition and tissue growth control. *Genes & Development*, 21(21), 2747–2761. <https://doi.org/10.1101/gad.1602907>
- Zhao, B., Ye, X., Yu, J., Li, L., Li, W., Li, S., Yu, J., Lin, J. D., Wang, C. Y., Chinnaiyan, A. M., Lai, Z. C., & Guan, K. L. (2008). TEAD mediates YAP-dependent gene induction and growth control. *Genes & Development*, 22(14), 1962–1971. <https://doi.org/10.1101/gad.1664408>
- Zhao, Y., Montminy, T., Azad, T., Lightbody, E. D., Hao, Y., Sengupta, S., Asselin, É., Nicol, C. J., & Yang, X. (2018). PI3K positively regulates YAP and TAZ in mammary tumorigenesis through multiple signaling pathways. *Molecular Cancer Research*, 16(6), 1046–1058. <https://doi.org/10.1158/1541-7786.mcr-17-0593>
- Zhu, A., Ibrahim, J. G., & Love, M. I. (2018). Heavy-tailed prior distributions for sequence count data: removing the noise and preserving large differences. *Bioinformatics*, 35(12), 2084–2092. <https://doi.org/10.1093/bioinformatics/bty895>

### **III. Discussion and Conclusions**

YAP and TAZ have been implicated in various tumor types for many years now. However, YAP or TAZ, and even their major regulatory pathway, the Hippo pathway, are rarely ever mutated in cancer (Franklin et al., 2023), thus understanding their contributions has not been straightforward. In this thesis, we showed the effects, or lack thereof, of YAP or TAZ loss in UM. Additionally, we established that TAZ functions as a potent oncogenic driver in melanocytic cells in our zebrafish model.

Research uncovering the importance of YAP in UM goes back to 2014, when two labs independently showed that oncogenic GNAQ (*GNAQ<sup>Q209L</sup>*), but not wild type GNAQ, could promote YAP nuclear localization and thus activity (Feng et al., 2014, Yu et al., 2014). *GNAQ<sup>Q209L</sup>* was shown to activate YAP independently from the Hippo pathway (Feng et al., 2014). Additional work over the years has further supported an important role for YAP in UM. This includes work from the Lees laboratory, which strongly de-emphasized the role of the MAPK pathway in promoting UM in our zebrafish model, while highlighting the YAP pathway as a critical promoter of tumorigenesis (Phelps, Hagen et al., 2022). Notably, MAPK activity was variable in UM tumors in general and it was even possible to generate UM in the absence of any detectable MAPK signaling in certain genetic backgrounds. However, YAP activity was a consistent presence, as determined by YAP nuclear localization, in all types and genetic backgrounds of UM.

Due to these striking results, work in this thesis investigated the dependency of YAP activity in UM. No other work has shown YAP dependence in *GNAQ<sup>Q209L</sup>* driven tumors in the *in vivo* context. We generated transgenic zebrafish expressing *GNAQ<sup>Q209L</sup>* with either *yap<sup>wt</sup>* or *yap<sup>-/-</sup>* genotypes. Contrary to our expectations, the *yap<sup>-/-</sup>* tumors did not have reduced tumorigenic potential compared to *yap<sup>wt</sup>*. This suggests that, although Yap may play an important role in UM, it is not necessary for *GNAQ*'s oncogenic signaling. This further argues that *GNAQ<sup>Q209L</sup>* must be driving tumorigenesis through another pathway or component, and we tested two possible alternatives. First, we considered whether *GNAQ<sup>Q209L</sup>* was relying on oncogenic signaling through the canonical MAPK pathway. However, when we examined the MAPK activity in these *yap<sup>-/-</sup>*



tumors, we found that the presence of pERK was highly variable, including many tumor cells with no detectable signal. This doesn't rule out the possibility that MAPK has some role in UM, but it seems unlikely that it can be the main driver of *GNAQ*'s oncogenic signaling. The second possibility we explored was whether the oncogenic signaling was occurring through the paralog of YAP, TAZ, since these proteins are known to have some overlapping functions (Reggiani et al., 2021). Taz nuclear expression was found to be present in the *yap*<sup>-/-</sup> tumors, supporting the notion that these tumors might be relying on Taz to transmit *GNAQ*'s oncogenic signal. Moreover, TAZ has been shown to play important roles in other tumor types, for example non-small cell lung cancer (Noguchi et al., 2014). Thus, we decided to test TAZ's oncogenic potential in melanocytic cells. Taking advantage of a constitutively active form of TAZ, we injected this into zebrafish under the control of a melanocyte promoter and saw incredibly rapid tumor formation. We note that other studies have previously identified TAZ dependent cancers, but efforts in different tissue types to show TAZ's oncogenic potential had proven fruitless, failing to achieve full transformation (Franklin et al., 2023). Our results are the first to show *in vivo* that activated TAZ, can function as an oncogene without the need for any cooperating mutation.

Following this finding, we asked whether *GNAQ*<sup>Q209L</sup> driven tumors depend on *taz* for tumorigenesis. Similar to our analyses of *yap*'s role, we generated transgenic zebrafish expressing *GNAQ*<sup>Q209L</sup> in a genetic background that is *tp53* mutant and either wildtype or mutant (*taz*<sup>-/-</sup>) for *taz*. Analyses of these fish clearly showed that *taz* is not necessary for *GNAQ*<sup>Q209L</sup> driven tumorigenesis. At this point, this result was not particularly surprising, given that these *taz*<sup>-/-</sup> tumors still express Yap. These results show the lack of necessity of either Yap or Taz for tumorigenesis, even though either of these proteins is capable of driving UM development, collectively arguing that Yap and Taz are playing important, but functionally redundant roles, in zebrafish UM. Additionally, these data drive home the point that UM tumors are highly adaptable and plastic.

Pathway plasticity, as defined by the ability to switch from relying on one pathway to another, is the main hypothesis that surrounds the results shown in chapter 2. Additional, to the work performed in zebrafish, we also studied the roles of YAP and TAZ in human UM cell lines. We generated clones with single knockout of YAP or TAZ in two UM cell lines, Mel202 and MP41, using CRISPR Cas9. Contrary to previously published work (Barbosa et al., 2023; Feng et al., 2014; Lyubasyuk et al., 2014; Yu et al., 2014), which showed that UM cell lines depend on YAP for survival, we were able to successfully generate multiple YAP KO single cell clones. This showed that UM cell lines can survive without YAP and further analyses established that this caused no impairment in proliferation compared to control wildtype clones. It is important to point out that many of the previous studies showing YAP dependence were conducted in the context of acute loss, using siRNAs to induce knockdown. Furthermore, a recent study showed that the UM cell line 92.1, widely used in the YAP knockdown experiments, has a higher dependence on YAP than another counterpart cell lines, including Mel202 (Barbosa et al., 2023). During this thesis work, another group reported successful generation of a YAP KO UM cell line without loss of viability, as well as little to no effect in the viability of multiple UM cell lines treated with a YAP inhibitor (Ma et al., 2020). Additionally, Kim et al. analyzed TCGA data for human UM and showed that higher YAP mRNA did not significantly correlate with worse survival when compared to lower YAP mRNA (Kim et al., 2020). We also see similar results when analyzing TCGA data. However, we found that, while YAP didn't correlate with poor progression free survival, higher TAZ mRNA does significantly correlate with poor progression free survival compared to lower TAZ mRNA patients (TCGA data).

Alongside our generation of YAP KO human cell lines, we also successfully generated TAZ KOs. These cells also showed no changes in viability, and even displayed a significant increase in proliferative capacity compared to control wildtype clones. This result could be due to the increased YAP protein expression found in the control clones\*, as well as potentially the observed increase in pERK, as discussed more below. There has been considerable focus on establishing the relative roles of YAP and TAZ, particularly identifying functions that are shared

versus differential (Reggiani et al., 2021). As one example, YAP and TAZ have been reported to differentially contribute to proliferation and migration/invasion in the context of lung and breast cancer (Shreberk-Shaked et al., 2020; Chan et al., 2008). We had hoped to use our human UM KO clones to identify potential differential roles for YAP and TAZ in UM. We did see a difference in proliferation between the two genotypes, with the TAZ KO cells showing increased proliferative capacity. However, the other properties we probed, including cell cycle and even the transcriptome, showed no consistent and significant differences between the KO cells and the control cells for both Mel202 and MP41. We also conducted some assays for invasion *in vitro*. Unfortunately, we observed a lot of experiment-to-experiment variation in this assay, even for a single clone, which made it hard to score altered properties. However, within these constraints, we saw no consistent results that pointed to the YAP or TAZ KO cell lines being more or less invasive. Taken together, these results imply that UM cells can easily adapt to loss of either YAP or TAZ, potentially as a result from overlapping roles. Another way our KO cells could be adapting to loss of YAP or TAZ is through upregulation of, or increased reliance on, an alternate signaling pathway. Canonically, GNAQ signals to the MAPK through PLC $\beta$ 4 and thus we asked whether the YAP/TAZ KO cell lines displayed increased dependence on MAPK. Treatment of UM cell lines, including Mel202 and MP41, with MAPK inhibitors is known to induce cell death (Ambrosini et al., 2012; Amirouchene-Angelozzi et al., 2014; Sugase et al., 2020), and thus we compare the response of knockout versus control clones to the MEK inhibitor, trametinib. This analysis showed that the YAP KO clones of both MP41 and Mel202 were significantly more sensitive to the MEK inhibitor than their control counterparts, as were the TAZ KO clones for Mel202. This, along with evidence for upregulation of pERK in the cultured KO clones, suggests that the YAP or TAZ KO cells increase their reliance on the MAPK pathways to enable cell viability. However, as we discuss below, once we put the cell lines *in vivo*, we saw no drastic differences in the level of MAPK signal across genotypes.

We assessed the tumorigenic potential of the YAP or TAZ KO cells via *in vivo* transplant assays. Prior analyses showed reduced tumorigenicity in response to YAP knockdown cells *in vitro* and *in vivo* (Barbosa et al., 2023; Feng et al., 2014; Lyubasyuk et al., 2014; Yu et al., 2014). Much of this prior published *in vivo* work was done via subcutaneous injections in mice. Our study took a different approach, using an intracardiac injection system to inject cells directly into the hearts of mice, which allows them to enter the circulation and spread throughout the body, mimicking the last steps of the metastatic cascade. In this assay, the control, YAP and TAZ KO MP41 and Mel202 clones showed high tropism for the liver, as well as to the adrenal glands. The formation of liver tumors was highly gratifying because this is the overwhelming site of metastatic tumors in UM patients. In contrast, the formation of adrenal gland tumors is atypical for UM, and thus unexpected. While YAP and TAZ KO clones were able to generate tumors, both of the Mel202 YAP KO clones tested, showed reduced tumor burden when compared to their TAZ KO or control counterparts. In contrast, one of the two MP41 YAP KO clones yielded the highest tumor burden seen for any of the clones. These results hint at the possibility of there being a difference in YAP dependence that is cell line dependent. As previously mentioned, this possibility has already been shown with regards to the UM cell lines 92.1 and Mel202 (Barbosa et al., 2023).

After performing IHC analyses on these tumors to look at YAP and TAZ, we confirmed the lack of expression of the deleted paralog in each KO line. Nuclear YAP staining was consistently high in MP41 parental, control, and TAZ KO cell lines. Notably, the levels of YAP in Mel202 TAZ KO were consistently present at the higher end of the range seen in parental and control lines. Nuclear TAZ staining displayed more variable levels but showed consistent low to mid-level staining across all of the samples. In particular, there was no obvious upregulation in the YAP KOs for either MP41 or Mel202. However, the upregulation of YAP in Mel202 TAZ KO tumors hints at an important role for TAZ in tumorigenesis, presumably that its loss is compensated for by increasing YAP activity. Collectively, all the tumor data argue that YAP and TAZ share important and functionally redundant roles in UM tumorigenesis.

We also assessed pERK expression and saw variable low expression in all of the tumors, irrespective of whether they were derived from parental cells or clones that were control, YAP KO or TAZ KO. While the MP41 tumors showed somewhat higher pERK than Mel202s, this signal was consistently low and heterogenous. Even though pERK levels were elevated in YAP and TAZ KO cell lines *in vitro*, we saw no evidence of pERK upregulation of signal in the YAP or TAZ KO tumors for either MP41 or Mel202. Thus, activation of this pathway shifts between the *in vitro* and *in vivo* contexts. We hypothesize that the cell lines exhibit an increased dependence on MAPK activity for their survival *in vitro*, but the act of removing them from tissue culture media, which contains growth factors that stimulate MAPK signaling, causes downregulation of this pathway when they are transplanted into the *in vivo* context.

These results highlight the importance of testing pathway contributions and sensitivities *in vitro* and *in vivo* to confirm that any observed dependencies and contributions are sustained in both contexts and not specific to culture conditions. This seems even more important when we consider the inconsistent results we observed regarding TEAD inhibition from the *in vitro* and *in vivo* contexts. As mentioned, we tested the importance of TEAD for UM tumorigenesis in our *in vivo* zebrafish model through genetic inhibition of the YAP/TAZ-TEAD interaction and showed that this was critical for tumorigenesis. Additionally, we showed that TEAD is important for oncogenic GNAQ biology in early melanocyte biology of zebrafish embryos. In contrast, when we tested the response of human UM cell lines to TEAD inhibition *in vitro*, we saw only modest impact on the viability of parental, control, and knockout cells. Furthermore, the YAP or TAZ KO clones did not show increased sensitivity to TEAD inhibition compared to parental or controls. This could be explained by the essentially fully redundant roles of YAP and TAZ we have observed, and that the remaining paralog shows some upregulation *in vitro*. Alternatively, or in addition, it could be due to the higher reliance of these knockout cells on MAPK signaling. To establish whether TEAD activity is required or dispensable for UM tumorigenesis, in humans/mammals, it will be necessary to validate the effect of TEAD inhibition of UM in the *in vivo* context, an experiment which has yet to be conducted by us or the field.

One thing we have not been able to address in this project is whether UM progression can continue in the absence of both YAP and TAZ. We put extensive effort into trying to knock out either YAP or TAZ in tumors of *yap*<sup>-/-</sup> or *taz*<sup>-/-</sup> zebrafish with CRISPR CAS9, to no avail. We have also worked hard to make double knockouts in the UM cell lines. Initially, we tried to use the dTAG system (Nabet et al., 2018) to specifically target the remaining *YAP* or *TAZ* genes in the single KOs and allow us to induce protein degradation in a dose dependent manner. However, after many trials, we failed to achieve successful dTAG knock-in due to issues with selection markers and particularly the low transfection efficiency of both UM cell lines. Thus, we have now shifted our efforts to the use of inducible shRNAs with the goal of achieving sufficient shRNA knockdown of the remaining TAZ or YAP paralog in the single KO cells, to get as close as possible to double knockout. Then, we could test the effect of shRNA induction on cell line viability. Given the importance of YAP and TAZ in development, and our inability to generate double KOs *in vivo*, we anticipate that the UM cell lines will be unable to tolerate simultaneous loss of YAP and TAZ.

## References

- Ambrosini, G., Pratilas, C. A., Li, Q., Tadi, M., Surriga, O., Carvajal, R. D., & Schwartz, G. K. (2012). Identification of unique MEK-Dependent genes in GNAQ mutant uveal melanoma involved in cell growth, tumor cell invasion, and MEK resistance. *Clinical Cancer Research*, 18(13), 3552–3561. <https://doi.org/10.1158/1078-0432.ccr-11-3086>
- Amirouchene-Angelozzi, N., Némati, F., Gentien, D., André, N., Agathe, D., Carita, G., Camonis, J., Desjardins, L., Cassoux, N., Piperno-Neumann, S., Mariani, P., Sastre, X., Decaudin, D., & Roman-Roman, S. (2014). Establishment of novel cell lines recapitulating the genetic landscape of uveal melanoma and preclinical validation of mTOR as a therapeutic target. *Molecular Oncology*, 8(8), 1508–1520. <https://doi.org/10.1016/j.molonc.2014.06.004>
- Arang, N., Lubrano, S., Ceribelli, M., Rigracciolo, D. C., Saddawi-Konefka, R., Faraji, F., Ramirez, S. I., Kim, D., Tosto, F. A., Stevenson, E., Zhou, Y., Wang, Z., Bogomolovas, J., Molinolo, A. A., Swaney, D. L., Krogan, N. J., Yang, J., Coma, S., Pachter, J. A., . . . Gutkind, J. S. (2023). High-throughput chemogenetic drug screening reveals PKC-RhoA/PKN as a targetable signaling vulnerability in GNAQ-driven uveal melanoma. *Cell Reports Medicine*, 4(11), 101244. <https://doi.org/10.1016/j.xcrm.2023.101244>
- Barbosa, I., Gopalakrishnan, R., Mercan, Ş., Mourikis, T. P., Martin, T., Wengert, S., Sheng, C., Ji, F., Lopes, R., Knehr, J., Altorfer, M., Lindeman, A., Russ, C., Naumann, U., Golji, J., Sprouffske, K., Barys, L., Tordella, L., Schübeler, D., . . . Galli, G. (2023). Cancer lineage-specific regulation of YAP responsive elements revealed through large-scale functional epigenomic screens. *Nature Communications*, 14(1). <https://doi.org/10.1038/s41467-023-39527-w>
- Chan, S. W., Lim, C. J., Guo, K., Ng, C. P., Lee, I., Hunziker, W., Zeng, Q., & Hong, W. (2008). A role for TAZ in migration, invasion, and tumorigenesis of breast cancer cells. *Cancer Research*, 68(8), 2592–2598. <https://doi.org/10.1158/0008-5472.can-07-2696>

- Chen, X., Wu, Q., Tan, L., Porter, D., Jager, M. J., Emery, C. M., & Bastian, B. C. (2013). Combined PKC and MEK inhibition in uveal melanoma with GNAQ and GNA11 mutations. *Oncogene*, *33*(39), 4724–4734. <https://doi.org/10.1038/onc.2013.418>
- Faião-Flores, F., Emmons, M. F., Durante, M. A., Kinose, F., Saha, B., Fang, B., Koomen, J. M., Chellappan, S., Maria-Engler, S. S., Rix, U., Licht, J. D., Harbour, J. W., & Smalley, K. S. (2019). HDAC inhibition enhances the in vivo efficacy of MEK inhibitor therapy in Uveal melanoma. *Clinical Cancer Research*, *25*(18), 5686–5701. <https://doi.org/10.1158/1078-0432.ccr-18-3382>
- Feng, X., Degese, M. S., Iglesias-Bartolomé, R., Vaqué, J. P., Molinolo, A. A., Rodrigues, M., Zaidi, M. R., Ksander, B. R., Merlino, G., Sodhi, A., Chen, Q., & Gutkind, J. S. (2014). Hippo-Independent Activation of YAP by the GNAQ Uveal Melanoma Oncogene through a Trio-Regulated Rho GTPase Signaling Circuitry. *Cancer Cell*, *25*(6), 831–845. <https://doi.org/10.1016/j.ccr.2014.04.016>
- Franklin, J., Wu, Z., & Guan, K. (2023). Insights into recent findings and clinical application of YAP and TAZ in cancer. *Nature Reviews Cancer*, *23*(8), 512–525. <https://doi.org/10.1038/s41568-023-00579-1>
- Hitchman, T. D., Bayshtok, G., Ceraudo, E., Moore, A. R., Lee, C., Jia, R., Wang, N., Pachai, M. R., Shoushtari, A. N., Francis, J. H., Guan, Y., Chen, J., Chang, M. T., Taylor, B. S., Sakmar, T. P., Huber, T., & Chi, P. (2021). Combined inhibition of GNAQ and MEK enhances therapeutic efficacy in uveal melanoma. *Clinical Cancer Research*, *27*(5), 1476–1490. <https://doi.org/10.1158/1078-0432.ccr-20-2860>
- Li, H., Li, Q., Dang, K., Ma, S., Cotton, J. L., Sun, Y., Zhu, L. J., Deng, A., Ip, Y. T., Johnson, R. L., Wu, X., Punzo, C., & Mao, J. (2019). YAP/TAZ Activation drives uveal melanoma initiation and progression. *Cell Reports*, *29*(10), 3200–3211.e4. <https://doi.org/10.1016/j.celrep.2019.03.021>



- Li, Y., Shen, H., Frangou, C., Yang, N., Guo, J., Xu, B., Bshara, W., Shepherd, L., Zhu, Q., Wang, J., Hu, Q., Liu, S., Morrison, C., Sun, P., & Zhang, J. (2015). Characterization of TAZ domains important for the induction of breast cancer stem cell properties and tumorigenesis. *Cell Cycle*, *14*(1), 146–156. <https://doi.org/10.4161/15384101.2014.967106>
- Lyubasyuk, V., Ouyang, H., Yu, F., Guan, K., & Zhang, K. (2014). YAP inhibition blocks uveal melanogenesis driven by GNAQ or GNA11 mutations. *Molecular and Cellular Oncology*, *2*(1), e970957. <https://doi.org/10.4161/23723548.2014.970957>
- Nabet, B., Roberts, J. M., Buckley, D. L., Paulk, J., Dastjerdi, S., Yang, A., Leggett, A. L., Erb, M., Lawlor, M. A., Souza, A., Scott, T. G., Vittori, S., Perry, J. A., Qi, J., Ciulli, A., Wong, K., Gray, N. S., & Bradner, J. E. (2018). The dTAG system for immediate and target-specific protein degradation. *Nature Chemical Biology*, *14*(5), 431–441. <https://doi.org/10.1038/s41589-018-0021-8>
- Noguchi, S., Saito, A., Horie, M., Mikami, Y., Suzuki, H., Morishita, Y., Ohshima, M., Abiko, Y., Mattsson, J. S. M., König, H., Lohr, M., Edlund, K., Botling, J., Micke, P., & Nagase, T. (2014). An integrative analysis of the tumorigenic role of TAZ in human Non-Small Cell lung Cancer. *Clinical Cancer Research*, *20*(17), 4660–4672. <https://doi.org/10.1158/1078-0432.ccr-13-3328>
- Paradis, J. S., Acosta, M., Saddawi-Konefka, R., Kishore, A., Lubrano, S., Gomes, F., Arang, N., Tiago, M., Coma, S., Wu, X., Ford, K., Day, C., Merlino, G., Mali, P., Pachter, J. A., Sato, T., Aplin, A. E., & Gutkind, J. S. (2021). Synthetic lethal screens reveal cotargeting FAK and MEK as a multimodal precision therapy for GNAQ-Driven uveal melanoma. *Clinical Cancer Research*, *27*(11), 3190–3200. <https://doi.org/10.1158/1078-0432.ccr-20-3363>

- Phelps, G. B., Hagen, H. R., Amsterdam, A., & Lees, J. A. (2022). MITF deficiency accelerates GNAQ-driven uveal melanoma. *Proceedings of the National Academy of Sciences of the United States of America*, *119*(19). <https://doi.org/10.1073/pnas.2107006119>
- Reggiani, F., Gobbi, G., Ciarrocchi, A., & Sancisi, V. (2021). YAP and TAZ Are Not Identical Twins. *Trends in Biochemical Sciences*, *46*(2), 154–168. <https://doi.org/10.1016/j.tibs.2020.08.012>
- Shreberk-Shaked, M., Dassa, B., Sinha, S., Di Agostino, S., Azuri, I., Mukherjee, S., Aylon, Y., Blandino, G., Ruppin, E., & Oren, M. (2020). A Division of Labor between YAP and TAZ in Non-Small Cell Lung Cancer. *Cancer Research*, *80*(19), 4145–4157. <https://doi.org/10.1158/0008-5472.can-20-0125>
- Sugase, T., Lam, B., Danielson, M., Terai, M., Aplin, A. E., Gutkind, J. S., & Sato, T. (2020). Development and optimization of orthotopic liver metastasis xenograft mouse models in uveal melanoma. *Journal of Translational Medicine*, *18*(1). <https://doi.org/10.1186/s12967-020-02377-x>
- Yu, F., Luo, J., Mo, J., Liu, G., Kim, Y. C., Meng, Z., Zhao, L., Peyman, G. A., Ouyang, H., Jiang, W., Zhao, J., Chen, X., Zhang, L., Wang, C., Bastian, B. C., Zhang, K., & Guan, K. (2014). Mutant GQ/11 promote uveal melanoma tumorigenesis by activating YAP. *Cancer Cell*, *25*(6), 822–830. <https://doi.org/10.1016/j.ccr.2014.04.017>